Pacific Northwest
NATIONAL LABORATORY

PNNL-ACT-10151

Nine Canyon Long-Duration Energy Storage

A Feasibility Study

August 2025

Mukesh Gautam [1]
Corey Wiggins [2]
Rebecka Iveson [1]
Jessica Kerby [1]
Di Wu [1]
Ross Rebich [3]
Diane Baldwin [1]
Russ Weed [2]
Swasti Saxena [1]
Kazi Tamaddun [1]
Jeremiah Miller [1]

[1] Pacific Northwest National Laboratory
[2] ARES North America
[3] Energy Northwest

U.S. DEPARTMENT OF ENERGY

Prepared for the U.S. Department of Energy
Under contract DE-AC05-76RL01830

DISCLAIMER

PACIFIC NORTHWEST NATIONAL LABORATORY
operated by
BATTELLE
for the
UNITED STATES DEPARTMENT OF ENERGY
under Contract DE-AC05-76RL01830

Printed in the United States of America

Available to DOE and DOE contractors from
the Office of Scientific and Technical Information,
P.O. Box 62, Oak Ridge, TN 37831-0062
www.osti.gov
ph: (865) 576-8401
fox: (865) 576-5728
email: reports@osti.gov

Available to the public from the National Technical Information Service
5301 Shawnee Rd., Alexandria, VA 22312
ph: (800) 553-NTIS (6847)
or (703) 605-6000
email: info@ntis.gov
Online ordering: http://www.ntis.gov

PNNL-ACT-10151

Nine Canyon Long-Duration Energy Storage

A Feasibility Study

August 2025

Mukesh Gautam [1]
Corey Wiggins [2]
Rebecka Iveson [1]
Jessica Kerby [1]
Di Wu [1]
Ross Rebich [3]
Diane Baldwin [1]
Russ Weed [2]
Swasti Saxena [1]
Kazi Tamaddun [1]
Jeremiah Miller [1]

[1] Pacific Northwest National Laboratory
[2] ARES North America
[3] Energy Northwest

Prepared for the U.S. Department of Energy
Under Contract DE-AC05-76RL01830
Pacific Northwest National Laboratory
Richland, Washington 99352

Executive Summary

Chartered in 1957 as a joint operating agency, Energy Northwest (EN) is a consortium of 29 public utility districts (PUDs) and municipalities across Washington state. EN takes advantage of economies of scale and shared services to help utilities run their operations more efficiently and at lower costs, to benefit more than 1.5 million customers. EN develops, owns, and operates a diverse mix of electricity generating resources, including hydro, solar, wind, and battery energy storage projects—and the Northwest's only nuclear energy facility. These projects provide enough reliable and affordable energy to power more than a million homes each year. EN continually explores new generation and storage projects to meet its customers' needs.

EN is targeting the future installation of a 50-200 MW Long Duration Energy Storage (LDES) system with a minimum duration of 10 hours at the Nine Canyon (9C) site, located in southeast Kennewick, Washington. The 9C site is characterized by hilly and broken terrain, with an elevation gain of over 1,000 feet from bottom to top. Of the 5,120-acre lease area, only about 75 acres are in actual use by existing generation facilities, access roads, and maintenance buildings. This provides ample space for siting an LDES system while leveraging existing infrastructure, including a substation and a transmission corridor with an established Interconnection Agreement with the Bonneville Power Administration (BPA).

EN intends to charge the facility with power supplied by the electrical grid from the BPA transmission system. The transmission line that services 9C is owned by BPA and originates approximately 15 miles to the south at the McNary Lock and Dam on the Columbia River. Although not specifically investigated in this report, siting the storage facility in a location that connects to the BPA system allows the facility to store energy generated from anywhere connected to the BPA grid.

EN is particularly interested in gravity-based mechanical rail storage technology that uses elevation to store potential energy. Gravity storage uses no chemicals, is not flammable, uses no water, and can take advantage of natural, locally sourced materials for ballast and weight in the mass cars. In addition to gravity storage, EN seeks to explore other promising LDES technologies and assess their techno-economic characteristics and performance. To achieve this, expert support is required to perform a comprehensive feasibility study to determine the most suitable LDES technology type, size, duration, economic value, and location to meet the project objectives.

Building on this vision, EN has been awarded funding through the Grid Modernization program administered by the Washington State Department of Commerce and the Department of Energy (DOE) Office of Electricity LDES Voucher Program to develop a feasibility study of the 9C LDES. Pacific Northwest National Laboratory (PNNL) applied its extensive expertise in LDES review, modeling, dispatch optimization, and techno-economic assessment (TEA) to support EN in achieving its goals.

At the core of this effort is the development of a generalized techno-economic modeling framework and evaluation tool designed to assess the value proposition of LDES

projects across a variety of contexts. The modeling tool is technology-agnostic and accommodates user-defined parameters such as rated power, energy duration, round-trip efficiency, capital and operational costs, and dispatch constraints. It also integrates economic inputs including market prices, energy revenue structures, and financing parameters to evaluate performance through key metrics. The tool provides utilities with a transparent, adaptable platform to support decision-making, investment prioritization, and portfolio planning for various storage technologies.

To guide scenario design and interpretation, the study first surveyed the LDES technology landscape—lithium-ion batteries, flow batteries, non-hydro gravity storage, and thermo-mechanical systems—comparing cost trajectories, technical performance, safety and hazards, materials sourcing and recyclability, and spatial/siting considerations. This literature-grounded review highlights technology trade-offs and reinforces the need to align technology choice with site characteristics, use cases, and project objectives. A companion chapter examines ownership structures (EN ownership, third-party ownership, shared models) and offtake options (energy marketing, capacity/energy PPAs, time-of-use PPAs, block-delivery PPAs, and tolling), where PPAs (power purchase agreements) represent contractual arrangements for buying and selling electricity. The chapter also highlights implications for risk allocation, capital access, operational control, and revenue certainty.

The study also evaluates supervisory control and data acquisition (SCADA) and transmission interconnection pathways, options include upgrading the existing SCADA at the substation or deploying a dedicated LDES controller, with attention to protection schemes, data telemetry, cybersecurity, and regulatory coordination with BPA. While sharing a geographical location and BPA interconnection agreement, the new storage asset will likely have different offtake utilities from the existing generation facility, making a separate SCADA system a preferred approach for coordinating operational activities. In addition, an ARES-specific geotechnical and hydrology assessment presented in appendix screens multiple corridors for slope stability, bearing capacity, cut-and-fill magnitude, and stormwater behavior. Most candidate corridors appear workable with conventional geotechnical measures; however, one expansion area would require significant earthwork and targeted drainage solutions. Follow-on stormwater design (e.g., terraced bioswales, energy-dissipating outfalls) is recommended for steeper sections.

The TEA examines three primary dimensions: sizing options, offtake structures, and economic/financial assumptions. To capture both broad insights and technology-specific dynamics, the analysis is organized into two levels:

- **Technology-agnostic case studies** that evaluate how capital cost assumptions and offtake structures influence financial outcomes.
- **In-depth assessments of ARES** that evaluate performance across multiple system sizes and financing assumptions.

For the technology-agnostic assessment, a reference LDES system was defined with 50 MW capacity, 10-hour discharge duration, 75% round-trip efficiency, a 20-year project

life, and annual O&M costs equal to 0.5% of CAPEX. These uniform assumptions provide a consistent baseline for comparison across technologies, despite differences in actual lifetimes and efficiencies. In particular, the 20-year horizon reflects a common planning period used in project finance, with shorter-lived technologies interpreted as requiring augmentation or replacement, and longer-lived technologies viewed as having residual value beyond year 20. Likewise, a 75% RTE was selected as a representative midpoint across technologies, balancing higher-efficiency batteries and lower-efficiency mechanical or thermal systems. This framing ensures that results highlight the influence of cost and offtake structures rather than becoming entangled in technology-specific details. Six scenarios were evaluated, reflecting three capital cost assumptions—low ($300/kWh), medium ($400/kWh), and high ($500/kWh)—under two offtake structures: energy marketing and tolling agreements. Energy marketing revenues were estimated using 2023 Mid-C market prices, while tolling revenues were modeled with a $30/kW-month tolling fee and a $20/MWh throughput fee.

Table ES.1. TEA results for high-level technology-agnostic scenarios

Offtake Option	CAPEX	Ann. Rev. ($M)	Ann. Chrg. Hrs.	Ann. Disch. Energy (GWh)	Chrg. Cost ($M)	NPV ($M)	IRR (%)	BCR	Payback Period (years)	LCOS (¢/kWh)
Market	Low	$14	2447	89	$5	-$34	1.8	0.75	None	19
	Med.	$14	2447	89	$5	-$85	-1.3	0.54	None	24
	High	$14	2447	89	$5	-$136	-3.6	0.42	None	29
Tolling	Low	$21	N/A	174	N/A	$108	13.1	1.78	9	7
	Med.	$21	N/A	174	N/A	$57	8.4	1.31	14	10
	High	$21	N/A	174	N/A	$7	5.3	1.03	20	12

Table ES.1 summarizes TEA results for these scenarios, including annual operation results together with net present value (NPV), benefit-cost ratio (BCR), internal rate of return (IRR), payback period, and levelized cost of storage (LCOS). Key insights and lessons learned are summarized as follows:

1. General Lessons Learned

   - Energy marketing in current wholesale energy markets may not provide sustainable revenue streams for LDES, even at relatively low capital cost assumptions.
   - Structured offtake agreements such as tolling can mitigate market risk by securing

predictable revenues, as reflected in positive NPVs and IRRs across all tolling cases, even at high CAPEX.

- The viability of LDES projects is highly sensitive to upfront capital costs, underscoring the importance of technology cost reductions, financing strategies, or supportive incentives to enable deployment.

2. Impacts of Capital Cost: Tolling agreement partially buffers higher CAPEX, but viability remains highly sensitive to upfront cost; a $100/kWh change shifts NPV by $50 million for both offtake options.

   - With tolling agreement, raising CAPEX from $300/kWh to $500/kWh reduced BCR by 0.75 (1.78 to 1.03), IRR by 7.8% (13.1% to 5.3%), and NPV by $101 million ($108 M to $7 M). Near break-even around $500/kWh.
   - With energy marketing, the same CAPEX increase reduced BCR by 0.33 (0.75 to 0.42), IRR by 5.4% (1.8% to -3.6%), and NPV by $101 million (-$34 M to -$136 M); NPV is negative across the assumed range.

3. Impacts of Offtake Structures: Tolling agreements provide stable revenues that sustain economic viability across the assumed CAPEX range, while energy marketing remains negative-NPV.

   - At a low CAPEX of $300/kWh, tolling improved outcomes by 1.03 in BCR (0.75 to 1.78), 11.3% in IRR (1.8% to 13.1%), and $74 million in NPV ($34 M to $108 M).
   - At a high CAPEX of $500/kWh, tolling remained marginally viable with a BCR of 1.03 and IRR of 5.3%, whereas energy marketing at the same cost level resulted in a BCR of just 0.42 and IRR of -3.6%.

4. LCOS Trends: At comparable CAPEX, LCOS under energy marketing is roughly 2-2.5 times higher than under tolling.

   - For tolling agreements, LCOS increased from 7 ¢/kWh at low CAPEX to 12 ¢/kWh at high CAPEX. Daily cycling (approximately 347 days per year) spreads fixed costs over more energy, keeping LCOS moderate despite higher total costs.
   - For energy marketing, LCOS increased from 19 ¢/kWh at low CAPEX to 29 ¢/kWh at high CAPEX. Because dispatch occurs only when energy price spreads are favorable, total discharged energy is much lower, leading to significantly higher LCOS.

The in-depth ARES case study evaluated 30 scenarios, combining five different system sizing candidates with three offtake structures (energy marketing, conservative tolling,

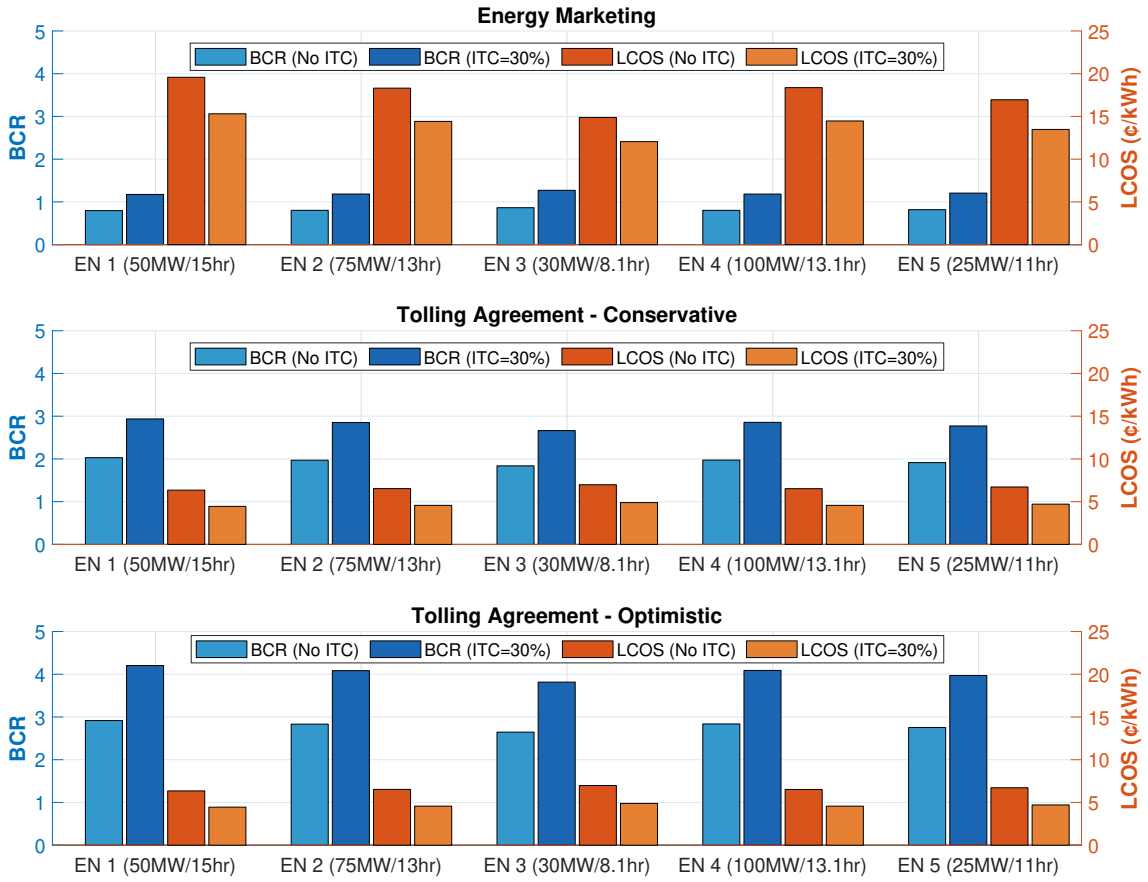

Figure ES.1. Comparison of BCR and LCOS under different offtake options for ARES system

and optimistic tolling) under two investment tax credit (ITC) conditions (with 0% and 30% ITC). This framework enabled systematic comparison of how project performance varies with storage duration, market structure, and financial incentives. Figure ES.1 summarizes BCR and LCOS results in all scenarios. The figure highlights the performance spread across offtake arrangements, clearly showing the stronger economic outcomes of tolling agreements compared with energy marketing. Tolling payments were modeled with a combination of capacity and throughput fees: conservative tolling assumes $30/kW-month for a 10-hour system (scaled for other durations) plus $20/MWh throughput, while optimistic tolling assumes $45/kW-month plus the same $20/MWh throughput. Key insights and lessons learned are summarized as follows:

- **Energy marketing favors shorter-duration systems**: Shorter-duration systems, such as EN 3 (30 MW / 8.1-hour), perform relatively better under energy marketing

because their duration is sufficient to capture most of the available price spreads. Increasing system duration beyond this provides diminishing additional revenue, while increasing capital costs. For example, without ITC, EN 3 achieves a BCR of 0.86 and IRR of 4.0%, whereas a longer-duration system like EN 1 (50 MW / 15-hour) shows lower financial performance (BCR = 0.80, IRR = 3.4%). Including the 30% ITC improves all cases, with EN 3 reaching BCR = 1.27 and IRR = 6.9%, but larger systems remain only marginally viable (EN 1: BCR = 1.17, IRR = 6.2%).

- **Tolling agreements significantly improve economic performance**: Tolling payments, structured with both capacity and throughput fees, yield consistently stronger outcomes. Under conservative tolling, EN 1 (50 MW / 15-hour) without ITC achieves a BCR of 2.03 and IRR of 11.7%, increasing to BCR = 2.94 and IRR = 17.1% with ITC. Optimistic tolling further amplifies returns, with EN 1 reaching BCR = 4.20 and IRR = 24.5% when paired with ITC. Longer-duration and larger-capacity systems benefit most, as revenues scale with both power and discharge duration (e.g., EN 4, 100 MW / 13.1-hour: BCR = 4.09, IRR = 23.8% with ITC under optimistic tolling).

- **Financial incentives matter:** Scenarios including the 30% ITC demonstrate significant improvements in profitability across all sizes and offtake arrangements. For example, under energy marketing, EN 1 moves from a negative NPV (-$51 million) without ITC to a positive NPV ($30 million) with ITC. Similarly, under tolling, EN 2 (75 MW / 13-hour) increases NPV from $610 million to $718 million with ITC under the optimistic structure. This underscores that financial support can turn marginal or borderline projects into financially compelling investments.

- **Best-performing scenario:** EN 1 under optimistic tolling with ITC achieves the highest BCR (>4) and lowest LCOS (<5 ¢/kWh), demonstrating the compounding benefits of favorable contract terms and financial support.

- **Cross-cutting insight:** No single factor—system size, CAPEX, offtake structure, or financial incentives—alone guarantees viability. For instance, EN 3 performs well under energy marketing due to low capital intensity, yet its BCR and IRR remain below tolling alternatives. Similarly, tolling structures consistently outperform energy marketing regardless of ITC, but returns are maximized when paired with financial support. Effective project design therefore requires integrated consideration of all three dimensions.

Acknowledgments

We gratefully acknowledge the guidance and oversight provided by Mr. Jeremy Berke, Senior Commerce Specialist with the Washington State Department of Commerce, in advancing this and other grid modernization initiatives. We also thank Mr. Benjamin Shrager, Storage Strategy Engineer with the U.S. Department of Energy's Office of Electricity (OE), for his support and commitment to the Long-Duration Energy Storage Technical Assistance Voucher. We appreciate the support from the OE Energy Storage Division, which has enabled numerous energy storage efforts at Pacific Northwest National Laboratory, including the development of advanced storage analytics used in this project. Finally, we extend our sincere thanks to Brian Cunnington, Allison Krienke, and Michael Connerly from Energy Northwest, as well as Mark Callaghan from ARES North America, for their invaluable collaboration, coordination, and data sharing.

Acronyms and Abbreviations

9C	Nine Canyon
ARES	Advanced Rail Energy Storage
BCR	benefit-cost ratio
BESS	battery energy storage system
BPUD	Benton Public Utility District
BPA	Bonneville Power Administration
CAES	Compressed-Air Energy Storage
CAISO	California Independent System Operator
CAPEX	capital expenditure
CASA	Control Area Services Agreement
CIP	Critical Infrastructure Protection
DEM	Digital Elevation Model
DNP	Distributed Network Protocol
DOD	depth-of-discharge
DOE	Department of Energy
EN	Energy Northwest
ESS	energy storage system
FERC	Federal Energy Regulatory Commission
HSG	hydrologic soil group
IBR	inverter-based resource
IA	Interconnection Agreement
ICCP	Inter-Control Center Communication Protocol
IEEE	Institute of Electrical and Electronics Engineers
IRR	internal rate of return
ISO/RTO	Independent System Operator / Regional Transmission Organization
ITC	investment tax credit
LAES	liquid-air energy storage
LCOS	levelized cost of storage
LDES	long-duration energy storage
LGIA	large generator interconnection agreement
LGIP	large generator interconnection procedures
LVRT	low-voltage ride-through
Mid-C	Mid-Columbia trading hub
Modbus	Modbus communications protocol
NLCD	National Land Cover Database

NOAA	National Oceanic and Atmospheric Administration
NERC	North American Electric Reliability Corporation
NPV	net present value
NRCS	Natural Resources Conservation Service
O&M	operation and maintenance
OATT	Open Access Transmission Tariff
OE	Office of Electricity
OEM	Original Equipment Manufacturer
OPEX	operating expenditure
PNNL	Pacific Northwest National Laboratory
PPA	power purchase agreement
PUD	Public Utility District
RTE	round-trip efficiency
RTU	remote terminal unit
SCADA	supervisory control and data acquisition
sCO_2	supercritical carbon dioxide
SOC	state-of-charge
TEA	techno-economic assessment
TMES	thermo-mechanical energy storage
USGS	U.S. Geological Survey

Notation

Parameters

Δt	Simulation time step (hours)
η^{ES}	Energy storage round-trip efficiency
$P^{\text{ES}}_{\text{max}}$	Energy storage rated charge and discharge power (MW)
$E^{\text{ES}}_{\text{max}}$	Energy storage energy capacity (MWh)
E_0	Energy storage initial energy state (MWh)
E_T	Energy storage final energy state (MWh)
r	Discount rate
N	Project lifetime (years)
π^{sell}_t	Selling price of electricity at time t ($/MWh)
π^{buy}_t	Purchase price of electricity at time t ($/MWh)
C_{capex}	Capital expenditure, upfront investment cost ($)
$C_{\text{O\&M}}$	Annual operations and maintenance cost ($)
C_{eol}	End-of-life cost incurred at project retirement ($)

Decision Variables

P^+_t	Energy storage discharging power at time t (MW)
P^-_t	Energy storage charging power at time t (MW)
P^{ES}_t	Net energy storage power at time t (MW)
E_t	State-of-charge of the energy storage at time t (MWh)
R_{annual}	Annual revenue from storage operation ($)
C_{charge}	Annual charging cost ($)
E_{dis}	Annual discharged energy (MWh)
H_{charge}	Annual charging hours(h)

Contents

Figures

Tables

CHAPTER 1

Introduction

1.1 Background and Motivation

The power grid faces growing challenges due to aging infrastructure and increasing operational complexity. Resource limitations and transmission constraints create regional imbalances and congestion. The rapid expansion of AI, data centers, and widespread electrification further intensifies these challenges, making grid stability and affordability urgent concerns (Li et al., 2023).

Energy storage is critical in enhancing grid flexibility, improving system reliability, and supporting cost-effective electricity. By storing excess electricity during periods of low demand and discharging it when needed, storage helps balance supply and demand fluctuations. It can provide a broad range of grid and end-user services, such as energy arbitrage, frequency regulation, load following, voltage support, congestion relief, critical infrastructure upgrade deferral, and outage mitigation (Wu and Ma, 2021).

In particular, long-duration energy storage (LDES) enables sustained power availability over extended periods, enhancing resource adequacy and grid reliability. By shifting large amounts of energy over hours, days, and weeks, LDES alleviates stress on transmission and generation infrastructure, reducing the need for costly and prolonged generation and transmission investments. Its ability to store low-cost energy for extended durations and discharge it during high-demand periods improves economic efficiency, making it a valuable tool for stabilizing energy markets. Additionally, LDES strengthens resilience by providing backup power during grid disruptions, ensuring continuous operation for critical services such as hospitals, military bases, and industrial facilities. As electricity demand grows and grid challenges intensify, LDES plays a vital role in securing an affordable, reliable, and resilient electric grid.

Building on these opportunities, Energy Northwest (EN) is targeting the future installation of a 50-200 MW LDES system with a minimum discharge duration of 10 hours sharing the locating with the existing Nine Canyon (9C), located in southeast Kennewick, Washington. The site features hilly terrain with over 1,000 feet of elevation gain and spans 5,120 acres, though only approximately 75 acres are currently in use. This leaves ample space to host LDES while leveraging existing infrastructure, including a substation, 115 kV transmission line, and a Bonneville Power Administration (BPA) interconnection.

1.2 Site Infrastructure and Suitability for LDES

The site's infrastructure includes a substation, grid connection facilities, and maintenance facilities that support the existing wind turbines. These assets provide a solid foundation for deploying LDES, though upgrades or additional components may be required to accommodate the new system.

- Substation and Transmission: The site includes an existing substation facility and an established transmission corridor. The project has an Interconnection Agreement with BPA, which allows for seamless integration with the grid.
- Communication and Control Systems: The current setup includes communication equipment and Supervisory Control and Data Acquisition (SCADA) systems. These systems may either be upgraded or replaced to ensure optimal integration with the LDES system.
- Transportation and Accessibility: Access roads and transport routes are critical for delivering and maintaining LDES equipment, especially bulk systems like rail-based gravity energy storage. Existing access infrastructure will be evaluated for compatibility with the project's logistical requirements.
- Maintenance and Operational Facilities: The 9C site has facilities for ongoing maintenance of existing generation facilities. These facilities may be able to play a role in maintaining LDES units, and the potential for co-use of these facilities can reduce project costs.

The 9C site offers a strong platform for LDES deployment by combining established infrastructure with favorable site characteristics. The presence of a substation and an existing transmission corridor, supported by a formal interconnection agreement with BPA, enables efficient integration with the regional grid and reduces the need for extensive new transmission development. This provides not only cost savings but also helps avoid the long lead times typically associated with permitting and constructing new transmission assets. Communication and SCADA systems are already in place at the site, providing a baseline for monitoring, control, and data acquisition. While these systems may require targeted upgrades or replacement, their availability offers a head start in ensuring compatibility with an LDES system.

Beyond electrical integration, the physical attributes of the site also contribute to its suitability. Ample land availability within the lease area creates flexibility to accommodate a range of LDES technologies, whether bulk rail-based gravity storage that requires significant elevation and space or modular systems such as flow batteries that can be deployed more compactly. Established access roads and transport routes further support construction and long-term maintenance by simplifying delivery of large equipment and ensuring year-round accessibility. Existing maintenance facilities can also be leveraged

for LDES, reducing the need for entirely new support infrastructure and helping lower ongoing operational costs.

Taken together, these elements make the site not only technically viable but also strategically advantageous. By leveraging infrastructure and facilities that are already in place, project development risks and costs are reduced, while site characteristics such as land availability, elevation, and accessibility provide flexibility in choosing among candidate LDES technologies. This combination of readiness and adaptability positions the 9C site as a practical and cost-effective location for LDES deployment.

1.3 Project Objectives and Scope

EN was awarded funding as part of the Grid Modernization program administered by the Washington State Department of Commerce and the U.S. Department of Energy (DOE) Office of Electricity (OE) LDES voucher program to develop a feasibility study of 9C LDES in Benton County, Washington. The study aims to evaluate the technical and economic feasibility of an LDES system at the site, with a focus on identifying optimal configurations that can strengthen system reliability, improve asset utilization, and deliver cost-effective grid services. The core objectives of the study are to:

- Assess the suitability of the 9C site for LDES deployment, leveraging existing land, infrastructure, and interconnection capacity.
- Identify and evaluate different technology and siting/sizing candidates, and ownership/offtake structures to determine economically favorable scenarios.
- Examine the technical requirements and benefits of LDES operation at the 9C site.

To support these objectives, Pacific Northwest National Laboratory (PNNL), in partnership with EN and ARES North America, will carry out the following activities:

- Review and compare promising LDES technologies and their techno-economic characteristics.
- Develop a customized framework to model LDES technical capabilities, optimize operations, and quantify potential benefits.
- Conduct techno-economic assessment (TEA) and sensitivity analyses across a range of scenarios, considering various sizing/siting candidates, ownership, and offtake structures.
- Perform engineering assessments of SCADA and interconnection pathways to ensure compatibility with existing infrastructure and identify potential upgrade needs.
- Provide site-level technical assessment, including topography, climate, and accessibility, to determine location-specific feasibility and construction constraints.

1.4 Report Organization

The remainder of this report is structured as follows: Chapter 2 provides a comprehensive review and comparison of various LDES technologies, including lithium-ion batteries, flow batteries, non-hydro gravity-based storage, and thermo-mechanical energy storage. Chapter 3 discusses potential ownership models and offtake agreement structures. Chapter 4 presents the modeling framework, mathematical formulation, scenario design, and assessment results from multiple scenarios. Chapter 5 outlines considerations related to SCADA integration and transmission interconnection. Chapter 6 concludes the report by summarizing key findings. Appendix A provides geotechnical and hydrological assessments specific to the ARES technology and the project site.

CHAPTER 2

Review and Comparison of LDES Technologies

There exist various LDES technologies, including but not limited to lithium-ion batteries, redox flow batteries, compressed-air energy storage, pumped storage hydro, and emerging solutions like thermal and gravity-based storage. Each technology has unique technical, economic, safety, and material-related characteristics, making it essential to evaluate trade-offs based on deployment needs. Factors such as spatial constraints, energy density requirements, urban versus rural siting, and site-specific geographic and geological characteristics play a key role in determining the most suitable technology for a given application. This chapter provides a comprehensive review and comparison of LDES technologies based on updated economic performance, safety considerations, spatial requirements, and impacts related to energy infrastructure and operations. Leveraging the Energy Storage Grand Challenge (ESGC) Cost and Performance Report (Pacific Northwest National Laboratory, 2023), alongside other relevant studies, this chapter offers insights into the current state of LDES technologies and provides recommendations for stakeholders in the energy sector.

To structure the analysis, the review highlights several dimensions that collectively determine the viability of a technology for deployment, capturing not only cost and performance, but also long-term sustainability, safety, and practical feasibility in real-world settings. The review and comparison are organized around the following key aspects:

- Economic Characteristics: Capital investment, maintenance costs, levelized cost of storage (LCOS), and long-term economic feasibility.
- Technical Characteristics: Efficiency, energy storage capacity, response time, scalability, and energy density.
- Safety and Hazards: Assessment of potential risks, including fire hazards, mechanical failures, and operational stability.
- Material Sourcing and Recycling: Resource intensity, sustainability, and recyclability considerations.
- Spatial and Siting Considerations: Space needed, land use restrictions, height and structural constraints, geographical suitability, and scalability in deployment.

2.1 Overview of Selected LDES Technologies

Various energy storage technologies are outlined in the DOE ESGC Roadmap (U.S. Department of Energy, 2020), many of which hold strong potential for LDES. Additionally, U.S. Department of Energy (2023) provides a structured framework for defining and categorizing LDES based on discharge duration. EN identified four LDES technologies for further exploration, and PNNL carried out a comparative review of these options: lithium-ion batteries, flow batteries, non-hydro gravity storage, and thermo-mechanical energy storage. For clarity, this report uses the term "gravity storage" to refer specifically to non-hydro gravity-based technologies, excluding conventional pumped storage hydro. In addition, the terms "efficiency" and "round-trip efficiency (RTE)" are used interchangeably, both denoting the AC RTE measured at the point of interconnection. In this report, technology scalability refers to the inherent ability of a storage technology to increase power and energy ratings within a single system, whereas deployment expandability reflects the practical ability to add capacity through modular or replicated installations.

2.1.1 Lithium-ion Batteries

Lithium-ion batteries are widely utilized in grid applications due to their technical maturity, fast response times, and modular deployment capabilities. As illustrated in Figure 2.1 (EverythingPE, 2023), these batteries work by moving lithium ions from the negative electrode to the positive electrode during discharge and back when charging. The widespread adoption of lithium-ion batteries is largely due to their high energy density and cycling performance, which makes them suitable for a variety of applications including consumer electronics, electric vehicles, and stationary storage for grid applications (Chen et al., 2020). At first optimized for short-duration applications, advancements in battery technology have enabled their use for longer discharge durations.

Presently, most commercial lithium-ion batteries consist of a graphite anode, a lithium-containing transition metal oxide or phosphate cathode, and a non-aqueous lithium-ion-conducting liquid electrolyte. The cells are often packaged in cylindrical, prismatic, or pouch formats to form the basic repeating unit. Two main chemistries dominate stationary lithium-ion energy storage projects: Lithium Iron Phosphate (LFP) and Nickel Manganese Cobalt (NMC). LFP modules are roughly 10% less expensive on a $/kWh basis than NMC modules, and due to safety considerations, the maximum state of charge for NMC is typically limited to 90%, unlike LFP (Pacific Northwest National Laboratory, 2023).

Key benefits of lithium-ion batteries include high efficiency (80-95%) in temperate climates, fast response times, modularity, and maturity, which make them suitable for various applications where a quick response and high efficiency are needed. However, challenges such as high initial costs, resource availability (particularly for lithium, cobalt, and nickel), lower efficiency in intemperate climates due to thermal management, and degradation over time remain significant considerations (Huang and Li, 2022). Additionally, lithium-ion batteries pose a high fire risk due to thermal runaway, requiring robust

safety measures, including advanced cooling systems and containment measures.

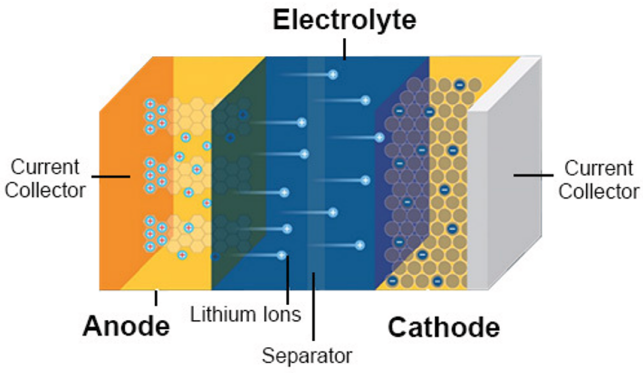

Figure 2.1. Schematic of a lithium-ion battery technology

2.1.2 Flow Batteries

Flow batteries store energy in liquid electrolytes contained in external tanks, which flow through a cell stack where the electrochemical reactions occur. Figure 2.2 (BE&R, 2023) illustrates the operating principle of a vanadium redox flow battery, where the electrolyte circulates between the tanks and the electrochemical cell stack. This design provides scalable, long-duration storage with minimal degradation as the reactants are cycled through the system rather than stored within the electrodes. Their ability to independently scale power and energy capacity makes them suitable for grid support and backup power applications (Aluko and Knight, 2023).

In solid battery designs like lithium-ion, the stored energy is directly related to the amount of electrode material, and increasing the power capacity of these systems also increases the energy capacity as more cells are added. In contrast, flow battery systems can vary power and energy capacity separately. The power of the system is determined by the size of the electrodes, the number of cells in a stack, and the number of stacks in the battery system, whereas the energy storage capacity is determined by the concentration and total volume of the electrolyte(s). This flexibility makes the flow battery an attractive technology for a variety of grid-scale applications with a wide range of power and energy needs (Pacific Northwest National Laboratory, 2023).

Flow batteries come in various chemistries, including vanadium redox, zinc-bromine, and iron-chromium systems, each with unique advantages and trade-offs in terms of efficiency, cost, and material availability (Soloveichik, 2015). Vanadium redox flow batteries are among the most commercially developed, benefiting from stable electrochemistry and long cycle life, while zinc-bromine and iron-chromium flow batteries offer alternative

cost structures with varying degrees of efficiency and scalability (Doetsch and Burfeind, 2022). More recent advancements explore organic flow batteries to reduce reliance on critical materials and improve cost-effectiveness (Wei et al., 2017).

Flow batteries offer advantages such as a long cycle life, high recyclability, and minimal operational degradation (Yuan et al., 2019). However, the initial capital costs are presently higher than lithium-ion, necessitating careful economic consideration for deployment. Some cost reduction strategies for the energy subcomponent include using cheaper low-metallurgical-grade vanadium with an ultrapurification step, electrolyte leasing models, and vertical integration to leverage manufacturing and logistics efficiencies (Pacific Northwest National Laboratory, 2023).

Safety-wise, flow batteries are low-risk for fires but require precautions for handling concentrated electrolytes (Whitehead et al., 2017). The chemical stability of the vanadium electrolyte across a wide range of states of charge reduces the risks associated with thermal runaway, which is a significant concern in traditional lithium-ion batteries. High power and energy requirements can be supported economically, making flow batteries a versatile choice for grid stabilization and support.

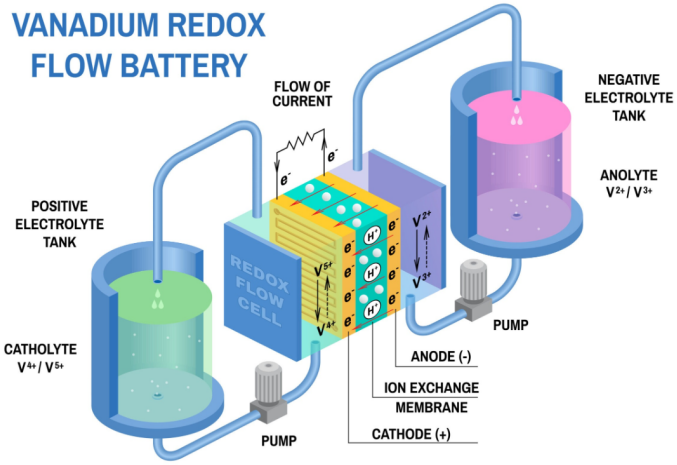

Figure 2.2. Schematic of a vanadium redox flow battery technology

2.1.3 Non-Hydro Gravity Storage

Non-hydro gravity storage technologies leverage gravitational potential energy by raising and lowering solid masses to store and release energy. Unlike traditional pumped hydro storage, which requires large water reservoirs and specific geographic conditions, non-hydro gravity storage systems can be deployed in a wider range of locations and offer scalable, modular designs. These systems generally involve lifting a solid mass–such as

concrete blocks, mass cars, or other dense materials–during charging and allowing it to descend during discharge, converting stored potential energy back into electricity.

One approach to non-hydro gravity storage involves lifting massive blocks using electric motors during periods of excess electricity generation. Companies such as Energy Vault have developed gravity-based storage systems where modular blocks are stacked into a tower and later lowered to drive generators when energy is needed (Li et al., 2024). Another approach is underground gravity storage, developed by companies such as Gravitricity, where masses are lifted and lowered with deep vertical shafts, leveraging high-density materials to optimize energy storage capacity (Li et al., 2024). Lifting-type mass storage systems share similar principles, relying on various mechanisms to raise and lower weights efficiently to store and discharge energy.

Advanced Rail Energy Storage (ARES) represents another form of non-hydro gravity storage system that utilizes heavy mass cars, which move up and down inclined tracks with rails to store and release energy based on gravitational potential energy. During periods of low electricity demand, the mass cars are driven up the incline using excess power; during high demand, they descend, generating electricity. ARES offers an alternative to pumped hydro storage without requiring large water reservoirs, making it suitable for arid areas. The key advantages include minimal operational costs and long asset life.

ARES system consists of several key components, also illustrated in Figure 2.3 (Trott, 2024), which are briefly discussed below:

- Motors/Generators: Stationary motor/generators installed at the top of a slope are used to move mass cars up the slope during charging, converting electrical energy to gravitational potential energy. The motors/generators do the reverse during discharge by moving the mass cars down the slope, converting the gravitational potential energy back into electrical power.

- Mass Cars and Generation Tracks/Rails: The storage media of the ARES system are the mass cars, which during charging are elevated by the motors/generators on inclined tracks/rails installed on the slope. These tracks leverage the natural elevation of the terrain to maximize energy storage efficiency. When energy is needed, the mass cars are lowered, converting potential energy back into electrical energy through motors/generators.

- Transformers and Control Houses: Transformers ensure that the generated power is compatible with the grid's voltage and frequency requirements. Control houses manage the operation of the entire ARES system, ensuring coordination between operation of the motors/generators, movement of the mass cars, and energy charging/discharging.

The non-hydro gravity storage technologies boast a high round-trip efficiency, estimated in the range of 75-85%. The higher efficiency is achieved by minimizing energy losses during the conversion between electrical and mechanical energy, including by the

ESS being engineered so it is unnecessary for the motors/generators to have gearboxes. Additionally, the non-hydro gravity storage is sustainable as it does not use chemicals, water, or flammable materials, making it an attractive option for bulk energy storage.

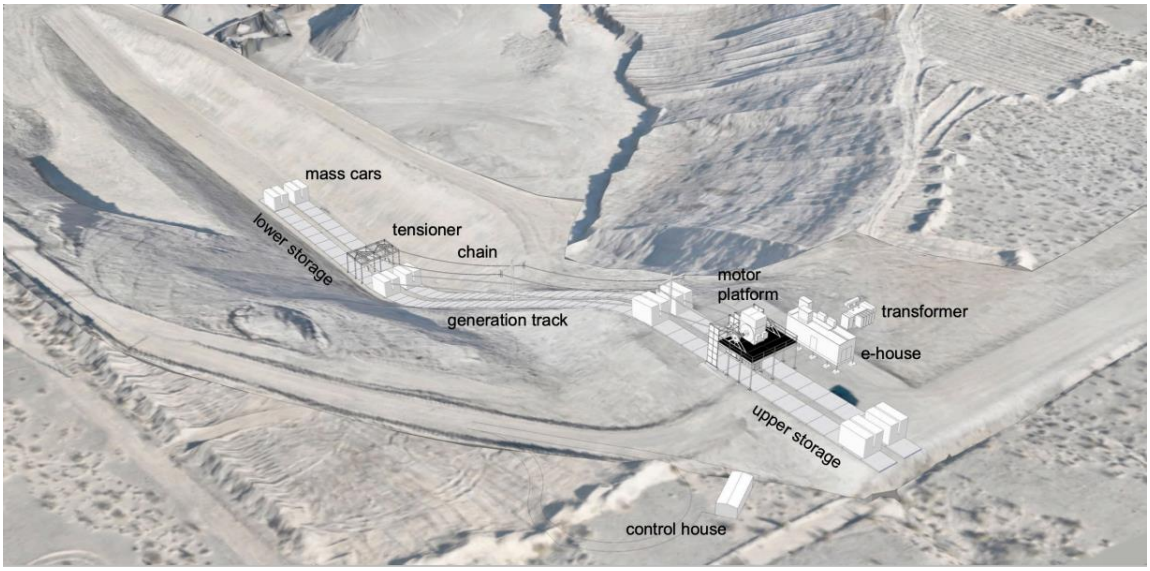

Figure 2.3. Major system components of an ARES technology

2.1.4 Thermo-Mechanical Energy Storage

Thermo-mechanical energy storage (TMES) technologies store energy by converting electricity into thermal and/or mechanical energy, which can later be converted back into electricity when needed. These systems typically rely on compressing gases, heating storage media, or leveraging phase-change materials to store energy. Among the various TMES approaches, compressed air energy storage (CAES) and liquid air energy storage (LAES) are well-established, using high-pressure air or liquefied air to store energy and release it through expansion to drive turbines.

A more advanced form of TMES involves supercritical carbon dioxide (sCO_2)-based energy storage, which uses sCO_2 as the working fluid in a closed-loop Brayton cycle. During charging, using electricity, a compressor generates high-pressure sCO_2 stored in a high-pressure tank, and a thermal energy storage (TES) system stores heat. During periods of high demand, the stored high-pressure sCO_2 is released to generate electricity using a turbine. The system also makes use of two TES units to enhance the efficiency of energy conversion and storage by storing heat. The sCO_2-TMES systems can achieve high round-trip efficiency and extended discharge durations due to the efficient thermal storage. A schematic representation of this technology is shown in Figure 2.4 (Pathak,

2024).

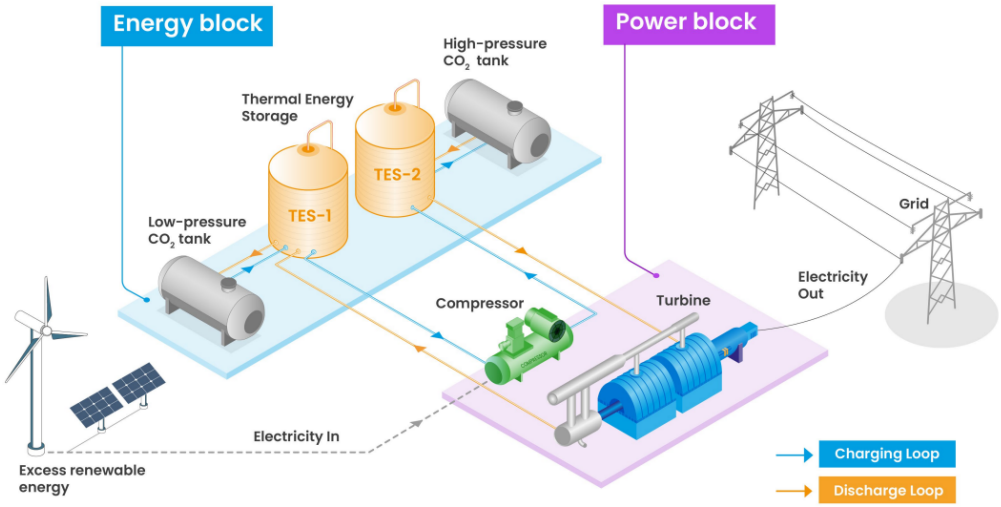

Figure 2.4. Schematic of a sCO_2-TMES technology

2.2 Comparison of LDES Technologies

This section provides a comparison of the selected LDES technologies based on key metrics essential for ensuring grid operational flexibility, reliability, and resilience. The analysis considers economic characteristics, technical characteristics, safety and hazards, and material sourcing and recycling.

It is important to note that the data provided for some technologies may not be fully mature as they have not been fully implemented or deployed yet. This could impact the accuracy of the cost projections and performance data.

2.2.1 Economic Characteristics

Economic feasibility is crucial in determining the adoption of LDES technologies. Key cost components include capital expenditure (CAPEX), operational and maintenance costs (OPEX), LCOS, and system lifespan, as summarized in Table 2.1.

- Lithium-ion batteries: While costs have declined significantly due to advancements in technology and economies of scale, lithium-ion batteries still have high upfront costs. These systems require periodic replacement of the battery cells due to degradation

over time, typically every 10-15 years. This creates a moderate LCOS that is influenced by the cycle life and depth of discharge (DOD) limitations. The high resource intensity for critical minerals like lithium, cobalt, and nickel also contributes to the overall cost (Peters and Weil, 2016).

- Flow batteries: Flow batteries have relatively higher initial capital costs but benefit from lower operational costs due to their long cycle life and minimal operational degradation (Weber et al., 2018). Flow batteries can last between 20-30 years with proper maintenance, which lowers the overall LCOS. Their ability to scale energy capacity independently of power capacity offers significant economic flexibility, making them a viable option for grid applications that require extended energy storage durations. Additionally, they have moderate resource intensity and high recyclability, contributing to their economic and environmental advantages (Rodby et al., 2023).

- Non-hydro gravity storage: Solid mass-based gravity storage systems, such as ARES and lifting-based storage, benefit from low material costs (steel, concrete, or natural rock or soil formations) and minimal degradation over time. These systems offer long asset life with relatively low maintenance costs, making them economically viable for bulk LDES applications. They also have low resource intensity, as they do not rely on rare or critical materials.

- TMES: TMES technologies, including CAES, LAES, and sCO_2 energy storage, utilize thermal and mechanical processes to store energy. Their long lifespans and in some cases high RTE make them promising solutions for bulk energy storage. However, CAPEX can be high, particularly for systems requiring large underground caverns or specialized heat exchangers (Shan et al., 2022).

Table 2.1. Economic characteristics comparison

Technology	CAPEX ($/kWh)	OPEX ($/kW-year)	LCOS ($/kWh)	Lifespan (Years)
Lithium-ion	300-600	5-25	0.15-0.30	10-15
Flow batteries	350-800	5-25	0.15-0.30	15-25
Gravity storage	250-600	15-35	0.12-0.25	30-50
TMES	100-600	10-50	0.10-0.30	25-40

2.2.2 Technical Characteristics

Technical performance is evaluated based on storage duration, efficiency, response time, and technical scalability, as summarized in Table 2.2. These technical characteristics highlight the unique strengths and suitability of each LDES technology for various grid applications.

- Lithium-ion batteries: Lithium-ion batteries are known for their high efficiency, ranging between 80-95% (in temperate climates), and fast response times, typically less than a second. This makes them suitable for applications requiring quick response, such as frequency regulation and short-term grid stabilization. However, their storage duration is limited to approximately 4-12 hours, making them less ideal for long-duration applications. The scalability of lithium-ion batteries is relatively high due to their modular nature, enabling easy integration into various grid settings.

- Flow batteries: Flow batteries have a moderate efficiency of about 60-85%, but they excel in providing long discharge durations of 6-24+ hours. This makes them well-suited for applications requiring continuous and extended energy storage, such as the integration of distributed energy resources and load shifting. Flow batteries are highly scalable, allowing independent scaling of power and energy capacities, providing great flexibility for grid support and backup power applications. With fit-for-purpose DC power electronics and AC power conditioning, their response times are the same as lithium-ion. Their ability to maintain capacity over a long cycle life without significant degradation further enhances their appeal.

- Non-hydro gravity storage: Non-hydro gravity storage systems, such as ARES and lifting-based systems, offer efficiency in the range of 75-85% and are capable of discharging energy for 4-24+ hours. These technologies are particularly beneficial for bulk energy storage over extended durations due to their mechanical storage approach using heavy solid masses. ARES's scalability is high, with the potential to be deployed in various locations with suitable geographic conditions. Non-hydro gravity storage technologies are ideal for applications requiring high-capacity energy storage with minimal operational costs and a long asset life.

- TMES: TMES systems store energy through mechanical compression and thermal processes. They are ideal for bulk energy storage with very long discharge durations. However, their efficiency is lower than electrochemical and gravity-based storage, and their response time is slower due to the use of turbines, making them more suitable for energy shifting where efficiency is not prioritized and not for fast-response grid support. Despite these limitations, their scalability is high, particularly for centralized storage in industrial or utility-scale applications.

Table 2.2. Technical characteristics comparison

Technology	Efficiency (%)	Response Time (sec)	Duration (hours)	Technical Scalability
Lithium-ion	80-95	0.01-10	4-12	Moderate
Flow batteries	60-85	0.01-10	6-24+	High
Gravity storage	75-85	10-70	4-24+	High
TMES	50-80	60-600	4-100+	High

2.2.3 Safety and Hazards

Safety considerations are critical when evaluating LDES technologies. This includes assessing the potential risks such as fire hazards, mechanical failures, and operational stability, as summarized in Table 2.3. Each technology has unique safety profiles that need to be carefully considered in the context of grid integration and operational environments.

- Lithium-ion batteries: Lithium-ion batteries are widely used but possess significant safety risks due to their high fire hazard and potential for thermal runaway. Thermal runaway refers to an uncontrollable increase in temperature that can lead to propagation and fires or explosions. To mitigate these risks, robust containment measures and advanced cooling systems are essential. Fire risk management strategies include the use of flame-retardant materials, advanced monitoring systems, and emergency response protocols (Huang and Li, 2022). Additionally, battery management systems (BMS) play a crucial role in monitoring cell temperatures and ensuring safe operating conditions. Improvements in electrolyte formulations and battery design are ongoing to enhance safety profiles and reduce the likelihood of thermal runaway (Huang and Li, 2022).

- Flow batteries: Flow batteries pose lower fire risks compared to lithium-ion batteries due to the high heat capacity of their aqueous electrolyte, which does not easily combust (Whitehead et al., 2017). However, safety concerns associated with flow batteries include the handling of concentrated acid or alkaline electrolytes, which can be corrosive and hazardous. To ensure safe operation, adequate personal protection equipment (PPE) and proper ventilation systems are needed to manage hydrogen and oxygen gases that may be released during electrochemical reactions (Paiss, 2017). Regular maintenance and monitoring systems are essential to detect and address any leaks or pressure build-ups in the electrolyte tanks and flow systems.

- Non-hydro gravity storage: Gravity storage systems, such as ARES and lifting-based technologies, have minimal fire hazards, as they do not involve chemical reactions or combustible materials. However, mechanical failures could occur due to equipment malfunction, track misalignment, structural failures, or mechanical wear of lifting systems. These risks necessitate regular inspections and maintenance to ensure system stability. Additionally, long-term exposure to environmental conditions could affect infrastructure reliability. Like all grid-connected ESS, ARES integrates with substations and transformers, thus electrical hazards such as electric shocks, arc flashes, and insulation failures must also be considered. Proper grounding, insulation, and protective equipment are essential to mitigate these risks. Routine electrical inspections and maintenance of transformers and power electronics are necessary to prevent potential failures that could impact overall system performance and safety.
- TMES: TMES systems introduce different safety challenges. Pressurized tanks and mechanical components pose risks of structural failure or leaks. Some systems, particularly those using hydrocarbons or organic Rankine cycles, may introduce fire hazards if flammable working fluids are involved. Additionally, high-temperature operations and thermal cycling can lead to material fatigue over time. Proper containment, pressure management, and thermal insulation are critical for ensuring safe and stable operation.

Table 2.3. Safety and hazards comparison

Technology	Fire Hazard Risk	Mechanical Failure Risk	Operational Stability Risk
Lithium-ion	High	Moderate	Moderate
Flow batteries	Low	Low	Moderate to High
Gravity storage	Negligible	Moderate	High
TMES	Varies	Low to Moderate	Moderate

2.2.4 Material Sourcing and Recycling

Material sourcing and end-of-life recycling are vital when evaluating LDES technologies. This includes assessing resource security, intensity, sustainability, and recyclability considerations, as summarized in Table 2.4.

- Lithium-ion batteries: Lithium-ion batteries have high resource intensity due to the need for critical minerals like lithium, cobalt, and nickel (Peters and Weil, 2016).

These materials are associated with significant environmental impacts from extraction and processing. While lithium-ion batteries produce no operational emissions, they face moderate to significant (at present) recycling challenges. Recycling processes are still evolving, and the environmental impacts of disposal and resource recovery are not negligible. Efforts are underway to improve recycling technologies to reduce the overall environmental impact of lithium-ion batteries.

- Flow batteries: Flow batteries exhibit moderate resource intensity and boast high recyclability. They produce no operational emissions, contributing positively to their environmental profile. The use of vanadium, which has a relatively abundant supply, and the potential for recycling the electrolyte system, enhances the sustainability of vanadium redox flow batteries (Rodby et al., 2023). The long cycle life of flow batteries further reduces the environmental impact by minimizing the need for frequent replacements.

- Non-hydro gravity storage: Gravity storage systems, such as ARES and lifting-based technologies, primarily use steel, concrete, and other bulk materials, which are more abundant and accessible compared to mined minerals. These systems offer high recyclability, as their structural components can be repurposed at the end of their operational life. While ARES requires dedicated tracks/rail and land for operation, lifting-based technologies often require vertical structures whether buildings or mines, both of which necessitate careful planning to optimize material use and system integration.

- TMES: TMES technologies primarily rely on steel, aluminum, and mechanical components, which have high recyclability. The working fluids, such as air or CO_2, are typically available and reusable. However, high-pressure storage tanks and thermal insulation materials require periodic replacement, affecting long-term material sustainability and system maintenance requirements.

Table 2.4. Material sourcing and recycling comparison

Technology	Resource Intensity	End-of-Life Management
Lithium-ion	High (lithium, cobalt, nickel)	Recycling challenges
Flow batteries	Moderate (vanadium, zinc, bromine)	High recyclability
Gravity storage	Low to moderate (steel, concrete)	Moderate
TMES	Low	Moderate

2.2.5 Spatial and Siting Considerations

LDES installation depends on available space, land use restrictions, height and structural constraints, geographical suitability, and scalability in deployment, as summarized in Table 2.5. Each technology has unique spatial and infrastructure requirements, which influence their suitability for different geographic locations and operational settings.

- Lithium-ion batteries: Lithium-ion battery systems are highly compact and modular, which makes them energy-dense for urban and suburban installations. Their compact nature allows for integration into existing grid infrastructure with minimal spatial disruptions. However, they require additional space for non-propagation and fire safety considerations, including fire suppression systems and adequate ventilation to manage thermal runaway risks. These extra space requirements can sometimes limit their deployment flexibility.

- Flow batteries: Flow batteries require more space than lithium-ion batteries because of the tanks needed to store the liquid (and in some cases, solid) electrolytes. However, their design allows for modular expansion, meaning energy capacity can be increased by adding more electrolyte without requiring significant additional infrastructure (Weber et al., 2018). This feature makes flow batteries suitable for larger installations, such as utility-scale projects developed by independent developers, utility-owned storage, and commercial and industrial sites, whether coupled with generation or stand-alone storage, where available space is not as restricted. Flow batteries can also be installed in less dense areas where land is more affordable and accessible.

- Non-hydro gravity storage: Gravity storage technologies, such as ARES or lifted-mass systems, require significant land area and structural support. Taller structures or deeper mine shafts are needed for lifted-mass systems, posing cost problems and engineering challenges in areas with strict zoning laws or geological limitations. Track/rail technologies like ARES using the ground for weight-bearing depend on specific terrain conditions, requiring natural or engineered height differences (e.g., hilly or mountainous regions). The availability of a suitable gradient is crucial for their operation.

- TMES: TMES systems, such as those utilizing underground caverns for compressed air or thermal storage, are highly dependent on geological conditions. These systems require specific rock formations or caverns for underground storage, making them geographically constrained (Shan et al., 2022). While they have high energy density and long-duration capabilities, their expansion is difficult since new underground formations cannot be easily created. The need for large surface-level infrastructure (compressors, heat exchangers, and turbines) also impacts land requirements.

Table 2.5. Spatial and siting considerations comparison

Technology	Land Requirement	Height/Structural Constraints	Deployment Expandability
Lithium-ion	Moderate	Low	Moderate
Flow batteries	Moderate	Low	Moderate to High
Gravity storage	High	High	Moderate
TMES	High	High	Low to moderate

Table 2.6. Comparison of LDES technologies

Characteristic	Lithium-ion	Flow Batteries	Gravity Storage	TMES
CAPEX ($/kWh)	300-600	350-800	250-600	100-600
OPEX ($/kW-year)	5-25	5-20	15-35	10-50
LCOS ($/kWh)	0.15-0.30	0.15-0.30	0.12-0.25	0.10-0.30
Lifespan (years)	10-15	15-25	30-50	25-40
Efficiency (%)	80-95	60-85	75-85	50-80
Resp. Time (s)	0.01-10	0.01-10	10-70	60-600
Duration (h)	4-12	6-24+	4-24+	4-100+
Tech. Scalability	Mod.	High	High	High
Fire Risk	High	Low	Low	Varies
Mech. Failure	Mod.	Low	Mod.	Low-Mod.
Oper. Stability	Mod.	Mod.-High	High	Mod.
Resource Intensity	High	Mod.	Low-Mod.	Low
EoL Mgmt. & Recycling	High	Low	Mod.	Mod.
Land Req.	Mod.	Mod.	High	High
Height/Struct. Const.	Low	Low	High	High
Deploy. Expansion	Mod.	Mod.-High	Mod.	Low-Mod.

2.2.6 Summary of Comparison

The comparisons discussed in previous subsections are consolidated in Table 2.6 to provide a clear and concise overview of key characteristics across the selected LDES technologies, namely lithium-ion batteries, flow batteries, non-hydro gravity storage, and TMES. The table includes key characteristics such as CAPEX, OPEX, LCOS, lifespan, efficiency, response time, duration, technical scalability, fire hazard, mechanical failure risk, operational stability, resource intensity, end-of-life management, land requirement, height/structural constraints, and scalability in deployment. This comprehensive comparison facilitates a better understanding of the relative strengths, limitations, and potential applications of each technology.

Moreover, to provide a visual representation of the trade-offs between these LDES technologies, radar (spider) charts have been used to illustrate their relative strengths and weaknesses across key performance metrics. Each chart highlights the performance of a given technology in terms of various key metrics such as economic characteristics, technical characteristics, safety and hazard, material sourcing and recycling, and spatial and siting considerations. Each chart highlights the performance of a given technology in these areas, enabling stakeholders to quickly understand their suitability for different grid resilience and reliability applications, as illustrated in Figure 2.5.

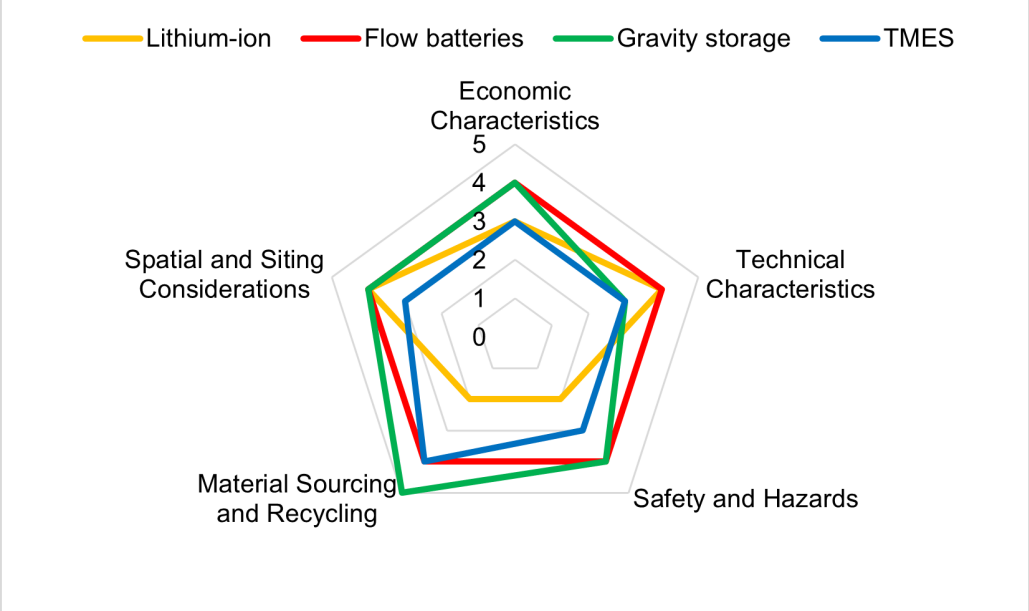

Figure 2.5. Radar charts illustrating key comparison characteristics of LDES technologies

CHAPTER 3

Ownership Structures and Offtake Agreement Options

This chapter outlines the potential ownership models and agreement options for integrating an LDES system at the 9C site. Establishing effective ownership and agreement structures is critical to maximizing the value of the LDES system for grid services, regulatory compliance, and overall project viability.

3.1 Ownership

The choice of operational responsibility and ownership structure plays a pivotal role in an energy storage project's financing, risk allocation, regulatory treatment, and long-term asset management, while also influencing stakeholder engagement and public trust. This study focuses on pathways where EN retains operational responsibility, consistent with its strong track record and established role in prior energy projects. Within this framework, three ownership models are examined to explore different pathways for asset ownership and risk allocation. The ownership options are compared in Table 3.1 across key dimensions such as financial responsibility, operational control, risk allocation, governance complexity, and policy alignment.

- EN Ownership

  Under this ownership model, EN fully owns and operates the LDES system and assumes complete responsibility for both the capital investment and operational management of the asset. Centralized ownership enables streamlined coordination between development, operations, and strategic planning, ensuring that project objectives are tightly aligned with EN's mission to deliver reliable, affordable, and sustainable energy. As a publicly governed, non-profit utility, EN can prioritize broader public interest goals such as energy affordability and reliable power, without external shareholder pressure.

  However, this model places the full burden of financing, asset ownership, and market exposure on EN. It requires substantial upfront capital investment, potentially constraining financial flexibility for other initiatives. EN also bears the financial risks

Table 3.1. Comparison of ownership models

Aspect	EN Ownership	Third-Party Ownership	Shared Ownership
Capital Investment	Fully borne by EN	Provided by third-party owner	Shared among multiple entities (may or may not include EN)
Operational Responsibility	EN operates the system	EN operates under service agreement	EN operates under shared governance
Financial Risk	Entirely borne by EN	Borne by third-party owner	Shared among owners
Control over Asset Decisions	Full control	Limited; requires contractual protections	Shared; requires governance mechanisms
Access to Incentives/Financing	Limited (public entity constraints)	Broader access (e.g., tax credits, private financing)	Depends on partner types
Governance Complexity	Low (internal governance)	Moderate (contractual coordination)	High (multi-owner governance structure)
Exposure to Technology Obsolescence	Direct exposure	Primarily third party's risk	Shared among owners
Alignment with Public Policy Goals	High	May be weaker depending on third-party priorities	Variable; depends on ownership mix
Administrative Burden	Relatively low	Moderate	High
Flexibility for Future Upgrades	High	Limited; subject to third-party agreement	Depends on governance arrangements

associated with technology performance, policy shifts, and evolving market conditions over the asset's lifetime. In addition, the rapid pace of technological innovation further introduces the risk that the selected storage technology could become economically less competitive before the end of its expected service life, potentially diminishing the long-term value of the investment.

- Third-Party Ownership

  Under the third-party ownership model, the LDES asset is owned by a third entity, such as a private developer, infrastructure fund, financial institution, or public agency,

while EN controls and is responsible for system operation through a long-term service agreement. This arrangement allows EN to leverage its operational expertise without committing capital to asset ownership. It enhances EN's financial flexibility and shields it from direct exposure to asset-related financial risks. The third-party owner may also access tax incentives or financing structures that are unavailable to EN as a public entity, potentially improving overall project economics.

Nevertheless, third-party ownership introduces several challenges. EN's ability to influence asset-level investment decisions, such as technology upgrades, may be limited, requiring strong contractual protections to safeguard operational performance. While clear, robust contracts can define service expectations and maintenance standards, they cannot fully eliminate the risk that a third-party owner underinvests in asset upkeep or upgrades, potentially affecting system reliability. EN also becomes partially dependent on the financial health and strategic priorities of the owner; ownership transitions, financial distress, or changes in business direction could destabilize long-term operations. Furthermore, future contract renegotiations may be necessary as market conditions and regulatory frameworks evolve, potentially reducing EN's leverage over key operational terms. Finally, alignment with broader public goals may be more difficult under third-party ownership, as private owners may prioritize financial returns over public interest objectives.

- Shared Ownership

  In the shared ownership model, the LDES asset is jointly owned by two or more entities, which may include EN, utilities, public agencies, or private investors. EN retains operational responsibility, ensuring technical continuity leveraging existing lease agreements, and electrical integration with the existing infrastructure. This structure can also foster broader partnerships across sectors, expanding access to expertise, funding opportunities, and regional support. This approach distributes capital requirements and asset risks across multiple stakeholders, enhancing financial feasibility while preserving EN's operational leadership. It also encourages cooperative investment in long-term performance and strategic alignment among participants.

  However, shared ownership could increases governance complexity and administrative burden. A formalized governance framework may be required to manage joint decision-making, cost and revenue allocation, and asset lifecycle planning. Differing risk appetites, investment priorities, or strategic goals among co-owners can create friction and slow decision-making. Decision-making delays could pose challenges during urgent operational needs, where quick action may be required to maintain system reliability. Ownership transitions or the exit of a co-owner could further introduce uncertainty and destabilize long-term management structures. Disputes may also arise regarding major reinvestment needs, particularly if co-owners have unequal financial strength. EN must carefully navigate these dynamics to maintain operational effectiveness and ensure that the system's performance remains aligned with broader public interest objectives.

Table 3.2. Comparison of offtake agreement options

Aspect	Energy Marketing	Power Purchase Agreements	Tolling Agreements
Revenue Predictability	Low; dependent on market prices	High; fixed or indexed price over long term	High; fee-based revenue independent of commodity price
Market Exposure	High; project owner exposed to market volatility	Low; insulated through fixed contractual terms	Low; insulated through tolling fee structure
Operational Complexity	Low for owner; handled by marketer	Medium; requires delivery, performance guarantees	Medium; requires operational availability
Credit Risk	Medium; risk on marketer performance	Medium to High; risk tied to offtaker's creditworthiness	Medium; depends on counterparty
Risk of Commodity Price Fluctuation	High; borne by owner	Low; price risk transferred to offtaker	Low; commodity procured by offtaker
Financial Attractiveness	Medium to Low; lenders may discount volatile revenues	High; favored by lenders due to stability	High; favored by lenders due to stability
Contract Negotiation Complexity	Medium	High; extensive terms and conditions	High; requires clear operational and performance standards

3.2 Offtake Agreements

Establishing clear and viable offtake agreement options is crucial for ensuring the financial viability and operational success of an energy storage project. These agreements define how the energy storage operation and associated services will be utilized, compensated, and allocated, providing revenue certainty and cost recovery mechanisms for investors and operators. This section outlines three distinct offtake agreement mechanisms: energy marketing, PPAs, and tolling agreements. Each mechanism is first introduced with a descriptive overview and then examined across several aspects, including benefits, challenges, applicability, and other relevant contractual and operational considerations. The three offtake agreement options are compared and summarized in Table 3.2 across key aspects related to revenue certainty, market risk, operational requirements, and financial attractiveness.

3.2.1 Energy Marketing

Under the energy marketing model, the LDES system monetizes energy and services through market-based transactions and/or bilateral agreements, depending on interconnection and regional access as well as commercial relationships. When participating in a market such as CAISO, the system can actively participate in day-ahead and real-time markets, leveraging dynamic price signals for arbitrage, capacity payments, and ancillary services. In the Pacific Northwest, including the Mid-Columbia (Mid-C) region, much of the electricity trading occurs through bilateral agreements, potential shaping services, and participation in custom reliability programs. Operators can optimize charging and discharging schedules to align with favorable pricing periods or contractual delivery terms, improving overall revenue potential.

The primary benefit of energy marketing is its high operational flexibility. It allows the project to respond dynamically to price signals and market demands, enabling value stacking across different services. However, the model also exposes the asset to significant market price volatility, creating uncertainty in revenue streams. Successful participation requires sophisticated forecasting, operational optimization, and real-time market trading capabilities. As such, this model is best suited for entities with strong experience in merchant market operations or those capable of employing active risk management strategies.

3.2.2 Power Purchase Agreements

PPAs offer a more structured and predictable revenue model for the LDES asset. A PPA is a long-term contract in which an offtaker agrees to purchase energy capacity, power capacity, or other energy storage services at pre-determined rates, typically spanning 10 to 20 years. By securing a guaranteed revenue stream, PPAs can substantially de-risk a project and facilitate access to financing. Several types of PPA structures can be applied to storage projects, each offering different trade-offs in terms of complexity, flexibility, and market responsiveness.

- Pro-rata Cost and Benefit Allocation PPAs

  In this structure, multiple offtakers share the costs and benefits of the project in proportion to their contracted share. Each party commits to paying its share of project costs (both fixed and variable) and receives a corresponding share of energy capacity, power capacity, or other services. This model is useful when a project serves multiple utilities or public agencies and can enhance project bankability by diversifying the offtaker base. However, coordinating among multiple participants can introduce administrative complexity and require detailed cost-sharing agreements.

- Traditional Energy and Capacity PPA

In a traditional structure, the offtaker contracts for delivery of energy capacity and/or power capacity at a fixed or escalating price schedule. The storage or the integrated system must meet minimum delivery obligations, with penalties or bonuses tied to performance metrics. This model provides clear revenue predictability and is widely accepted by lenders and investors. However, the project operator may have limited ability to optimize dispatch to take advantage of spot market conditions, potentially leaving some value on the table.

- Time-of-Use PPAs

  Time-of-use PPAs introduce variable pricing based on the time when energy, power, or services are delivered. Higher prices may apply during peak demand periods, with lower prices during off-peak times. This model is particularly well-suited to LDES assets that can strategically discharge during peak pricing windows, thus aligning operational behavior with grid needs. Time-of-use PPAs create a middle ground between fixed-price certainty and market-based optimization but require careful forecasting and operational discipline to maximize value.

- Block Delivery PPAs

  In a block delivery arrangement, the LDES project commits to deliver specified quantities of power during predefined time blocks (e.g., 6–10 AM, 5–9 PM). These blocks are often structured to align with system peak periods or resource adequacy requirements. Block PPAs provide clarity for both the seller and buyer regarding delivery expectations and pricing. However, they can constrain operational flexibility, particularly if grid needs or market conditions evolve over time.

The primary advantage of a PPA is the provision of long-term revenue certainty, which greatly supports project financing and investment. PPAs align well with integrated resource planning processes and help utilities and agencies plan for future grid needs. However, PPAs can involve complex negotiations and contractual structures, requiring careful tailoring to balance project economics with offtaker needs. One downside is that PPAs often limit the asset's ability to flexibly respond to emerging market opportunities. Static pricing mechanisms might not fully capture future upside potential from ancillary services or evolving market dynamics. PPAs are particularly suited for risk-averse public utilities, municipal agencies, or load-serving entities seeking predictable costs, resilient infrastructure, and a hedge against future market volatility.

3.2.3 Tolling Agreements

In a tolling agreement structure, the offtaker provides the input energy—such as electricity for charging a storage system—and pays the storage asset owner a fee for using the storage infrastructure (Baxter, 2019). Essentially, the offtaker "tolls" energy through the storage asset, paying primarily for operational performance rather than taking ownership of energy transactions.

The major advantage of tolling agreements is that they shield the owner from commodity price risk and complexities associated with energy procurement. This structure allows the owner to focus purely on the performance and availability of the storage system. However, the model can restrict opportunities for maximizing revenues through value stacking, as operational decisions may be more narrowly defined. Additionally, tolling agreements require close operational coordination between the asset owner and offtaker. Tolling arrangements are ideal for entities seeking access to storage services without wishing to operate, own, or directly manage energy market participation.

3.3 Relationship Between Ownership and Offtake Options

While ownership and offtake options are discussed separately, understanding their relationship is important for fully evaluating the viability and structure of storage projects.

Ownership structures primarily influence the distribution of costs, risks, and revenues among stakeholders. Regardless of the ownership option, the overall project economics in terms of total capital costs and total revenue potential remain largely unchanged. Ownership decisions determine who bears financial risks and how benefits are allocated, but they do not fundamentally alter the system's ability to generate revenue.

Offtake agreements, in contrast, directly shape the project's total revenue potential and its financial predictability. They determine how and at what value the energy, power, and associated services are monetized. Different offtake mechanisms carry different levels of market exposure, price stability, and lender attractiveness, all of which significantly impact the project's overall financial performance.

Although ownership and offtake options are not directly coupled, they influence each other in practice. For instance, a third-party owner may strongly prefer a long-term PPA to secure predictable cash flows and facilitate project financing, whereas EN ownership may allow for more risk tolerance and flexibility in market participation. Therefore, ownership structures may inform the selection of appropriate offtake strategies, and conversely, the feasibility of certain offtake models may influence preferred ownership arrangements.

PNNL's role is to provide technical assistance by identifying and analyzing ownership and offtake options, but not to select or recommend a preferred pathway. Final decisions regarding ownership structures and offtake agreements will be made by EN and other project stakeholders. All technical and economic assessments conducted by PNNL will be based on assumptions, inputs, and priorities provided by EN.

CHAPTER 4

Techno-Economic Assessment and Sensitivity Analysis

This chapter presents a comprehensive TEA framework developed to evaluate energy storage technologies under a variety of design and market scenarios. The analytical platform builds upon the Energy Storage Evaluation Tool (ESET) developed at PNNL, enabling systematic evaluation of performance and cost-effectiveness for different storage configurations.

The framework is designed to serve as a scenario-based decision-support tool. By combining detailed system-level modeling with flexible input parameterization, it allows exploration of a broad range of sizing strategies, financial assumptions, and offtake agreement structures. Each simulation yields a consistent set of economic and performance metrics enabling comparison across scenarios.

In this chapter, the underlying modeling formulation is first described, followed by a summary of key input parameters and assumptions used in the analysis. The final sections present the description of performance and economic evaluation metrics used to assess scenario outcomes, and a set of sensitivity analyses illustrating how results respond to changes in various input parameters and assumptions.

4.1 Modeling Framework and Mathematical Formulation

The modeling framework is designed to evaluate the operational and economic performance of LDES systems across multiple deployment and offtake scenarios. It supports both optimization-based and rule-based dispatch approaches, depending on the contractual structure. For merchant or market participation, the framework formulates and solves an optimization problem to determine the dispatch that maximizes net revenue subject to system and market constraints. In contrast, for fixed-contract structures such as certain PPAs, dispatch is prescribed by the contract, and no optimization is required. This dual capability ensures consistent and comparable results across fundamentally different operational regimes.

The energy storage system is modeled using a simplified scalar dynamic formulation that captures the essential operational behavior of grid-connected storage technologies.

This generalized approach accounts for key constraints such as energy balance, charging/discharging limits, state-of-charge (SOC) bounds, and round-trip efficiency, while maintaining computational efficiency. The model structure is sufficiently flexible to represent various storage types, including electrochemical and mechanical systems.

Let P_t^- and P_t^+ denote the charging and discharging power of the storage system at time t, respectively. The evolution of stored energy is represented by the following first-order difference equation:

$$E_t = E_{t-1} + \eta^{\text{ES}} \cdot P_t^- \cdot \Delta t - P_t^+ \cdot \Delta t \tag{4.1}$$

where E_t is the energy stored at time t, η^{ES} is the round-trip efficiency, and Δt is the simulation time step (set to one hour in this study).

The net storage power injected into the grid is given by:

$$P_t^{\text{ES}} = P_t^+ - P_t^- \tag{4.2}$$

where positive values indicate discharging (net export to the grid) and negative values represent charging (net import from the grid).

The operation of the storage system is constrained by its rated power and energy capacity:

$$0 \leq P_t^- \leq P_{\text{max}}^{\text{ES}} \tag{4.3a}$$
$$0 \leq P_t^+ \leq P_{\text{max}}^{\text{ES}} \tag{4.3b}$$
$$0 \leq E_t \leq E_{\text{max}}^{\text{ES}} \tag{4.3c}$$

where $P_{\text{max}}^{\text{ES}}$ is the rated power (in MW) and $E_{\text{max}}^{\text{ES}}$ is the maximum energy capacity (in MWh) of the storage system.

To ensure consistency of operation and enforce energy neutrality over the simulation horizon, the storage system is required to return to its initial state-of-charge at the end of the year:

$$E_T = E_0 \tag{4.4}$$

4.2 Scenario Design and Input Parameters

A multi-dimensional scenario framework is employed to evaluate combinations of storage system sizes, offtake agreement structures, and financial assumptions in a systematic manner. Each scenario represents a distinct configuration, which is analyzed through a unified optimization model to determine both operational performance and financial outcomes.

The scenario framework is organized along three principal dimensions to capture the variability in system design, contractual arrangements, and economic/financial assumptions:

- **Sizing Option (i):** The sizing options are designed to reflect both practical deployment constraints and variations in technology characteristics. Key parameters for each configuration include:
  - Rated energy capacity $E_{\text{max}}^{\text{ES}}$ (MWh)
  - Rated power capacity $P_{\text{max}}^{\text{ES}}$ (MW)
  - Round-trip efficiency (η^{ES})

- **Offtake Agreement Type (j):** The revenue potential of the storage system is closely tied to the chosen offtake arrangement. While Chapter 3 reviewed five types of offtake structures—energy marketing, energy/capacity PPA, time-of-use PPA, block-delivery PPA, and tolling agreements—only two of these are directly relevant for standalone LDES. Time-of-use and block-delivery PPAs are excluded in this context because they require coordinated scheduling with a co-located variable generation resource to meet fixed delivery profiles. Since the present analysis focuses solely on standalone storage, these arrangements are not applicable. Similarly, energy/capacity PPAs for storage essentially converge to tolling constructs, where the offtaker compensates based on capacity and availability. To avoid redundancy, these are treated as equivalent to tolling agreements and are not analyzed separately. Accordingly, two offtake structures are considered most relevant for standalone LDES: energy marketing and tolling agreements.

- **Economic/Financial Parameter Set (k):** Each scenario is associated with a set of economic/financial parameters that define the investment environment, operational costs, and long-term cash flows of the storage project. These assumptions provide the basis for post-simulation benefit-cost analysis, enabling evaluation of financial performance across different configurations. Key parameters in this set include:
  - Capital expenditure (CAPEX)
  - Operating expenditure (OPEX)
  - End-of-life (EOL) costs
  - Discount rate
  - Project lifetime
  - Investment tax credit (ITC)

  Together, these parameters allow systematic evaluation of how capital costs, operational expenses, financial incentives, and financing assumptions affect the long-term economic viability of the energy storage system.

Each scenario is uniquely indexed by the tuple (i, j, k) and simulated independently. The outcomes are then collected and analyzed to facilitate comparative assessment of operational performance and financial viability across all scenario configurations.

4.3 Performance and Economic Evaluation Metrics

The evaluation of each scenario combines operational and financial performance indicators to provide a holistic assessment of the storage system. Operational metrics quantify how the system performs in energy throughput and utilization, while economic metrics assess the long-term investment viability of each configuration. These metrics are derived from the simulation outputs and post-processed to account for both annual performance and project lifetime considerations.

4.3.1 Annual Operational Metrics

Annual operational metrics provide insight into the physical performance and utilization patterns of the storage system over a typical year. These include:

- **Annual Revenue ($):** Total income generated by the storage system from energy sales, capacity payments, or contractual agreements. Revenue is calculated as the sum of energy discharged to the grid multiplied by corresponding electricity prices for each hour:

$$R_{\text{annual}} = \sum_{t=1}^{T} \pi_t^{\text{sell}} \cdot P_t^{\text{dis}} \cdot \Delta t \tag{4.5}$$

  where π_t^{sell} is the selling price of electricity at hour t, P_t^{dis} is the discharging power (MW), and $\Delta t = 1$ hour.

- **Charging Cost ($):** Total expenditure associated with charging the storage system, accounting for electricity procurement costs:

$$C_{\text{charge}} = \sum_{t=1}^{T} \pi_t^{\text{buy}} \cdot P_t^{\text{ch}} \cdot \Delta t \tag{4.6}$$

  where π_t^{buy} is the electricity price of hour t, and P_t^{ch} is the charging power (MW).

- **Total Discharged Energy (MWh):** Cumulative energy delivered over the year:

$$E_{\text{dis}} = \sum_{t=1}^{T} P_t^{\text{dis}} \cdot \Delta t \tag{4.7}$$

- **Total Charging Hours (h):** Number of hours during which the system is actively charging, which reflects the utilization and cycling pattern:

$$H_{\text{charge}} = \sum_{t=1}^{T} \mathbb{1}(P_t^{\text{ch}} > 0) \tag{4.8}$$

  where $\mathbb{1}(\cdot)$ is the indicator function.

4.3.2 Economic Performance Indicators

Economic metrics evaluate the long-term financial performance of storage projects, taking into account capital costs, operational expenses, revenue streams, and project lifetime. The following metrics are computed using discounted cash flow analysis over the assumed project lifetime N years, using discount rate r.

- **Net Present Value (NPV):** NPV represents the present value of net benefits (revenue minus costs) over the project lifetime:

$$\text{NPV} = -C_{\text{capex}} + \sum_{y=1}^{N} \frac{B_y - C_y}{(1+r)^y} - \frac{C_{\text{eol}}}{(1+r)^N} \tag{4.9}$$

  where C_{capex} is the upfront capital cost, B_y is the annual revenue, C_y is the annual O&M plus charging cost, and C_{eol} is the end-of-life cost.

- **Benefit-Cost Ratio (BCR):** BCR evaluates the efficiency of investment by comparing discounted benefits to discounted costs:

$$\text{BCR} = \frac{\sum_{y=1}^{N} \frac{B_y}{(1+r)^y}}{C_{\text{capex}} + \sum_{y=1}^{N} \frac{C_y}{(1+r)^y} + \frac{C_{\text{eol}}}{(1+r)^N}} \tag{4.10}$$

- **Internal Rate of Return (IRR):** IRR is the discount rate r^* at which NPV becomes zero, representing the effective annualized return of the project:

$$0 = -C_{\text{capex}} + \sum_{y=1}^{N} \frac{B_y - C_y}{(1+r^*)^y} - \frac{C_{\text{eol}}}{(1+r^*)^N} \tag{4.11}$$

- **Discounted Payback Period (years):** It represents the minimum number of years Y required for the cumulative discounted net benefits to offset the initial capital investment:

$$\sum_{y=1}^{Y} \frac{B_y - C_y}{(1+r)^y} \geq C_{\text{capex}} \tag{4.12}$$

- **Levelized Cost of Storage (LCOS):** LCOS represents the effective cost per unit of energy discharged, accounting for capital, O&M, charging costs, and end-of-life costs, discounted over the project lifetime:

$$\text{LCOS} = \frac{C_{\text{capex}} + \sum_{y=1}^{N} \frac{C_y}{(1+r)^y} + \frac{C_{\text{eol}}}{(1+r)^N}}{\sum_{y=1}^{N} \frac{E_{\text{dis},y}}{(1+r)^y}} \tag{4.13}$$

  where $E_{\text{dis},y}$ is the discharged energy during year y.

4.4 Assessment Results

This section presents the LDES TEA assessment results through structured case studies. The analysis is organized into two parts. The first presents a high-level, technology-agnostic assessment, examining how factors such as technology costs and offtake structures (e.g., energy marketing versus tolling agreements) influence a range of economic and financial performance metrics. The second provides a detailed assessment using ARES as an example, where multiple sizing configurations and potential incentives are systematically explored. Together, these complementary perspectives provide valuable insights: the first highlights broad sensitivities and key drivers relevant to LDES technologies in general, while the second offers a focused evaluation of ARES across diverse sizing options, market structures, and potential incentive scenarios.

4.4.1 High-Level Technology-Agnostic Assessment

This subsection presents a set of simplified, technology-neutral case studies designed to illustrate how cost assumptions and offtake agreement structures influence key financial performance metrics. We consider a 50 MW/10-hour LDES system with a round-trip efficiency (RTE) of 75%, a project lifetime of 20 years, annual O&M costs equal to 0.5% of CAPEX, and end-of-life recycling costs of $1 million.

In practice, storage technologies differ widely in their technical parameters and expected lifetimes. For example, lithium-ion BESS may last 10–15 years, while gravity-based systems may operate for 30–50 years or more. Such variations complicate direct comparisons across technologies. To maintain clarity, we adopt a uniform 20-year project horizon, with assumed installed cost values that can be interpreted flexibly depending on the technology. For shorter-lived systems, the assumed cost may reflect vendor-supported capacity maintenance over 20 years (through augmentation, oversizing, or partial replacement) or an implicit mid-life replacement. For longer-lived systems, it can be interpreted as a net cost after accounting for residual value at year 20. This approach simplifies the comparison while preserving economic relevance.

An RTE of 75% is assumed as a representative value across technologies. While actual efficiencies vary—lithium-ion systems may reach 85-90% whereas other technologies, such as some thermo-mechanical or flow systems, may fall in the 60–75% range, using a common midpoint avoids bias toward any one technology and keeps the focus on financial structures rather than technical details.

The remaining assumptions, such as fixed O&M and end-of-life recycling costs, are likewise applied in a uniform and simplified manner. These values are not meant to reflect technology-specific details but to provide a consistent baseline for highlighting the influence of cost structures and offtake arrangements.

A 5% discount rate is applied to account for the time value of money when evaluating NPV and other financial metrics. Six scenarios are designed and evaluated to capture

the effect of offtake structures and capital cost assumptions. Three CAPEX values are considered: low ($300/kWh), medium ($400/kWh), and high ($500/kWh).

- Energy Marketing: Historical hourly energy prices from the Mid-C trading hub for 2023 are used to estimate potential arbitrage revenue, and capacity payments are assumed to be $10/kW-month.
- Tolling Agreement: A tolling fee of $30/kW-month and an energy throughput fee of $20/MWh are assumed.

Table 4.1. TEA results for high-level technology-agnostic scenarios

Offtake Option	CAPEX	Ann. Rev. ($M)	Ann. Chrg. Hrs.	Ann. Disch. Energy (GWh)	Chrg. Cost ($M)	NPV ($M)	IRR (%)	BCR	Payback Period (years)	LCOS (¢/kWh)
Energy Marketing	Low	$14	2447	89	$5	-$34	1.8	0.75	None	19
	Medium	$14	2447	89	$5	-$85	-1.3	0.54	None	24
	High	$14	2447	89	$5	-$136	-3.6	0.42	None	29
Tolling Agreement	Low	$21	N/A	174	N/A	$108	13.1	1.78	9	7
	Medium	$21	N/A	174	N/A	$57	8.4	1.31	14	10
	High	$21	N/A	174	N/A	$7	5.3	1.03	20	12

Table 4.1 shows the TEA results for the above six generic case study scenarios. The results and observations are discussed below:

- Tolling Agreements Outperform Energy Marketing: Across all CAPEX levels, the tolling agreement scenarios achieve a BCR greater than 1, indicating economic viability. Even for the highest CAPEX ($500/kWh), the project remains financially feasible under tolling arrangements. In contrast, energy marketing scenarios consistently produce BCR values below 1, reflecting the combined impact of market price variability and limited arbitrage opportunities. This suggests that standalone energy storage relying solely on energy and capacity market revenues may struggle to achieve profitability under current conditions.
- CAPEX Sensitivity: For both offtake options, higher CAPEX results in worse financial performance. Lower CAPEX ($300/kWh) produces the highest BCR values, reaching approximately 1.78 for the tolling agreement, while the high CAPEX scenario

($500/kWh) significantly reduces economic attractiveness. This highlights the importance of capital cost control in ensuring financial viability for LDES projects.

- Implications: The results demonstrate that contractual structure and cost assumptions are critical determinants of financial performance. Tolling agreements provide a more predictable and robust revenue stream for standalone storage systems, making them a promising option when market-based energy revenues are insufficient. Energy marketing remains sensitive to both CAPEX and market conditions, which may limit its attractiveness in isolation for certain project configurations.

4.4.2 In-Depth Assessment of ARES

To systematically assess the techno-economic performance of different sizing candidates for ARES, a comprehensive sensitivity analysis was conducted across three key dimensions: system sizing, offtake arrangements, and economic/financial assumptions. This structured approach enables a clear understanding of how each factor affects both operational outcomes and long-term financial viability, while also capturing the interplay between design choices and market structures.

- The first dimension of the sensitivity analysis focused on sizing candidates, capturing variations in energy and power capacity to reflect both practical deployment limits and technology-specific characteristics. Five candidate configurations were selected to reflect realistic deployment scales:
  - EN 1 (50 MW / 15-hour),
  - EN 2 (75 MW / 13-hour),
  - EN 3 (30 MW / 8.1-hour),
  - EN 4 (100 MW / 13.1-hour), and
  - EN 5 (25 MW / 11-hour).

  These options span a broad range of discharge durations and power ratings, providing insight into how scale and duration influence economic competitiveness under different offtake arrangements. The estimated RTE of the ARES system is 81% across all sizing candidates.

- The second dimension explored two offtake structures—energy marketing and tolling agreements—to evaluate how different revenue structures influence project economics. The assumptions and parameters used for each offtake structure are discussed below.
  - **Energy Marketing:** In this option, dispatch is actively optimized to maximize revenue from energy arbitrage and capacity markets. Historical hourly energy prices from Mid-C for 2023 are used to estimate arbitrage potential. Capacity payments are assumed to be $10/kW-month for a 10-hour duration system, scaled proportionally for other storage sizes.

  - **Tolling Agreement:** Under a tolling agreement, the storage owner is compensated based on energy throughput and pre-negotiated tolling rates. However, due to the limited number of projects using this model and the lack of standardized data, there is significant uncertainty in determining appropriate tolling rates. To capture this uncertainty, the analysis considers both conservative and optimistic assumptions. In the conservative case, a 10-hour storage system is assumed to receive $30/kW-month, while the optimistic case assumes $45/kW-month, with both scaled for other durations. In addition, a throughput fee of $20 per MWh cycled through the system is applied.

- The third dimension examined variations in economic/financial parameters, such as discount rates, capital expenditure assumptions, and operational costs, representing diverse financing conditions and levels of market maturity. Key parameters used in the in-depth assessment of ARES are:
  - CAPEX: The base CAPEX for the storage system is assumed to be $350/kWh for an 8-hour discharge duration. CAPEX is reduced by $5/kWh for each additional hour of discharge duration, reflecting potential economies of scale for larger storage capacities.
  - OPEX: Annual OPEX is set at 0.5% of CAPEX. In addition, a major mid-life maintenance event is assumed, with a cost of 9.5% of CAPEX, expressed in present value terms.
  - EOL costs: Decommissioning and residual costs at the end of the project's life are assumed to be $500,000, accounting for dismantling, disposal, and any site restoration requirements.
  - Discount rate: A 5% discount rate is applied to account for the time value of money when evaluating NPV and other financial metrics.
  - Project lifetime: The storage project is assumed to operate for 40 years, covering its full economic lifecycle and allowing assessment of long-term profitability under different operational and contractual scenarios.
  - ITC: Two cases are considered: no ITC and 30% ITC. This allows analysis of how government incentives influence overall project economics and investment attractiveness.

By integrating the three key dimensions of analysis—system sizing, offtake structure, and financial assumptions—the study framework yields a total of 30 distinct scenarios. These scenarios are organized as follows:

- 10 energy marketing scenarios, covering five sizing candidates under both economic/financial parameter sets (with and without ITC).

- 10 tolling agreement scenarios under conservative assumption, again evaluated across the same five sizing candidates and two economic/financial parameter sets.

- 10 tolling agreement scenarios under optimistic assumption, following the same structure.

Each scenario represents a unique case study that combines sizing, offtake arrangement, and financial assumptions. This design ensures coverage of a wide spectrum of potential market and financial environments while retaining comparability across cases.

Figure 4.1 provides a comparative overview of financial performance by presenting BCR and LCOS across all scenarios. Tables 4.2– 4.4 summarize TEA results for all 30 scenarios, detailing the configuration, offtake arrangement, and financial assumptions for each case. The results indicate that scenario outcomes are strongly influenced by the interplay between storage sizing and offtake structures. The key results and observations are discussed as follows.

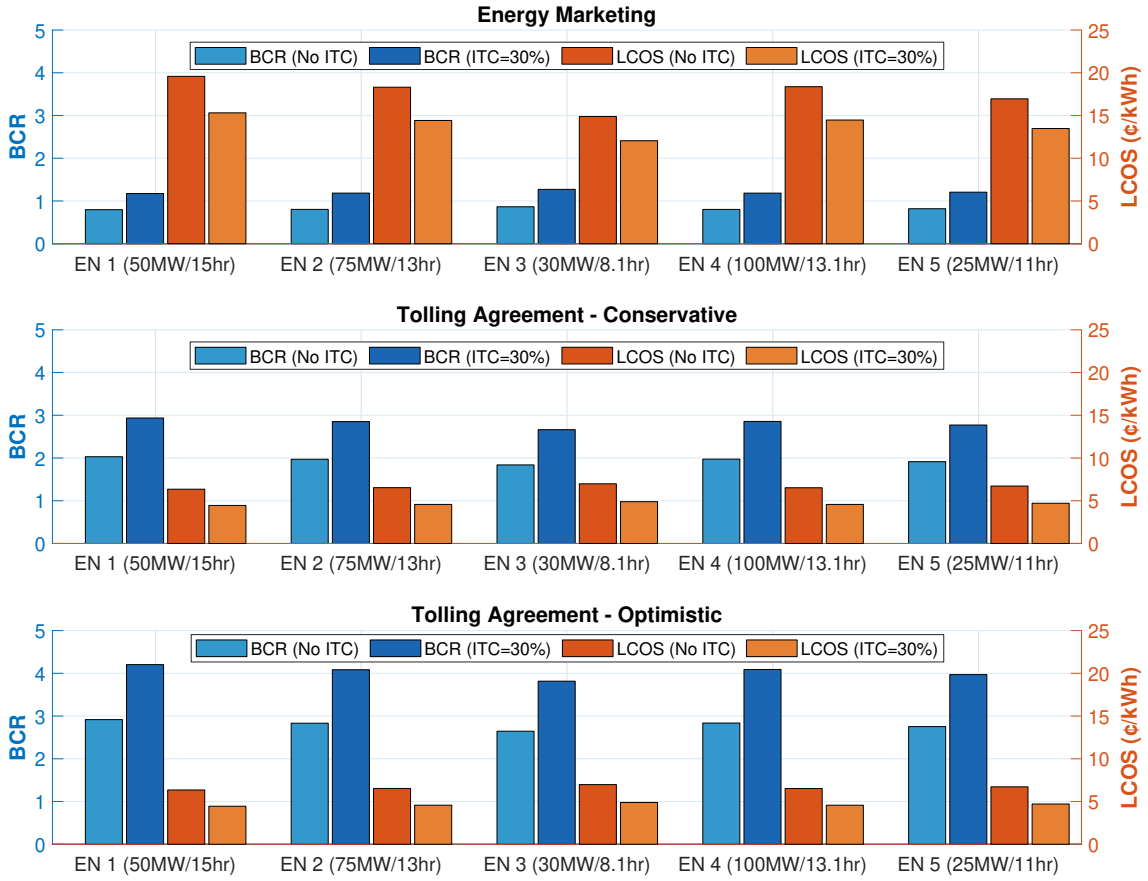

Figure 4.1. Comparison of BCR and LCOS under different offtake options for ARES system

Table 4.2. TEA results for ARES system with energy marketing

Sizing Cand.	Finan. Param. Set	Ann. Rev. ($M)	Ann. Chrg. Hrs.	Ann. Disch. (GWh)	Chrg. Cost ($M)	NPV ($M)	IRR (%)	BCR	Payback Period (years)	LCOS (¢/kWh)
EN 1	No ITC	$20	2932	116	$6	-$51	3.4	0.80	None	20
50MW/15hr	ITC = 30%	$20	2932	116	$6	$30	6.2	1.17	27	15
EN 2	No ITC	$27	2888	171	$9	-$65	3.5	0.80	None	18
75MW/13hr	ITC = 30%	$27	2888	171	$9	$43	6.3	1.18	27	14
EN 3	No ITC	$9	2648	62	$3	-$12	4.0	0.86	None	15
30MW/8.1hr	ITC = 30%	$9	2648	62	$3	$17	6.9	1.27	23	12
EN 4	No ITC	$36	2891	228	$12	-$88	3.5	0.80	None	18
100MW/13.1hr	ITC = 30%	$36	2891	228	$12	$57	6.3	1.18	27	14
EN 5	No ITC	$8	2828	56	$3	-$18	3.6	0.82	None	17
25MW/11hr	ITC = 30%	$8	2828	56	$3	$14	6.5	1.21	26	13

Table 4.3. TEA results for ARES system with conservative tolling agreement

Sizing Cand.	Finan. Param. Set	Ann. Rev. ($M)	Ann. Chrg. Hrs.	Ann. Disch. (GWh)	Chrg. Cost ($M)	NPV ($M)	IRR (%)	BCR	Payback Period (years)	LCOS (¢/kWh)
EN 1	No ITC	$32	N/A	260	N/A	$256	11.7	2.03	12	6
50MW/15hr	ITC = 30%	$32	N/A	260	N/A	$337	17.1	2.94	8	4
EN 2	No ITC	$42	N/A	338	N/A	$323	11.3	1.97	12	7
75MW/13hr	ITC = 30%	$42	N/A	338	N/A	$431	16.6	2.85	8	5
EN 3	No ITC	$10	N/A	84	N/A	$74	10.5	1.84	13	7
30MW/8.1hr	ITC = 30%	$10	N/A	84	N/A	$103	15.5	2.66	8	5
EN 4	No ITC	$56	N/A	455	N/A	$435	11.4	1.97	12	7
100MW/13.1hr	ITC = 30%	$56	N/A	455	N/A	$580	16.6	2.86	8	5
EN 5	No ITC	$12	N/A	95	N/A	$88	11.0	1.91	13	7
25MW/11hr	ITC = 30%	$12	N/A	95	N/A	$120	16.1	2.77	8	5

Table 4.4. TEA results for ARES system with optimistic tolling agreement

Sizing Cand.	Finan. Param. Set	Ann. Rev. ($M)	Ann. Chrg. Hrs.	Ann. Disch. (GWh)	Chrg. Cost ($M)	NPV ($M)	IRR (%)	BCR	Payback Period (years)	LCOS (¢/kWh)
EN 1	No ITC	$46	N/A	260	N/A	$477	17.0	2.92	8	6
50MW/15hr	ITC = 30%	$46	N/A	260	N/A	$558	24.5	4.20	5	4
EN 2	No ITC	$59	N/A	338	N/A	$610	16.5	2.83	8	7
75MW/13hr	ITC = 30%	$59	N/A	338	N/A	$718	23.8	4.08	5	5
EN 3	No ITC	$15	N/A	84	N/A	$146	15.4	2.65	9	7
30MW/8.1hr	ITC = 30%	$15	N/A	84	N/A	$175	22.2	3.82	6	5
EN 4	No ITC	$80	N/A	455	N/A	$820	16.5	2.84	8	7
100MW/13.1hr	ITC = 30%	$80	N/A	455	N/A	$965	23.8	4.09	5	5
EN 5	No ITC	$17	N/A	95	N/A	$169	16.0	2.75	8	7
25MW/11hr	ITC = 30%	$17	N/A	95	N/A	$200	23.1	3.97	5	5

- For energy marketing, EN 3 (30 MW / 8.1-hour), the configuration with the shortest duration, demonstrates the best overall economic performance. The relatively low capital cost of the sizing candidate and favorable balance between energy throughput and market price variability contribute to higher IRR and BCR values.
- Conversely, under tolling agreements, scenarios with longer-duration storage, such as EN 1 (50 MW / 15-hour), achieve better performance because payments are tied to the capacity and discharge duration, directly rewarding larger energy capacities.
- Among the 30 scenarios, EN 1 under optimistic tolling agreement with ITC exhibits the highest BCR and lowest LCOS, highlighting the significant impact of favorable contractual and financial incentives. The BCR of 4.203 and LCOS of 4.45 ¢/kWh in this scenario underscore the potential for high financial returns when long-duration storage is paired with optimistic contract structures and favorable financial support.

In summary, the case studies demonstrates that standalone LDES systems can achieve robust economic performance, but optimal sizing and careful selection of contractual structures are critical. Energy marketing favors smaller, more agile systems capable of capturing price fluctuations, whereas tolling agreements reward larger-duration storage with sustained capacity. The sensitivity analysis provides a detailed understanding of how design and market choices influence operational efficiency and financial viability.

CHAPTER 5

SCADA and Transmission Interconnection Considerations

This chapter analyzes SCADA and transmission interconnection requirements for deploying an LDES system at the 9C site. Two primary options are considered: (1) utilizing and adapting the existing SCADA and interconnection infrastructure, and (2) developing a new, dedicated SCADA and interconnection pathway for LDES. In both cases, the LDES facility is assumed to be charged with power supplied by the electrical grid from the BPA transmission system. The findings will guide the deployment strategy to ensure seamless operation, reliability, and regulatory compliance.

The existing and future SCADA system includes, but may not be limited to, the existing controllers and inverter/converter systems; LDES controllers and inverter/converter systems, remote-interface units; meteorological sensors; substation equipment; fault and protection systems; communication cabling; communication network; communication protocol(s); plant grid interface inverter/converter systems and any associated supplemental compensation systems; and SCADA server including database and historian.

The current SCADA system is specified as per Figures 5.1 and 5.2. As is common in the industry, 9C's SCADA is built out of DAQ Electronics and Schweitzer Engineering Laboratories (SEL) components.

5.1 SCADA and Control System Considerations

The proposed LDES system will require SCADA and control systems that comply with evolving grid performance standards. Over the past decade, reliability events involving inverter-based resources (IBRs) have revealed vulnerabilities in how such resources respond to normally cleared grid faults, underscoring the need for more rigorous performance standards and operating requirements (NERC, 2025a,c). In response, the Federal Energy Regulatory Commission (FERC) has issued new orders on IBR performance (e.g., Orders 901, 2023, etc.), and North American Electric Reliability Corporation (NERC) is working to update existing standards and likewise create new standards, such as in the protection and control (PRC) series: PRC-024, -028, -029, -030, etc.

These regulatory developments are directly relevant to the LDES project, and the system to be deployed should be planned with the latest requirements in mind. Deci-

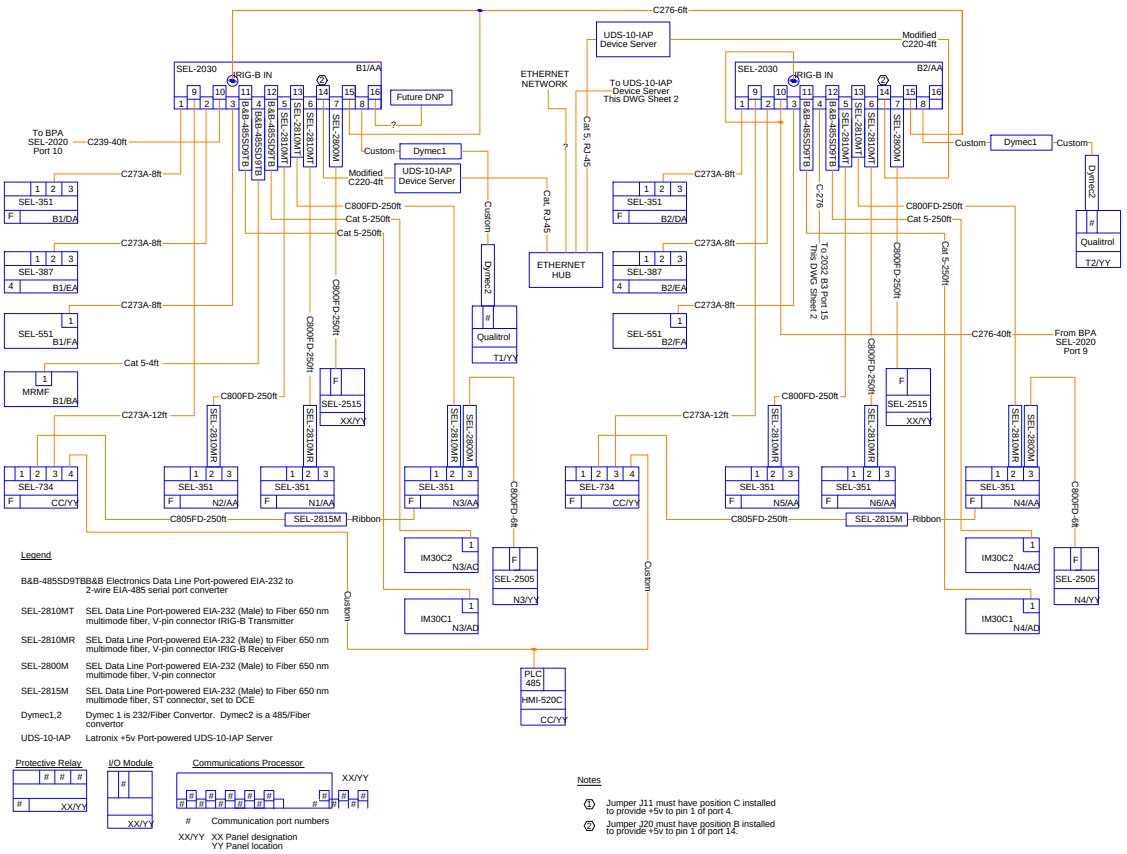

Figure 5.1. 9C's SCADA system - Part I

sions about configuring its SCADA/controls, or designing a dedicated solution, ought to consider these evolving standards. Updated IBR requirements are expected to guide baseline specifications for SCADA, communication, protection, and control to support compliance, interoperability, and long-term reliability.

Our analysis incorporates the most recent requirements, with IEEE 2800-2022 serving as the foundation for baseline SCADA considerations. IEEE 2800-2022, *IEEE Standard for Interconnection and Interoperability of IBRs Interconnecting with Associated Transmission Electric Power Systems* (IEEE, 2022), also illustrated in Figure 5.3, establishes a comprehensive technical framework for IBR performance that has gained broad stakeholder consensus and now informs ongoing NERC standards development. The BPA, as the transmission system operator, has also recently indicated they are seeking to adopt IEEE 2800 and have already included some IEEE 2800 elements in their latest interconnection code (BPA, 2024, 2025c,b).

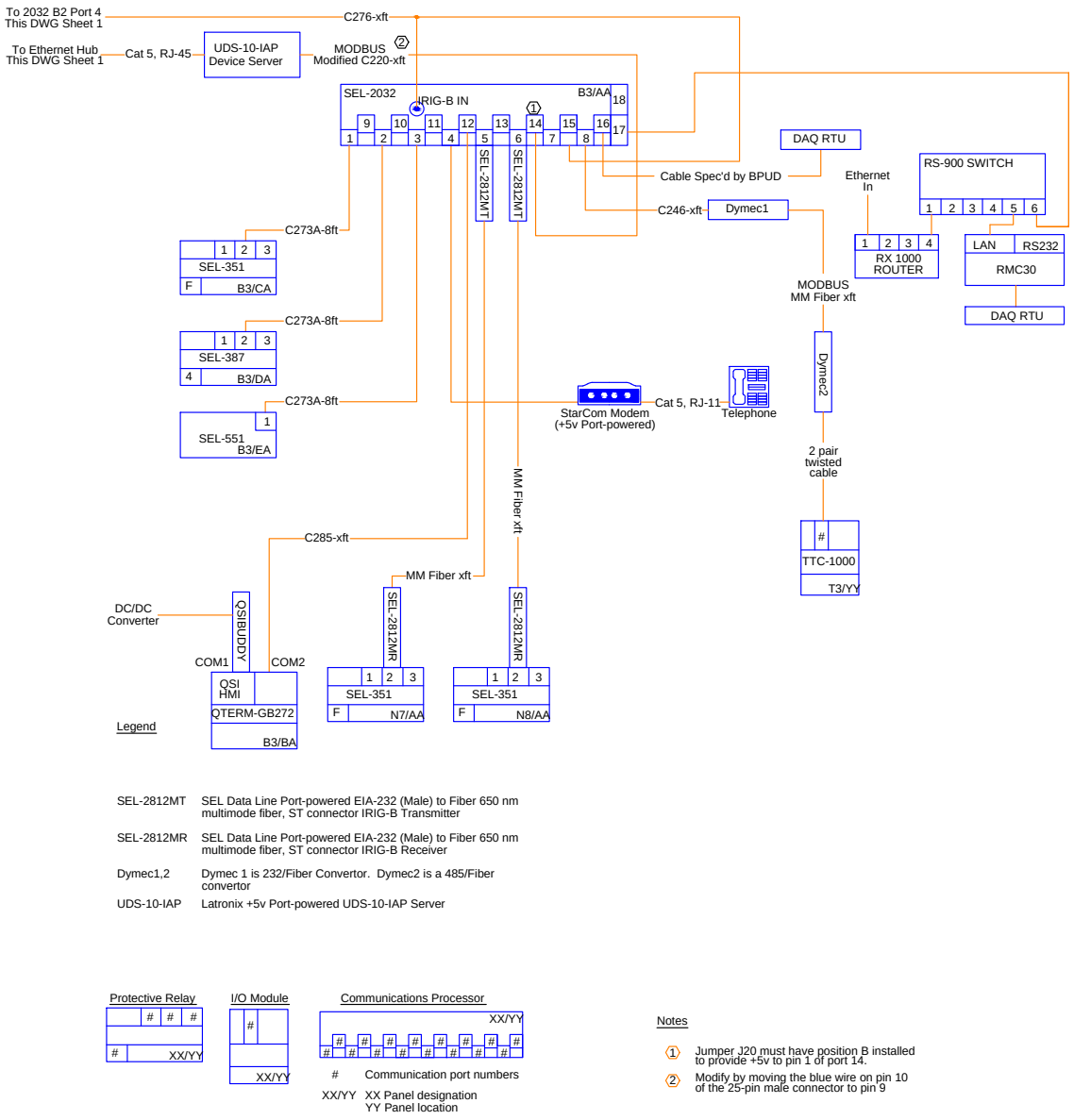

Figure 5.2. 9C's SCADA system - Part II

5.1.1 Control System Requirements for LDES

The deployment of LDES requires control systems capable of supporting reliable operation, regulatory compliance, and interoperability with BPA's SCADA and market platforms. Two approaches are considered: (1) leveraging and upgrading the existing control and

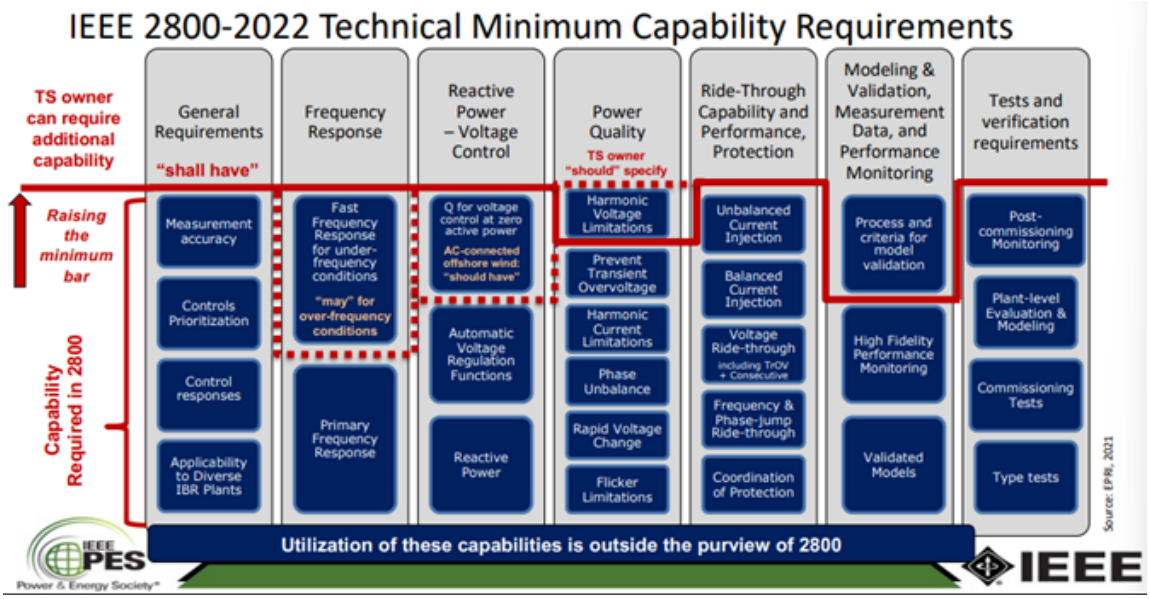

Figure 5.3. IEEE 2800 minimum technology capability requirements

SCADA infrastructure at the site, or (2) developing a new, dedicated control and SCADA system designed specifically for LDES.

- **Option 1 – Leveraging Existing SCADA and Controls** This option would involve adapting the current SCADA and communication systems to accommodate LDES operations. Key considerations include compatibility of existing hardware and software, adequacy of communication protocols, and the ability to expand functionality for monitoring LDES-specific parameters such as state of charge, inverter performance, and fault management. While potentially more cost-effective, this option may be limited by the early-2000s design philosophy of the existing infrastructure.

- **Option 2 – Developing a New SCADA and Control System** A new, stand-alone system would be purpose-built for LDES, providing maximum flexibility to meet modern standards and future requirements. This option would allow full alignment with IEEE 2800 standards and BPA interconnection requirements, reduce risks of integration with legacy systems, and ensure that LDES-specific functions are incorporated from the outset. However, it would require a higher capital investment.

5.1.1.1 Real-Time Monitoring

Regardless of the option selected, advanced monitoring capabilities are required to ensure safe and efficient LDES operation:

- State of charge and health management, including fault detection and maintenance status.
- Power management, encompassing regulation of output, ramping, and other grid-support functions.
- Performance diagnostics and alerts, supporting predictive maintenance and rapid response.

5.1.1.2 Data Exchange Requirements

Both options must ensure robust data exchange with supervisory systems to satisfy BPA requirements:

- Remote control and monitoring through SCADA RTUs, with polling intervals of approximately two seconds as defined by BPA.
- Telemetry for energy flows, system health, and protection functions.
- Support for existing communication protocols (e.g., Modbus RTU, SEL serial, DNP3) or equivalent modern protocols if a new system is deployed.

5.1.1.3 Compliance with IEEE 2800 Standards

To support IBR operation in either mode, the LDES must meet IEEE 2800 requirements:

- Fault ride-through and controlled return-to-service following tripping.
- Reactive power control and voltage regulation, including at zero active power output.
- Active frequency control and fast frequency response for grid stability.
- Capability to operate in low short-circuit strength conditions.
- Support for ancillary services such as balancing, oscillation damping, and blackstart restoration.

5.1.1.4 BPA SCADA Data Requirements

Compliance with BPA's SCADA requirements is necessary:

- Alignment with BPA's interconnection technical requirements, including monitoring, control, and telemetry functions.

Table 1010.— Generation Data Requirements for VERs, New Technologies and Batteries

Generation Plant to BPA Control Center(s):	
1.	Net instantaneous power output (MW) (BPA meter point)
2.	Net instantaneous MVAR output (BPA meter point)
3.	Instantaneous MVAR output of each collector line
4.	Instantaneous MW output of each collector line
5.	Instantaneous MVAR output of each reactive element (dynamic and switched)
6.	Voltage of each bus (kV) High side and each collector bus
7.	Available generation capability (MW) [1]
8.	Plant operation limit (MW) [2]
9.	Estimated Total MW Output (MW) [4]
10.	Plant high speed cutout (MW – wind only) (sum of all units out due to high winds)
11.	Automatic voltage control status (on/off), each controller
12.	Automatic voltage mode status (voltage/power factor), each controller
13.	Total plant MVAR capacity boost (MVAR) [3]
14.	Total plant MVAR capacity buck (MVAR) [3]
15.	Status of each generation and reactive element Breaker or switcher
16.	Status of each high side Breaker between generation and BPA system
17.	Acknowledge Limit Generation to Schedule
18.	Status of inverters blocking real/reactive power output (solar, batteries & type 3 or type 4 wind)
19.	Max/min calculated frequency by the inverters (Hz; solar & batteries)
20.	Max/min temperature of the inverters (ºF; solar & batteries)
21.	Status of grid island detection by the inverters (solar & batteries)
22.	State of charge/discharge for batteries
23.	Status of availability to generate for batteries
24.	Charge of batteries (MWh)
25.	Frequency Response provided by Generator (Calculated; MW)

Figure 5.4. BPA's SCADA data requirements—generation plant to BPA control centers

- Capability to manage reactive voltage control and LDES-specific parameters such as state of charge, thermal/fault conditions, and inverter operations.
- Figures 5.4 and 5.5 summarize BPA's SCADA data requirements relevant to LDES integration.

5.1.2 SCADA Upgrade vs. Standalone LDES Control System

As briefly discussed in Section 5.1.1, there are two approaches for implementing control and monitoring of the LDES at the 9C site: (1) upgrading the existing SCADA infrastructure, or (2) deploying a standalone control system dedicated to LDES. Each approach has distinct advantages and limitations. Choosing between a SCADA upgrade and a standalone LDES control system involves trade-offs between integration, scalability, and operational flexibility. A SCADA upgrade provides centralized control but may be constrained

Table 1111.— Generation Control and Data Requirements for VERs and Batteries

BPA Control Center(s) to Generation Plant:	
1.	Low Reserves Notification
2.	Limit Generation to Schedule– command (limit level 1, 2, etc.)
3.	Limit Generation to Schedule- MW Target amount
4.	Bus voltage schedule(s) in kV (future requirement for secondary voltage control)
5.	Dispatch trip control – to the agreed upon generation breaker
6.	Ramp limit initiated (Batteries Only)
7.	Frequency controller Dispatch initiated (future)

Figure 5.5. BPA's SCADA data requirements—BPA control centers to generation plant

by legacy hardware and limited expansion capacity, whereas a standalone system offers autonomy and flexibility but may require additional infrastructure and coordination efforts for grid integration. The two options are briefly discussed below.

5.1.2.1 Option 1: SCADA System Upgrade

Upgrading the existing DAQ Electronics Callisto SCADA system allows LDES to be integrated into the current site operations. This approach would involve:

- Expanding existing hardware and software to incorporate real-time LDES monitoring and control.
- Modifying database structures to accommodate new data types, including state of charge, energy flows, and fault conditions.
- Leveraging existing communication protocols and SCADA Masters to maintain centralized oversight.

This approach streamlines operator workflows but faces limitations. The current hardware is approaching the end of its expected life, and the system was originally designed for early-2000s operations, limiting its scalability. Additionally, the substation lacks spare feeder positions and distribution bays, restricting expansion capacity. Extending existing circuits would provide only limited charging capacity during high production periods and impose rate limits on discharging. Any SCADA upgrade must therefore consider not only functional enhancements but also potential hardware replacement or platform migration. Transitioning to a modern platform from a vendor with significant market share could offer benefits such as improved workforce support, reduced supply chain complexity, and access to advanced SCADA features, including enhanced data historian capabilities.

5.1.2.2 Option 2: Standalone LDES Control System

An alternative approach is to implement an independent control system dedicated to LDES operation. This option provides flexibility and does not rely on the existing SCADA system, enabling:

- Full autonomous operation of the LDES system, including charging, discharging, and state-of-charge management.
- Easier adoption of advanced control strategies and communication protocols without constraints imposed by legacy SCADA architecture.
- Simplified deployment for future expansions or relocations of energy storage assets, independent of existing generation infrastructure limitations.

The standalone approach may reduce the need for immediate SCADA upgrades but could require additional operator training and separate monitoring infrastructure. Integration with the broader grid and participation in ISO/RTO markets would need careful design to ensure coordination between the independent LDES system and existing generation operations.

5.1.3 Communication Protocols and Cybersecurity Considerations

The limited use of ethernet-based communication protocols in the existing system design reduces the attack surface and minimizes the need for advanced management systems. Industry trends, however, increasingly favor protocols like DNP3 and IEC 61850. Implementing new protection and SCADA systems with a Zero Trust Architecture and a Deny by Default ethernet network, alongside device and user management services, will enable secure utilization of enhanced ethernet-based SCADA devices.

As outlined in BPA's interconnection requirements, the Inter-Control Center Communication Protocol (ICCP) serves as the standard for real-time data exchange. Defined by the IEC 870-6 TASE.2 standard, ICCP protocols are regularly updated, requiring retrofitting of current and future SCADA ICCP servers when new protocol versions are released. Additional protocols such as IEEE 1815 (DNP3) or IEEE 2030.5 may also be applicable, depending on the transmission owner/operator specifications. Early engagement with BPA on communication protocol requirements is advisable, especially as certain U.S. regions (e.g., California) now mandate IEEE 2030.5 for distributed energy resource integration into utility systems, discontinuing support for protocols like IEEE 1815 or Modbus.

Regarding cybersecurity, the existing 9C facility already complies with NERC Critical Infrastructure Protection (CIP) standards for low-impact resources (aggregate capacity $\geq$ 75 MVA and connected at $\geq$ 100 kV). The addition of LDES systems would need to

maintain these standards until aggregate capacity reaches 1,500 MVA. These minimum, low-impact resource CIP requirements include:

- Cybersecurity policies and procedures
- Physical security measures
- Personnel training and awareness
- Incident response and recovery plans
- Reporting of certain events and compliance documentation

Medium-impact resource CIP requirements require all low impact controls plus enhanced access controls, real-time cyber monitoring and alerting, and additional requirements. For details on CIP and other NERC standards, their One-Stop-Shop spreadsheet provides links to standards, adoption / implementation status, implementation plans, project pages, Reliability Standards Audit Worksheets, FERC Orders, and compliance guidance (NERC, 2025b).

5.2 Transmission Interconnection Options

The current interconnection agreement was signed in the early 2000's before a significant number of FERC initiatives and interconnection reforms. Notably, FERC established the Large Generator Interconnection Agreement (LGIA), which includes several key components directly relevant to the deployment of an LDES at the 9C site. Because the 9C interconnection agreement (IA) was signed prior to the adoption of the pro-forma LGIA and subsequent FERC reforms, knowing how today's requirements differ and what triggers a need for a new or amended agreement is critical for evaluating new interconnection options. For example, a deployment of LDES would likely be deemed a "qualified change" and therefore may require the IA to be updated to align to current LGIA requirements. The following are, therefore, key components of the present day LGIA:

- Standardized Interconnection Process
  - The LGIA is part of a standardized process (LGIP/LGIA) applicable to all large generators (over 20 MW) connecting to the transmission grid.
  - The agreement is incorporated into every transmission provider's Open Access Transmission Tariff (OATT), ensuring comparability and transparency.

- Interconnection Request and Queue Management
  - Entry into the interconnection queue now requires: Financial deposits and demonstration of site control to ensure only viable projects proceed. A cluster study process: Multiple projects are studied together to improve efficiency and cost allocation, as opposed to the former serial, project-by-project studies.

  - Firm deadlines for study completion are imposed on transmission providers, with penalties for delays to enhance accountability and reduce queue backlogs.

- Types of Interconnection Service: The LGIA distinguishes between:
  - Energy Resource Interconnection Service (ERIS): Allows delivery of energy on an as-available basis.
  - Network Resource Interconnection Service (NRIS): Allows the facility to be designated as a network resource and participate in network integration transmission service.

- Modifications and Materiality
  - Any material modification (such as increasing plant capacity, changing turbine type, or adding storage) typically requires a new interconnection request or a significant amendment, triggering new studies and possibly new network upgrade requirements.
  - The threshold for what constitutes a "material modification" can vary by region and is subject to case-by-case review, but adding storage is likely to be considered material.

- Incorporation of Technological Advancements
  - The LGIA now explicitly accommodates energy storage resources:
    - Storage can be co-located with generation behind a single point of interconnection and included in a single interconnection request.
    - The agreement requires study assumptions to reflect the charging and discharging behavior of storage resources.
    - Storage is recognized as a "generating facility," affording it the same rights and obligations as traditional generation.
  - The LGIA also supports alternative transmission technologies and sets performance standards for IBRs.

- Surplus Interconnection Service
  - Provisions exist for utilizing surplus interconnection capacity—if the maximum output does not fully utilize its interconnection rights, storage or additional generation can be added up to the original interconnection limit without triggering a full restudy, subject to transmission provider review.

- Reliability and Performance Standards
  - Modern LGIAs require compliance with updated reliability standards, such as Low Voltage Ride-Through (LVRT) and power factor requirements, which may not have been present in 2002 agreements.

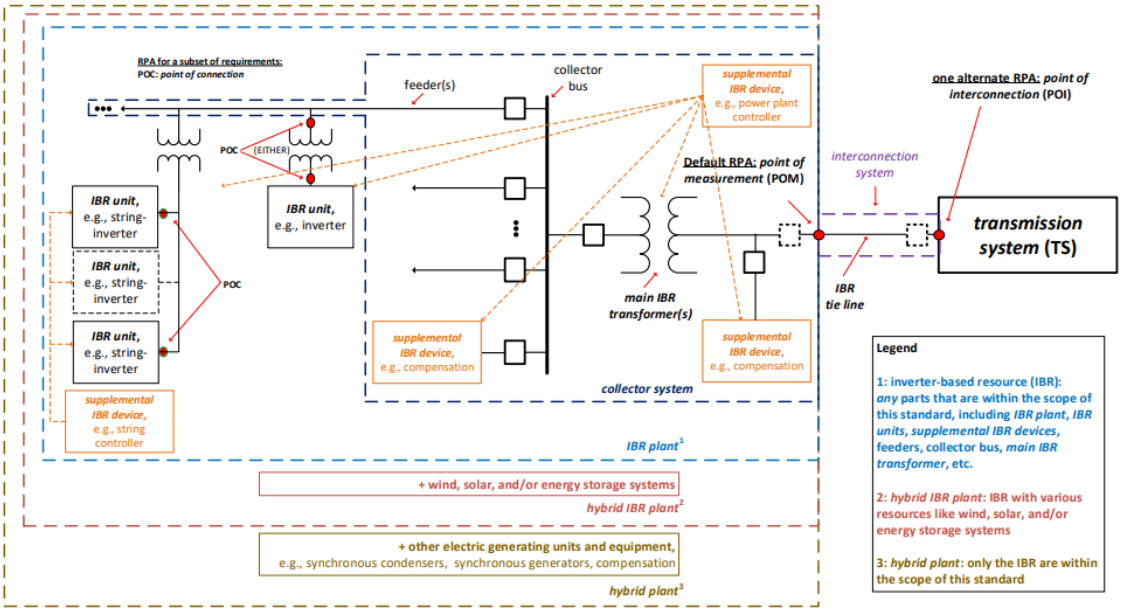

Figure 5.6. Diagram showing IBR plant, IBR units, and optional supplemental systems

  - Any new or upgraded facility must meet current technical and operational standards, which may require equipment upgrades.

- Affected Systems and Coordination
  - The LGIA mandates coordination with affected systems (neighboring transmission providers) and includes uniform modeling standards and pro forma affected system agreements to address broader grid impacts.

As mentioned prior, upgrading the facility and/or adding an energy storage system may necessitate compliance with IEEE 2800 performance requirements. Within IEEE 2800, the location where interconnection and interoperability performance requirements apply is the reference point of applicability (RPA), as shown in Figure 5.6. For the IBR plant, a default RPA is the common point of measurement on the high-side of the main IBR plant transformer, but also noted on the diagram is an alternate RPA at the point of interconnection further up the transmission system beyond the IBR plant's boundary.

In practice for 9C, as the interconnecting transmission system owner/operator, BPA may adopt some or all IEEE 2800 performance requirements and move the RPA to another location, including the point of interconnection. Applicable voltage and applicable frequency are therefore measured at the RPA as defined by BPA. For instance, low/high voltage ride-through, transient over-voltage, and rate of change of frequency (ROCOF) ride-through are all measured at the RPA relative to the nominal voltage and frequency

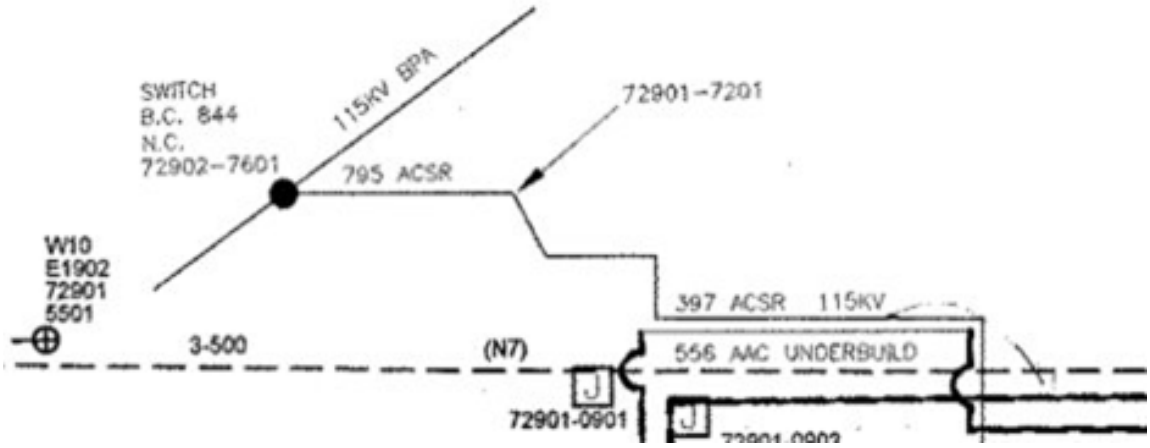

Figure 5.7. Overview of the current transmission system at the 9C site

that BPA would specify. Additionally, some IBR plants may require supplemental equipment to compensate for voltage and frequency capabilities at the RPA. Early engagement with BPA may be necessary to address performance requirements, particularly if new equipment such as voltage and frequency compensation devices are triggered by the addition of energy storage. Similarly, RPA location and performance standards will significantly influence whether the energy storage system shares the same interconnection as the existing facility or pursues an independent interconnection arrangement with BPA.

5.2.1 Existing Transmission Infrastructure

The 9C site is interconnected at 115 kV to BPA's transmission system, stepping down to 34.5 kV via three feeder bays as illustrated in Figure 5.7. The facility operates under a legacy Control Area Services Agreement (CASA), executed prior to the establishment of standardized FERC interconnection procedures. The CASA outlines requirements for maintaining system reliability through reference to the Reliability Coordinator's standards. Additionally, two agreements between BPA and Benton PUD—a construction agreement and an operations and maintenance agreement—govern aspects of the facility's operation. Review of these agreements is recommended before undertaking upgrades or adding an LDES system to evaluate potential modifications or replacements.

Transmission capacity, congestion, and stability are key considerations for future upgrades. Should a qualified change be pursued—by adding LDES—BPA will perform interconnection studies to assess the capability of the existing transmission system to accommodate increased generation or storage output. Existing interconnection requests

in the vicinity of 9C may further constrain available capacity, potentially limiting options for LDES deployment while maintaining full capacity operation (Figures 5.8–5.11).

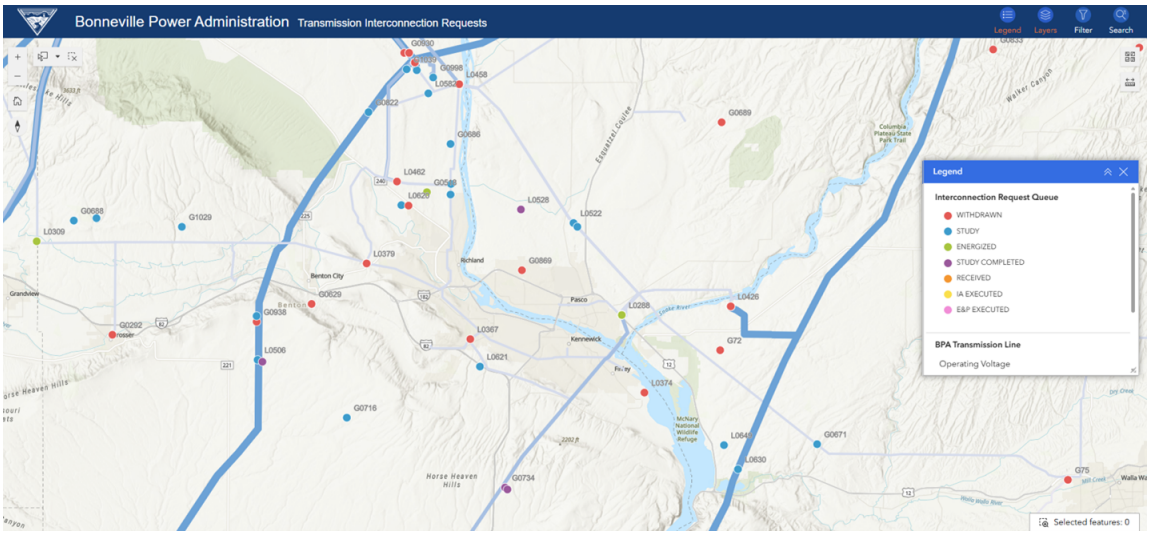

Figure 5.8. Snapshot of BPA's transmission interconnection queue requests in region

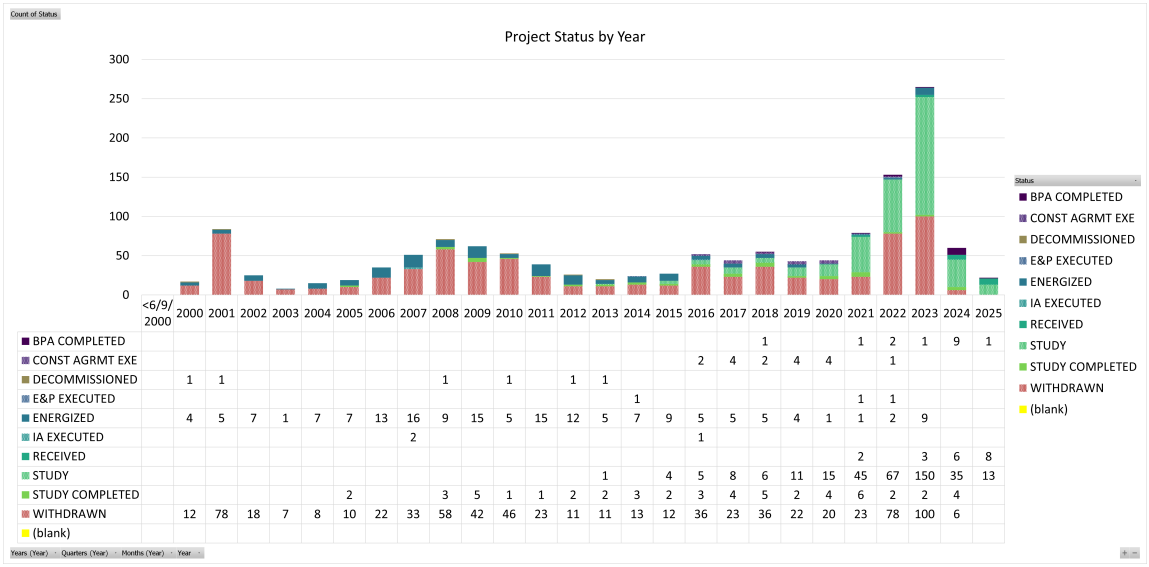

	<6/9/2000	2000	2001	2002	2003	2004	2005	2006	2007	2008	2009	2010	2011	2012	2013	2014	2015	2016	2017	2018	2019	2020	2021	2022	2023	2024	2025
BPA COMPLETED																				1			1	2	1	9	1
CONST AGRMT EXE																		2	4	2	4	4		1			
DECOMMISSIONED		1	1							1		1		1	1												
E&P EXECUTED																1							1	1			
ENERGIZED		4	5	7	1	7	7	13	16	9	15	5	15	12	5	7	9	5	5	5	4	1	1	2	9		
IA EXECUTED									2									1									
RECEIVED																							2		3	6	8
STUDY															1		4	5	8	6	11	15	45	67	150	35	13
STUDY COMPLETED							2			3	5	1	1	2	2	3	2	3	4	5	2	4	6	2	2	4	
WITHDRAWN		12	78	18	7	8	10	22	33	58	42	46	23	11	11	13	12	36	23	36	22	20	23	78	100	6	
(blank)																											

Figure 5.9. BPA's interconnection queue - project status by project year

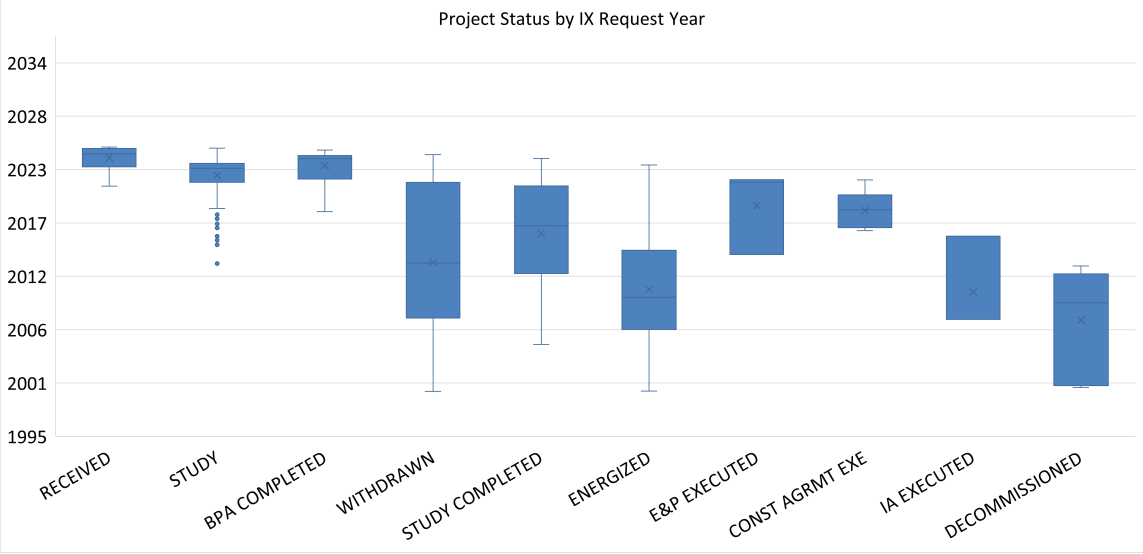

Figure 5.10. BPA's interconnection queue - project status by project year (box plot view)

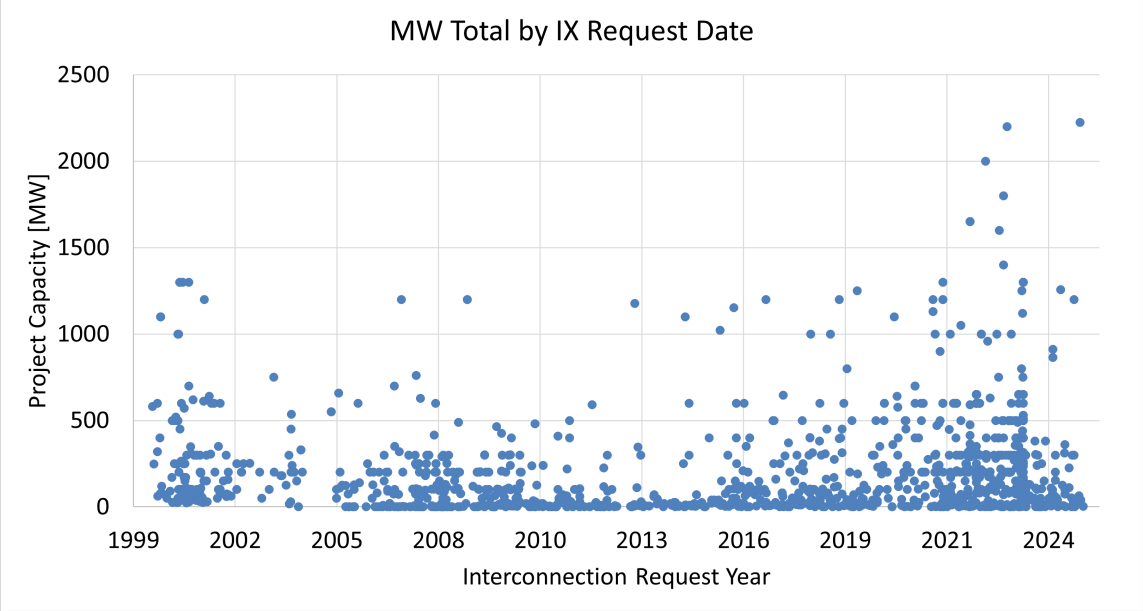

Figure 5.11. BPA's interconnection queue - project capacity by project year

5.2.2 Interconnection Process and Qualified Changes

BPA maintains a long interconnection queue, and applicants for new generation have experienced steadily increasing wait times. No new interconnection applicant has completed the study process and executed an agreement since 2017. The current process is described in the Large Generator Interconnection: BPA Transmission Business Practice (BPA, 2025a), though updates in compliance with FERC Order 2023 are pending.

The addition of an LDES system at the 9C site would likely constitute a qualified change, requiring compliance with updated interconnection requirements, including alignment with IEEE 2800 performance standards. Qualified changes may necessitate:

- A system impact study to evaluate effects on the transmission system.
- A facilities study to determine interconnection costs.
- Execution of a final interconnection agreement before commercial operation.

According to BPA guidance and NERC FAC-002-4 Requirement 6 (R6), facility owners must notify BPA of any qualified changes and meet all applicable interconnection requirements. BPA reviews the proposed changes and determines specific interconnection obligations, with a response within five business days to schedule discussions.

The LDES system may require a separate interconnection agreement, even if it shares the same point of interconnection as the existing 9C site. The final interconnection study will include a complete system impact assessment, a facilities study with costs determined by BPA, and execution of a binding interconnection agreement before commercial operation.

BPA is implementing a cluster study process under FERC Order 2023. It remains uncertain whether qualified changes to existing interconnected projects will be included in cluster studies or processed independently. Historical precedent shows that requests for modifications or upgrades to existing interconnections are limited but actionable: since 2019, five such requests have been submitted in BPA's queue, including three in study, one energized, and one withdrawn (Table 5.1).

Table 5.1. Pending interconnection requests in BPA queue

Year	Point Of Inter-connection	Status	State	County	Requested In-Service Date	Max Summer MW
2025	Jones Canyon Substation at 230 kV	STUDY	OR	Gillman	6/30/2027	111
2023	Rock Creek Substation	WITHDRAWN	WA	Klickitat	9/1/2025	150
2023	Jones Canyon Substation	STUDY	OR	Gilliam	9/2/2025	91
2022	John Day–Klondike Schoolhouse 230 kV No 1 Line	STUDY	OR	Sherman	12/16/2024	25
2019	BPA's John Day 230 kV	ENERGIZED	OR	Sherman	12/31/2020	6

CHAPTER 6

Conclusions

This report provided a comprehensive assessment of LDES options for potential deployment at the 9C site. The analysis integrates technical, economic, and system integration considerations to evaluate the viability of an independent LDES asset under a range of scenarios. As part of this effort, a generalized TEA framework was developed. The framework is technology-neutral and designed to evaluate storage systems based on input parameters such as power and energy capacity, round-trip efficiency, capital and operational costs, dispatchability, and lifetime. It enables scenario-based analysis to support decision-making on system sizing, economic performance, and operational strategies. The tool is intended to be broadly applicable for utilities considering storage investments under diverse conditions and business models.

The study conducted a literature survey and comparative assessment of four LDES technologies: lithium-ion batteries, flow batteries, non-hydro gravity storage, and thermo-mechanical energy storage. Each technology was assessed in terms of technical performance, economic outcomes, safety profile, material sourcing, and spatial requirements. These comparisons provide insight into the relative strengths and limitations of different technologies, highlighting their suitability under specific siting and operational conditions. In addition to the technology assessment, the study examined ownership structures and offtake agreement models. Ownership pathways considered included EN ownership, third-party ownership, and shared models. Offtake options included energy marketing, PPAs, and tolling arrangements, which were incorporated into the TEA as key scenario dimensions. The study also assessed system integration aspects, including SCADA and transmission interconnection requirements. The presence of existing site infrastructure—such as the substation and the interconnection agreement with BPA—presents potential advantages for deploying LDES at the 9C site. Nonetheless, coordination with grid operators and targeted control system upgrades will be essential to ensure reliable and effective operation.

The TEA results underscore the decisive role of offtake structure. Across multiple scenarios, tolling agreements consistently outperformed energy marketing by providing stable and predictable revenues. Energy marketing under current Mid-C market conditions yielded negative value in all cases, even at lower capital costs, while tolling maintained positive economics with benefit-cost ratios above 1. Sensitivity analysis further showed that financial performance decreases as CAPEX rises, but tolling arrangements

buffer this risk more effectively than energy marketing.

An in-depth assessment of ARES expanded these findings by testing multiple system sizes, financing conditions, and contract terms. Results confirmed that tolling agreements—especially when combined with financial incentives such as ITC—deliver superior financial performance. Optimistic tolling assumptions paired with ITC support produced highly attractive outcomes, including BCR values above 4 and LCOS below 5 ¢/kWh. Importantly, the analysis highlighted that no single driver—technology, contract, or financial—guarantees success. Instead, project viability depends on aligning system sizing, contractual structures, and financial conditions to reinforce one another. Together, these insights suggest that successful LDES deployment at 9C will depend on negotiating robust offtake agreements, pursuing opportunities for cost reduction and financial support, and selecting technologies that align with site-specific characteristics.

CHAPTER 7

References

Aluko, A. and A. Knight 2023. A review on vanadium redox flow battery storage systems for large-scale power systems application. *IEEE Access 11*, 13773–13793.

Baxter, R. 2019. Energy storage financing: Advancing contracting in energy storage. *SAND2019-12793). Albuquerque, NM and Livermore, CA: Sandia National Laboratories*.

BE&R 2023. Vanadium flow batteries revolutionise energy storage in Australia. https://berconsulting.com.au/2023/11/07/vanadium-flow-batteries-revolutionise-energy-storage-in-australia/. Accessed: 2025-03-06.

BPA 2024. Bonneville power administration voltage control strategies. Presented at DOE's Forum for the Implementation of Reliability Standards for Transmission (i2X FIRST), December 17, 2024.

BPA 2025a. BPA transmission business practice: Large generator interconnection. Referenced in BPA Interconnection Process.

BPA 2025b. Metering application guide for BPA transmission interconnection. Referenced in BPA Interconnection Standards.

BPA 2025c. Technical requirements for interconnection to the BPA transmission grid. Revision STD-N-000001 - Rev 09; Revision Date: April 3, 2025.

Chen, T., Y. Jin, H. Lv, A. Yang, M. Liu, B. Chen, Y. Xie, and Q. Chen 2020. Applications of lithium-ion batteries in grid-scale energy storage systems. *Transactions of Tianjin University 26*(3), 208–217.

Doetsch, C. and J. Burfeind 2022. Vanadium redox flow batteries. In *Storing energy*, pp. 363–381. Elsevier.

EverythingPE 2023. What is a Lithium-ion battery? https://www.everythingpe.com/community/what-is-a-lithium-ion-battery. Accessed: 2025-03-06.

Huang, Y. and J. Li 2022. Key challenges for grid-scale lithium-ion battery energy storage. *Advanced Energy Materials 12*(48), 2202197.

IEEE 2022. Ieee std 2800-2022: Interconnection standard for large-scale solar, wind, and energy storage. Accessed on July 20, 2025.

Li, F.-F., J.-Z. Xie, Y.-F. Fan, and J. Qiu 2024. Potential of different forms of gravity energy storage. *Sustainable Energy Technologies and Assessments 64*, 103728.

Li, X., D. Lepour, F. Heymann, and F. Maréchal 2023. Electrification and digitalization effects on sectoral energy demand and consumption: A prospective study towards 2050. *Energy 279*, 127992.

NERC 2025a. Essential actions to industry: Inverter-based resource performance and modeling. Issued May 20, 2025.

NERC 2025b. One-stop-shop. Technical report, North American Electric Reliability Corporatipn.

NERC 2025c. IBR registration initiative Q1 update. Relevant to IBR standards and reliability certification.

Pacific Northwest National Laboratory 2023. Energy Storage Cost and Performance Database. https://www.pnnl.gov/ESGC-cost-performance. Accessed: 2024-08-30.

Paiss, M. 2017. Energy storage system safety: Comparing vanadium redox flow and lithium-ion based systems. *Energy Response Solutions*.

Pathak, M. 2024. sCO2-based thermo-mechanical energy storage. https://www.sandia.gov/app/uploads/sites/82/2024/08/PR2024_203_Pathak_Manas_MLDES.pdf. Accessed: 2025-03-06.

Peters, J. F. and M. Weil 2016. A critical assessment of the resource depletion potential of current and future lithium-ion batteries. *Resources 5*(4), 46.

Rodby, K. E., R. L. Jaffe, E. A. Olivetti, and F. R. Brushett 2023. Materials availability and supply chain considerations for vanadium in grid-scale redox flow batteries. *Journal of Power Sources 560*, 232605.

Shan, R., J. Reagan, S. Castellanos, S. Kurtz, and N. Kittner 2022. Evaluating emerging long-duration energy storage technologies. *Renewable and Sustainable Energy Reviews 159*, 112240.

Soloveichik, G. L. 2015. Flow batteries: current status and trends. *Chemical reviews 115*(20), 11533–11558.

Trott, H. 2024. Rail-based gravity storage - the advantages of pumped hydro without the disadvantages. https://www.sandia.gov/app/uploads/sites/82/2024/08/PR2024_205_Trott_Howard_MLDES.pdf. Accessed: 2025-03-06.

U.S. Department of Energy 2020. Energy Storage Grand Challenge Roadmap. https://www.energy.gov/energy-storage-grand-challenge/articles/energy-storage-grand-challenge-roadmap. Accessed: 2025-03-28.

U.S. Department of Energy 2023. Pathways to Commercial Liftoff: Long Duration Energy Storage. https://www.sandia.gov/app/uploads/sites/256/2023/09/Pathways-to-Commercial-Liftoff-LDES-May-5_UPDATED.pdf. Accessed: 2025-03-28.

Weber, S., J. F. Peters, M. Baumann, and M. Weil 2018. Life cycle assessment of a vanadium redox flow battery. *Environmental science & technology 52*(18), 10864–10873.

Wei, X., W. Pan, W. Duan, A. Hollas, Z. Yang, B. Li, Z. Nie, J. Liu, D. Reed, W. Wang, et al. 2017. Materials and systems for organic redox flow batteries: status and challenges. *ACS Energy Letters 2*(9), 2187–2204.

Whitehead, A., T. Rabbow, M. Trampert, and P. Pokorny 2017. Critical safety features of the vanadium redox flow battery. *Journal of Power Sources 351*, 1–7.

Wu, D. and X. Ma 2021. Modeling and optimization methods for controlling and sizing grid-connected energy storage: A review. *Current Sustainable/Renewable Energy Reports 8*, 123–130.

Yuan, X.-Z., C. Song, A. Platt, N. Zhao, H. Wang, H. Li, K. Fatih, and D. Jang 2019. A review of all-vanadium redox flow battery durability: Degradation mechanisms and mitigation strategies. *International Journal of Energy Research 43*(13), 6599–6638.

Appendix A – ARES Geotechnical and Hydrological Study

This appendix section presents a site-specific study on the feasibility of deploying ARES at the 9C site. The assessment includes slope suitability and inclination constraints, geotechnical feasibility, and hydrological feasibility studies required for successful deployment. The goal is to evaluate the suitability of the site, identify key infrastructural needs, and assess potential operational impacts.

A.1 Maximum Slope Incline Consideration

A.1.1 DEM Processing for Slope Analysis

To assess the slope characteristics of the proposed site footprints, a high-resolution 1-meter Digital Elevation Model (DEM) was processed using ESRI ArcGIS Pro 3.4.0 (Python 3). The DEM data were obtained from the USGS National Map (originally collected in 2018–2019).[1] A slope raster was generated using the `Slope` tool in the Spatial Analyst toolbox, which calculates the maximum rate of elevation change (i.e., gradient or steepness) between each DEM cell and its eight surrounding neighbors. The resulting slope values are expressed in degrees. Figure A.1 presents the clipped DEM (terrain elevation) and the corresponding slope raster, with borehole locations used in the geotechnical analysis shown for reference.

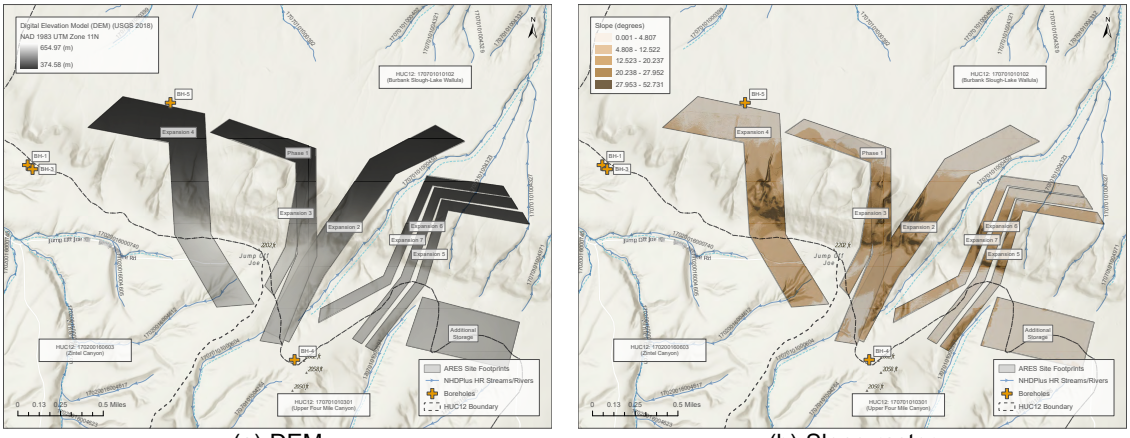

(a) DEM (b) Slope raster

Figure A.1. Site DEM and derived slope raster showing terrain elevation and slope distribution across proposed development footprints.

Following preprocessing in ArcGIS Pro, the DEM and corresponding slope rasters were clipped to the spatial extent of the inclined track segments within each site footprint

[1] https://apps.nationalmap.gov/viewer/

(e.g., EN 1–7). These clipped raster datasets were subsequently used for visualization, terrain analysis, and longitudinal profile computations in Python 3. A custom Python script was developed to generate 3D terrain surface plots, elevation profiles along the primary slope direction, and slope distribution histograms for each inclined track segment. An overview of slope classifications across the inclined track segments is shown in Figure A.2.

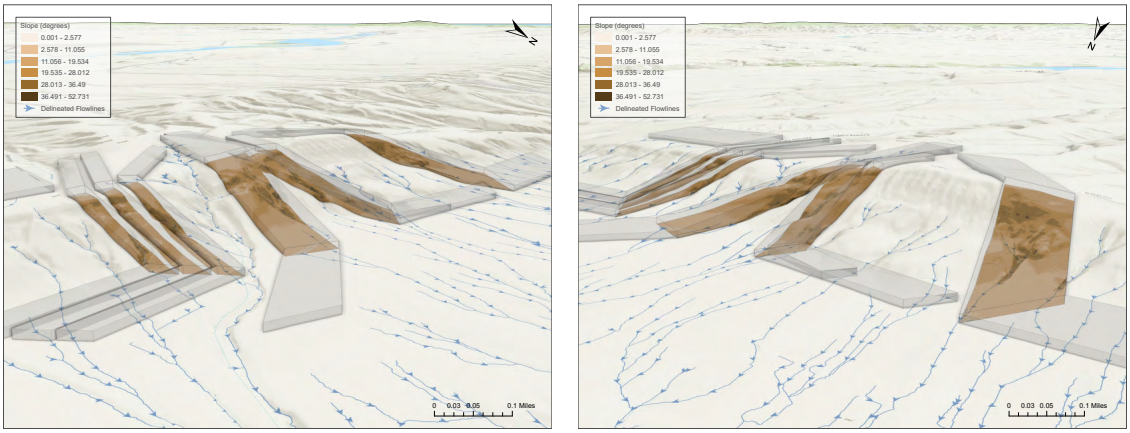

(a) Inclined footprint tracks with slope (NE view) (b) Inclined footprint tracks with slope (NW view)

Figure A.2. 3D visualization of slope classifications along the inclined track segments of proposed development footprints.

For each footprint, the script generated a 3D terrain surface with slope classifications, calculated a longitudinal elevation profile along the direction of greatest terrain extent (viewed from east to west), and produced a slope distribution histogram. The profile analysis determined the total rise and run of the terrain and computed the overall slope. Additionally, the elevation profile was compared against a straight-line baseline to estimate potential cut and fill areas, offering insight into the earthwork requirements. Slope statistics—including minimum, maximum, and mean values—were also calculated at the raster cell level across each footprint segment. These outputs are illustrated in Figures A.3-A.9.

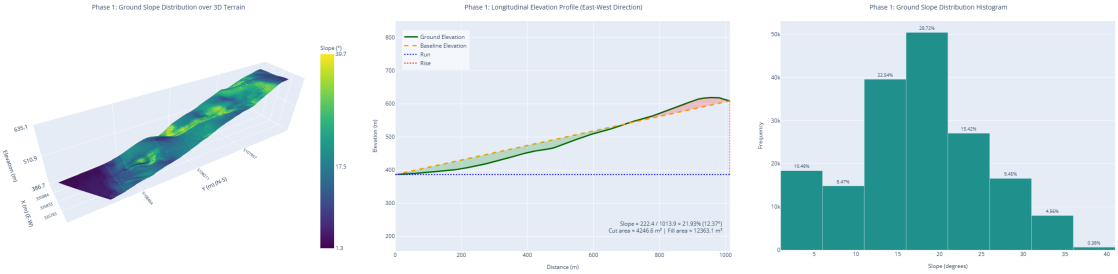

(a) 3D terrain view (b) Longitudinal elevation profile (c) Slope distribution histogram

Figure A.3. Terrain and slope visualizations for the EN 1 inclined track segment.

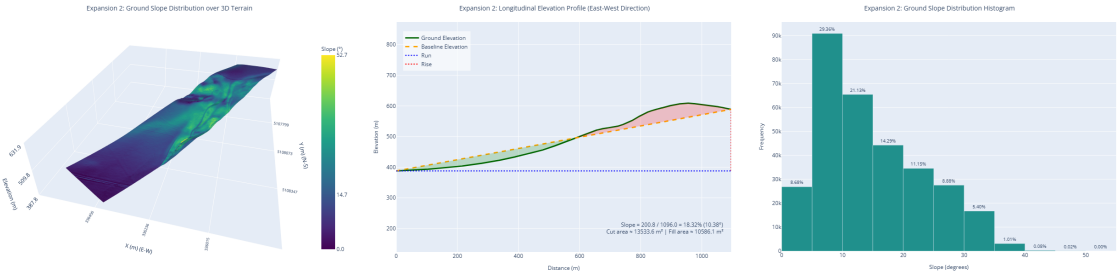

(a) 3D terrain view (b) Longitudinal elevation profile (c) Slope distribution histogram

Figure A.4. Terrain and slope visualizations for the EN 2 inclined track segment.

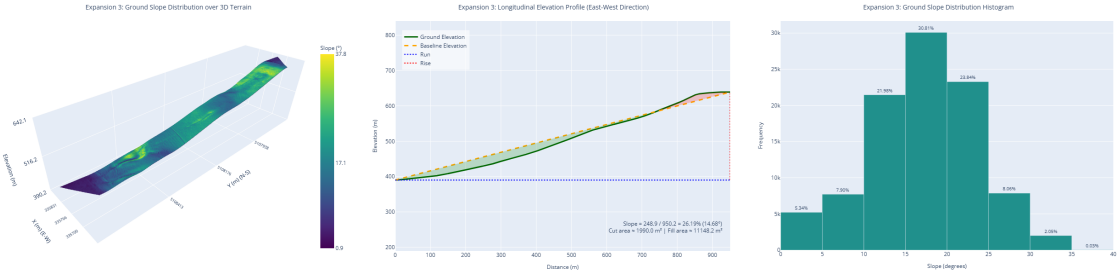

(a) 3D terrain view (b) Longitudinal elevation profile (c) Slope distribution histogram

Figure A.5. Terrain and slope visualizations for the EN 3 inclined track segment.

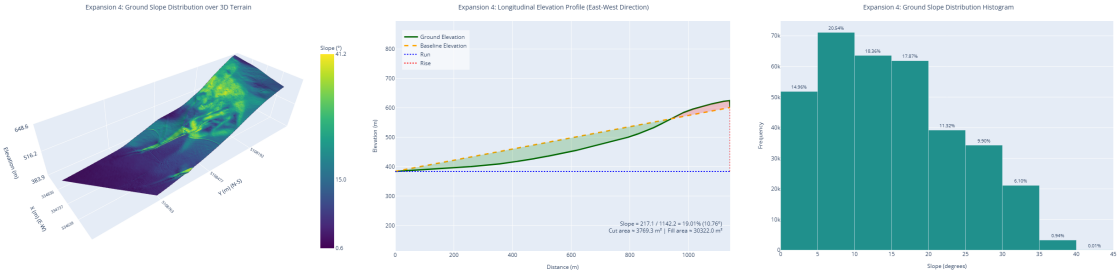

(a) 3D terrain view (b) Longitudinal elevation profile (c) Slope distribution histogram

Figure A.6. Terrain and slope visualizations for the EN 4 inclined track segment.

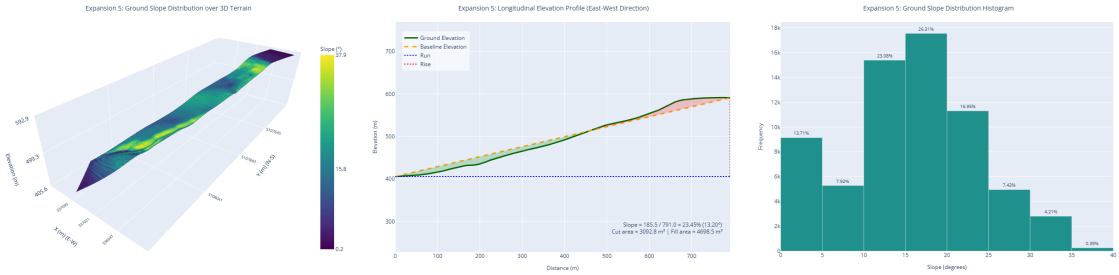

(a) 3D terrain view (b) Longitudinal elevation profile (c) Slope distribution histogram

Figure A.7. Terrain and slope visualizations for the EN 5 inclined track segment.

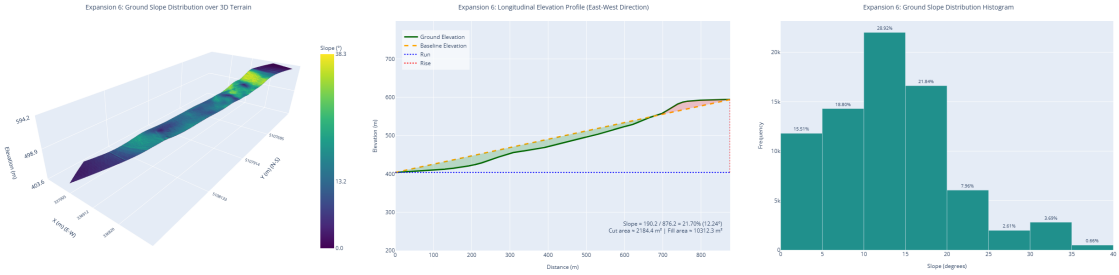

(a) 3D terrain view (b) Longitudinal elevation profile (c) Slope distribution histogram

Figure A.8. Terrain and slope visualizations for the EN 6 inclined track segment.

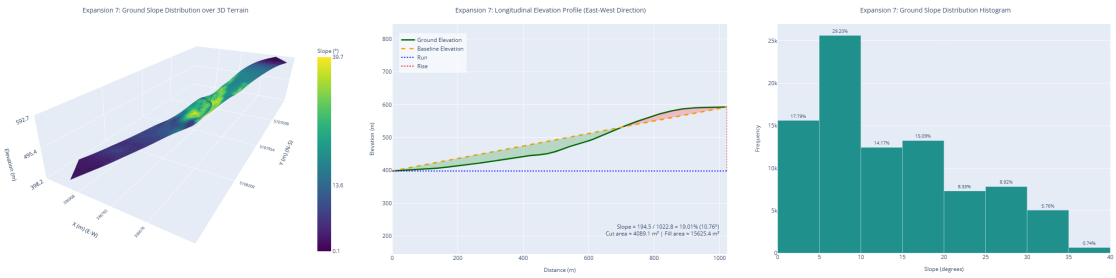

(a) 3D terrain view (b) Longitudinal elevation profile (c) Slope distribution histogram

Figure A.9. Terrain and slope visualizations for the EN 7 inclined track segment.

A.1.2 Slope Ranking for Site Feasibility

Slope plays a pivotal role in evaluating the feasibility of each proposed site footprint for a gravity rail energy storage system. While pixel-level slope statistics—derived from the 1-meter DEM raster—capture localized variations in terrain steepness (e.g., small ridges or depressions), the longitudinal baseline slope, calculated along the primary alignment direction (viewed from east to west), offers a more practical metric for assessing grading requirements, alignment feasibility, and operational energy demands.

Table A.1 presents both pixel-based slope metrics (maximum, minimum, and average) and longitudinal alignment parameters (rise, run, and slope angle), along with estimated earthwork volumes (cut and fill areas per unit width in the east–west direction).

Among the candidate sites:

- **EN 1** shows a moderate **average pixel slope** of 17.5°and a **longitudinal slope** of 12.4°, suggesting balanced terrain with moderate grading and earthwork requirements.
- **EN 2** features the steepest **maximum pixel slope** (52.7°), indicating sharp localized inclines. However, its longitudinal slope (10.4°) is relatively moderate, suggesting manageable alignment challenges with more substantial cut volumes.
- **EN 3** has the steepest **longitudinal slope** (14.7°), which may increase construction complexity, system braking energy demands, and grading effort. Its average pixel slope is also high at 17.1°.
- **EN 4**, while moderate in longitudinal slope (10.8°), is **fill-dominated**, requiring over 30,000 m^2 of fill area (per unit width). This suggests significant earth import and terrain modification needs.
- **EN 5** combines a relatively steep **longitudinal slope** of 13.2°and a high **average pixel slope** (15.8°), but requires relatively less fill volume compared to EN 4, which may benefit construction staging.
- **EN 6** presents a favorable terrain profile, with a baseline slope of 12.2°, modest cut and fill requirements, and the lowest **average pixel slope** (13.2°) among the main

site segments.

- **EN 7** is similar to EN 6 in average and longitudinal slope (13.6°and 10.8°, respectively), but with slightly higher fill needs, making it a viable option from a terrain-grading perspective.

Table A.1. Slope statistics and earthwork estimates for each site footprint based on 1 m × 1 m DEM terrain.

Footprint	Slope (1 m DEM)			Baseline Gradient			Earthwork Estimates		
	Max. (°)	Min. (°)	Avg. (°)	Rise (m)	Run (m)	Slope (°)	Cut Area (m^2)	Fill Area (m^2)	Width (m)
EN 1	39.7	1.3	17.5	222.4	1013.9	12.4	4246.6	12363.1	174.3
EN 2	52.7	0.0	14.7	200.8	1096.0	10.4	13533.6	10586.1	284.0
EN 3	37.8	0.9	17.1	248.9	950.2	14.7	1990.0	11148.2	103.6
EN 4	41.2	0.6	15.0	217.1	1142.2	10.8	3769.3	30322.0	305.5
EN 5	37.9	0.2	15.8	185.5	791.0	13.2	3092.8	4698.5	86.3
EN 6	38.3	0.0	13.2	190.2	876.2	12.2	2184.4	10312.3	88.5
EN 7	39.7	0.1	13.6	194.5	1022.8	10.8	4089.1	15625.4	87.9

A.1.3 Updated Cut-Fill Analysis

Based on the newly provided profiles for each system, an updated cut-fill analysis was performed. Table A.2 summarizes the estimated cut and fill volumes for each system and profile. Key observations include:

- **EN 1** is cut-dominated across all profiles, with minimal fill requirements. The East Profile shows the highest cut volume in the system at over 1.02 million m^3 (36.36 million ft^3), while the Middle Profile has the smallest fill requirement in the entire dataset (834 m^3 or 29,440 ft^3), indicating favorable grading conditions with minimal backfill needs.

- **EN 2** exhibits greater variation between profiles. The Middle Profile is heavily fill-dominated, requiring nearly 698,000 m^3 (24.64 million ft^3) of fill, whereas the West Profile has a more balanced earthwork distribution but still demands significant backfill volumes. The East Profile has moderate cut and fill needs, suggesting a less extreme grading effort compared to the Middle Profile.

- **EN 3** shows the lowest total cut volumes among all systems, with the West Profile requiring only 41,911 m^3 (1.48 million ft^3) of cut. However, it demands substantial fill (197,627 m^3 or 6.98 million ft^3), reflecting localized depressions or low terrain. The East Profile is cut-dominated, with over 290,000 m^3 removed and relatively low fill requirements.

- **EN 4** has the largest earthwork magnitudes overall. The West Profile alone accounts for over 1.63 million m^3 (57.80 million ft^3) of cut, the highest single-profile cut volume recorded. The Middle and East Profiles also have high cut demands (over 1.04 million m^3 and 0.78 million m^3, respectively), suggesting a terrain that requires extensive excavation across alignments.

- **EN 5** (Middle Profile) is cut-dominated, requiring 723,176 m^3 (25.54 million ft^3) of excavation with negligible fill demand, indicating a uniformly high terrain relative to design grade.

- **EN 6** (Middle Profile) presents moderate earthwork needs with roughly 279,000 m^3 (9.85 million ft^3) of cut and 102,000 m^3 (3.59 million ft^3) of fill, reflecting a more balanced terrain modification profile.

- **EN 7** (Middle Profile) shows a relatively high cut volume (425,209 m^3 or 15.02 million ft^3) paired with substantial fill (282,441 m^3 or 9.97 million ft^3), indicating both elevated and depressed segments along the alignment.

A.2 Geotechnical Feasibility Analysis

A geotechnical feasibility analysis is essential for ensuring that the site can support the weight and operational stresses of the ARES tracks and mass cars. Three primary geotechincal considerations were addressed as part of the feasibility analysis: bearing capacity, allowable settlement, and slope stability.

A.2.1 Geotechnical Data Collection

The 9C project, developed between 2002 and 2007, involved comprehensive geotechnical investigations to assess the subsurface conditions of the proposed site, located on agricultural land in the Horse Heavens Hills, southeast of Kennewick, Benton County, Washington. This hilly area, featuring undulating terrain, was subjected to a series of field tests performed by GN Northern, Inc., a geotechnical consulting firm based in Kennewick.

The initial geotechnical exploration commenced in January 2001 with three exploratory borings (BH-5, BH-6, BH-9), strategically positioned to align with the proposed turbine locations (Figure A.10). During this phase, subsurface strata were visually assessed

Table A.2. Cut and fill volumes for each site and profile

Site	Profile	Cut (m^3)	Fill (m^3)	Cut (ft^3)	Fill (ft^3)
EN 1	West Profile	792,909	4,031	28,001,340	142,371
EN 1	Middle Profile	745,798	834	26,337,637	29,440
EN 1	East Profile	1,029,597	2,559	36,359,892	90,356
EN 2	West Profile	353,344	461,360	12,478,249	16,292,797
EN 2	Middle Profile	178,706	697,805	6,310,937	24,642,763
EN 2	East Profile	274,294	557,938	9,686,613	19,703,422
EN 3	West Profile	41,911	197,627	1,480,074	6,979,122
EN 3	East Profile	290,262	38,897	10,250,515	1,373,644
EN 4	West Profile	1,636,718	90,817	57,800,221	3,207,162
EN 4	Middle Profile	1,045,528	271,257	36,922,523	9,579,343
EN 4	East Profile	775,819	446,432	27,397,798	15,765,611
EN 5	Middle Profile	723,176	266	25,538,739	9,385
EN 6	Middle Profile	278,896	101,686	9,849,128	3,591,007
EN 7	Middle Profile	425,209	282,441	15,016,135	9,974,316

at depth intervals wherever material changes were observed. Split spoon and Shelby tube samples were extracted for laboratory testing, including unconfined compressive strength tests performed exclusively on samples from BH-5, along with sieve analysis and moisture density tests. Additionally, Standard Penetration Tests (SPT) were conducted to determine blow counts per 6 inches of spoon penetration and “N values” at varying depths. Due to the relative rather than exact positioning of these boreholes, their soil profiles serve as representations of the diverse soil conditions and strengths prevalent around Jump-Off Joe.

The subsequent phase of subsurface exploration occurred between September 11-16, 2002. It involved five boreholes (Figure A.10), three of which (BH-1, BH-2, BH-3) were positioned at the proposed quarry site, approximately one mile west of Jump-Off Joe. Jump-Off Joe is the peak of an east-west trending ridge, situated approximately one mile east of the proposed quarry. The fourth borehole was situated southeast of Jump-Off Joe in a plowed field, while the fifth was located at its base. The material source at BH-1 to BH-3 was assessed for its potential application as crushed aggregate for road infrastructure construction pertaining to the 9C project. Core borings were drilled at three locations (BH-1, BH-2, BH-3) to depths ranging from 30 to 35 feet below the existing ground surface, mainly revealing basalt bedrock. Notably, basalt started within one foot

of the surface across all boreholes, although the quality of the upper five feet was compromised by weathering and calcium cement filling fractures. Despite moderate weathering conditions extending below five feet, the basalt was predominantly robust, with certain zones exhibiting considerable strength. Split spoon sampling was performed using a 140-pound hammer for BH-4 and BH-5. Blow counts and “N values” were recorded at various depths.

It must be noted that two profiles were provided for BH-5 in the geotechnical reports based on prior studies conducted by EN during the construction phases of the 9C project. As seen in (Figure A.10), the two profiles have been distinguished as BH-5_1, which is the borehole log provided with BH-1 to BH-5 in 2002. The second log is retrieved from the field tests conducted in 2001, that is BH-6, BH-5, and BH-9, and this profile is named BH-5_2. No coordinates were provided for BH-5_2 and estimating the locations from provided maps, it seems unlikely that BH-5_1 and BH-5_2 are at the same location.

These field and laboratory tests at the quarry site proved insightful in planning subsequent geotechnical evaluations closer to the site for LDES, that is Jump-Off Joe. No groundwater was encountered during any of the drilling operations. According to findings made by GN Northern, Inc, the site has a moderate seismic risk. Though the preliminary study performed here does not include seismic risk analysis, it is essential to take this into account when designing the foundation for the gravity rail tracks.

A.2.2 Soil Bearing Capacity Analysis

The bearing capacity of soil is defined as the maximum load per unit area that the ground can support without risk of failure. Bearing capacity failures are typically caused by shear failures within the soil. Hence, it is essential to determine the shear strength parameters, namely cohesion and the angle of internal friction, through direct laboratory tests or correlations from field tests.

Prototype soil profiles were created using borehole investigations conducted around the Jump-Off Joe area during the project construction period. Four profiles were selected for analysis due to their proximity to the proposed site: two from soft soils, identified as BH-5_2 and BH-6, and two with more stable subsurface conditions, labeled BH-1 and BH-2. Notably, bedrock was not encountered at BH-6, even though the borehole extended to 90 feet, whereas slightly weathered basalt was detected at about 60 feet in BH-5. In contrast, at BH-1 and BH-2, medium to slightly weathered basalt was found at a depth of about 30 feet or less during shallow explorations.

Standard Penetration Tests (SPT) were conducted at boreholes BH-5_2 and BH-6, and the results were referenced or adapted for N-values associated with BH-1 and BH-2, based on a visual inspection of the soil strata. SPT testing assesses density and strength of soil layers. The derived N-value were corrected to account for overburden pressures.

Estimates for overburden pressure require an assumption of soil density. The geotechnical report provided two different soil density values. Samples from BH-4 and BH-5-1 underwent laboratory testing and were found to have a density of 90 pounds per cubic

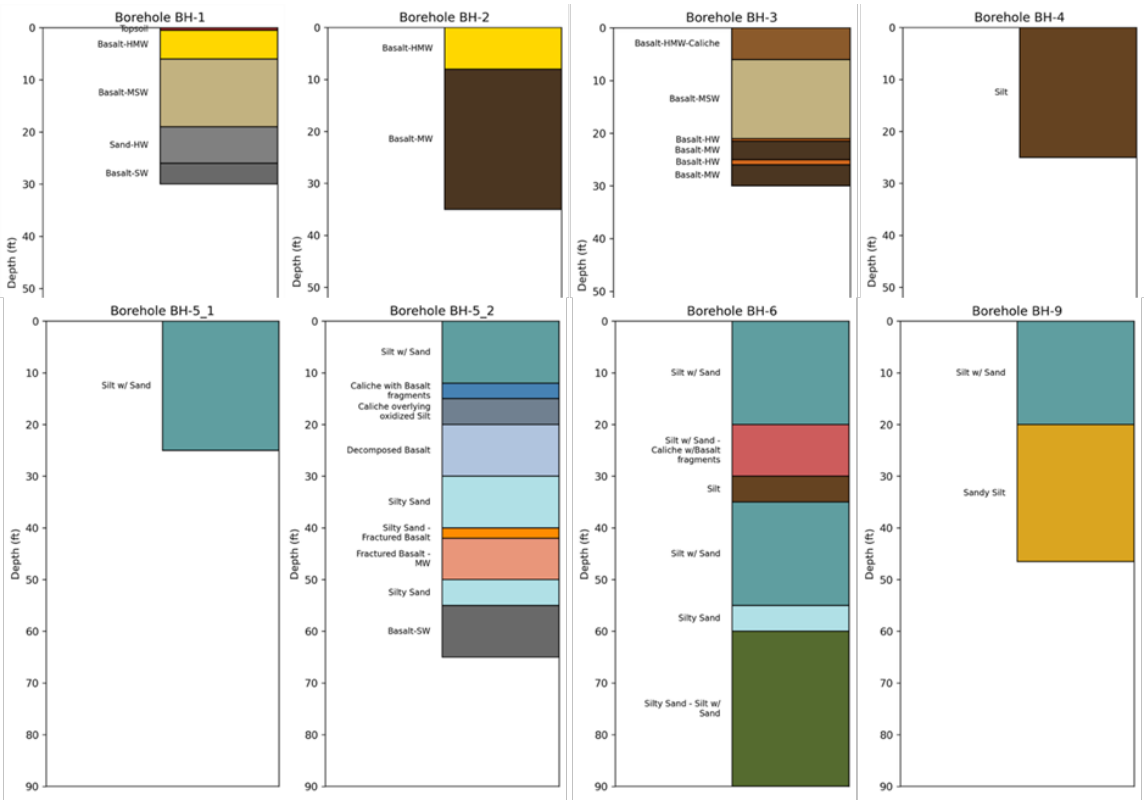

Figure A.10. Soil profiles reconstructed from the boring logs based on site investigations conducted by GN Northern, Inc. for EN. H=Highly, M=Moderately, S=Slightly, W=Weathered.

foot (pcf). The maximum dry density for a combined sample at BH-6 was estimated to be 104 pcf. These densities reflect the range of soil density in the soft soils at BH-5_2 and BH-6. According to literature, the density for basalt typically falls between 143 pcf and 168 pcf. Considering the basalt at BH-1 and BH-2 is in varied weathered states, generic assumptions were made regarding the densities within those strata using a graded approach.

When N-values were adopted for BH-1 and BH-2, they were adjusted to be more representative of the soil type. The N-value for moderately weathered basalt at BH-2 was assigned slightly lower than that for fractured basalt with moderate weathering at BH-5-2. Fractured basalt tends to have greater strength than a matrix consisting purely of weathered basalt due to its inherent structural integrity. Consequently, moderately-slightly weathered basalt was given a slightly higher N-value at the top of the range, while highly-moderately weathered basalt at both boreholes was assigned a lower N-value than the preceding assumptions. Basalt that is highly weathered and contains sand-sized

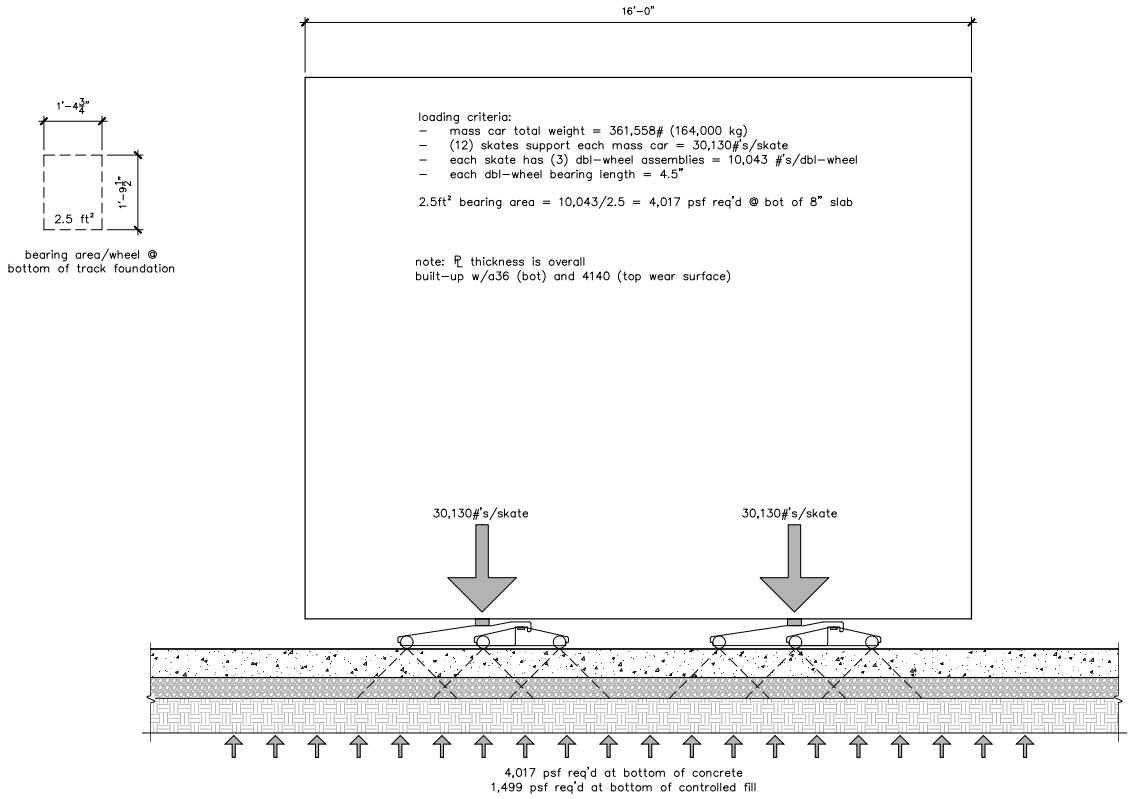

Figure A.11. Schematic provided by ARES for car loading on the tracks.

particles was assigned a similar, albeit slightly lower, strength (N-value) compared to highly-moderately weathered basalt.

According to ARES, the depth of foundation is set at 8 inches. However, Figure A.11 indicates the presence of a controlled fill extending almost 12 inches below the foundation. It also shows the necessity of a bearing capacity of 4017 psf at the bottom of the concrete foundation or 1499 psf at the base of the controlled fill. Typically, bearing capacity is averaged over a depth equivalent to twice the width of the foundation. In this case, a 24-foot depth (2 times 12 feet) or the end of the layer encompassing this depth is used for calculations.

A commonly applied method to compute bearing capacity requires shear strength parameters. Due to the limited details available from laboratory tests of site samples empirical relationships based on N-values were utilized instead. In 1977, J.E. Bowles offered a modified formula for foundations with width greater than 1.22 m, to ascertain

the net allowable bearing capacity (qnet) in kN/m² using the N-value-

$$q_{\text{net}} = \frac{N_{60}}{0.08}\left(\frac{B+0.3}{B}\right)^2 F_d\left(\frac{S_e}{25}\right) \tag{A.1}$$

where

q_{net} = net bearing capacity = $q_{\text{ult}} - q' = q_{\text{ult}} - \gamma D_f$
γ = unit weight (density) of the soil layer
N_{60} = standard penetration resistance corrected for field conditions
F_d = depth factor = $1 + 0.33\frac{D_f}{B}$
B = width of the foundation (m)
S_e = maximum allowable settlement (mm)
D_f = depth of foundation (m)

All the input parameters, overburden pressure, depth of foundation, etc., are converted into SI units for the calculations, and the computed ultimate bearing capacity is converted back into FPS units (Table A.3).

A.2.3 Allowable Settlement

Allowable settlement considers the immediate settlement, primary consolidation settlement, and secondary settlement of soil both during and after construction.

- **Immediate Settlement**: Occurs right after loading, primarily affecting non-cohesive soils like sands where drainage is efficient.
- **Primary Consolidation Settlement**: A time-dependent stiffness change in cohesive soils (such as clays) due to expulsion of pore water and subsequent soil compaction.
- **Secondary Settlement**: Happens over a long period as soils slowly adjust under sustained loads, more evident in organic soils and highly compressible clays.

Understanding these settlements helps in predicting potential site deformations and ensuring that any settlement remains within tolerable limits to maintain the structural integrity and performance of the ARES tracks.

The soil layers encountered in the four prototype profiles are mainly composed of coarse-grained material or weathered rock, and there was no presence of groundwater near the zone influenced by the applied stresses. Accordingly, both primary and secondary consolidation settlements will be negligible, and the immediate settlement is expected to prevail in terms of overall settlement at the site. To calculate the immediate settlement of the foundation of the rail tracks, Burland and Burbridge's method from 1985

is employed, using measurements from the Standard Penetration Test (N-value) –

$$\frac{S_e}{B_R} = \alpha_1 \alpha_2 \alpha_3 \left[\frac{1.25 \frac{L}{B}}{0.25 + \frac{L}{B}} \right]^2 \cdot \left(\frac{B}{B_R} \right)^{0.7} \cdot \frac{q' \cdot 1000}{p_a} \tag{A.2}$$

where

$S_e =$ average immediate settlement (mm)
$B_R =$ reference width $= 0.3$ m
$B =$ width of the foundation (m)
$\alpha_1 =$ a constant $= 1.4$ (for normally consolidated sand)
$\alpha_2 =$ compressibility index $= \frac{1.71}{N'^{1.4}}$
(for normally consolidated sand)
$\alpha_3 =$ correction for depth of influence $= 1.0$
(for normally consolidated sand and $H > z'$)
$H =$ depth of compressible layer $= 30$ ft
(minimum depth where bedrock could be present)
$z' = 1.4 \left(\frac{B}{B_R} \right)^{0.75} B_R$
$q' = q_{\text{net}}$ for normally consolidated sand and $H > z'$
$q_{\text{net}} = \bar{q} - \gamma D_f$
$\bar{q} =$ stress at foundation level $= 4017$ psf
$\gamma =$ unit weight of top soil layer
$D_f =$ depth to bottom of foundation
$N' =$ average N-value over depth of influence
(corrected for dilatancy but not for overburden pressure)

Assuming an average foundation length of 800 meters, the L/B ratio is approximately 2500. By using these parameters in the settlement equation, a range of minimum to maximum settlement values are determined, drawing on the observed N-values and soil densities for each layer. These results are detailed in Table A.4, where settlements are ranked based on their lowest values. Typically, a settlement limit of 25 mm is deemed acceptable, but stricter criteria apply to rail tracks with concrete foundations due to their rigidity, which can lead to cracking or structural damage. In this scenario, settlement between 10 mm and 20 mm is considered permissible.

A.2.4 Slope Stability Assessment

In assessing the stability of a finite slope, complex computations in extensive analyses are necessary. However, a simplified assessment can be conducted in an idealized context where the slope is assumed to be infinitely long, with a length-to-height ratio of the slope exceeding 16 [Ref]. This scenario considers a homogeneous $c - \phi$ soil with uniform stress distribution while ignoring boundary effects. In such cases, the depth (z) at which slope failure may occur can be estimated by setting the factor of safety (FOS) to 1:

$$z = \frac{c}{\gamma_t \cos^2 i \, (\tan i - \tan \phi)} \tag{A.3}$$

In this equation, c symbolizes the soil's cohesion (strength parameter), γ_t is the total soil density, i denotes the slope's angle of inclination, and ϕ signifies the soil's friction angle (another strength parameter). If $i > \phi$, the calculated depth z becomes negative, which is meaningless in practical terms.

A.2.5 Ground Improvement and Modification

There are several alternatives to consider for improving the soil conditions observed around Jump Off Joe. One option involves replacing 2 to 3 feet of silty layers with slightly weathered basalt sourced from a nearby borrow site. This alternative can enhance foundational stability due to the increased density and strength offered by the basalt. Another approach is to use 12 inches of Type II aggregate, as considered by ARES in Figure A.11, which can improve the foundation's load-bearing capacity and drainage characteristics.

Additionally, in-situ densification methods can be explored for sands or coarse-grained soils. One such method is the use of compaction/displacement piles. In this technique, a hollow tubular pipe is driven to the desired depth, densifying the sand displaced around it. As the pipe is retrieved, extra sand or gravel is backfilled into the created space.

Impact or dynamic compaction, also known as heavy tamping, involves dropping a heavy weight to increase the density of the underlying soil. This method effectively compacts soil layers and is suitable for various soil types. Vibration methods like vibroflotation (also known as vibro compaction) can also be effective at the site. An important consideration while employing methods that can generate vibrations in the surrounding soil is the vicinity to other structures, which in this specific case can be turbines, meteorological/communication towers, and other civil infrastructure.

Grouting methods provide another alternative for soil improvement using a mixing additive like cement, lime, and bentonite. Lime can be suitable for expansive soils, while bentonite is beneficial for creating impermeable barriers. Each method offers unique advantages, ensuring a tailored approach to enhancing soil conditions.

The appropriate method to be employed will be determined by the Geotechnical Engineer based on the site-specific conditions determined through supplementary field ex-

ploration and laboratory testing. If the soil is found to be too weak, incorporating soil reinforcements using geotextiles (geogrids) or steel elements could prove to be more economically viable alternatives compared to deep foundations.

A.3 Geotechnical Analysis Results and Site Feasibility

A.3.1 Results

This section presents the findings investigations into the bearing capacity, settlement, and slope stability of the four soil profiles. Table A.3 details the net bearing capacity calculations for each profile, accompanied by an evaluation of their capability to bear the gravity rail loads in the LDES system. Additionally, Table A.3 outlines the immediate settlement for the soil profiles, followed by an in-depth analysis of their appropriateness for the rail system. The section concludes with a brief assessment of slope stability at the prospective LDES system locations.

Table A.3. Net bearing capacity calculated using prototype soil profiles around Jump Off Joe.

Soil Profile	Lower End of Range (psf)	Upper End of Range (psf)
BH-1	2406.63	3779.37
BH-2	3438.25	4459.77
BH-5_2	2147.70	2188.46
BH-6	1152.74	2550.00

The net bearing capacity is not used directly in practice. A factor of safety (FOS), generally ranging from 3 to 5, is used to modify the net bearing capacity to account for uncertainties such as variations in soil, site differences, and measurement inaccuracies. The allowable bearing capacity (qall) is derived by dividing the net bearing capacity (qnet) by the FOS. It is recommended that future feasibility studies generate an allowable bearing capacity.

Foundations placed on sloped terrains undergo a decrease in bearing capacity. Given that the average slope inclination at the prospective sites ranges from 13°to 19°, the bearing capacity is anticipated to diminish by approximately 10% to 20%. Bearing capacity is also reduced in the presence of water table but since no groundwater was encountered in any of the field tests conducted near the sites from open-source data for well borings, and the soil is primarily coarse graded with good drainage characteristics, any effect of rainwater infiltration is considered to be negligible.

The net bearing capacities of the four prototype soil profiles in Table A.3. show that the stiffer sites, BH-1 and BH-2 are more suitable to support the loads from gravity rails compared to BH-5_2 and BH-6, which have significantly lower capacities and will require ground improvement. The details of the aggregate fill (Figure A.11) were not available at the time of the computations, hence they could not be included. However, its presence will enhance the bearing capacity. Please see section B.1.2.4 for different techniques that can be utilized for ground improvement at the site.

Table A.4. Immediate settlement calculated using prototype soil profiles around Jump Off Joe.

Soil Profile	Lower End of Range (mm)	Upper End of Range (mm)
BH-1	10.16	19.11
BH-2	7.84	11.28
BH-5_2	21.85	21.85
BH-6	106.51	106.51

Table A.4 indicates that the profiles like BH-1 and BH-2, where basalt layers are near the surface, are better suited to bear the loads of the LDES system without excessive settlement. However, BH-5-2 can be considered viable using the intermediate strong basalt layers and caliche, provided the upper soft soil layers are replaced with high-density compacted fill. BH-6 will require significant ground improvement before it can be considered a candidate for the LDES site. The bulk of settlement occurs in the upper layers directly beneath the foundation, meaning that a strong, competent subgrade or fill will absorb the most settlement.

For a railway track, controlling differential settlement - ideally maintaining it between 5mm and 10mm - is critical to prevent misalignments that pose safety risks. In the absence of data regarding adjacent soil profiles, hypothetical scenarios assuming any combination of the four prototype soil profiles indicate that BH-1, BH-2, and densified BH-5_2 are suitable for supporting the gravity rails. Similar to the total settlement considerations, utilizing BH-6 is advisable only if ground modification is undertaken to avert significant misalignment issues.

Given the average slope inclination constraint of 15°at Jump Off Joe and a derived ϕ exceeding 25°on average for the prototype profiles, the slope is anticipated to be stable across all four soil conditions, though localized failure may occur. In scenarios involving fully saturated flow, the maximum permissible slope inclination can be reduced by 50%, necessitating a minimum friction angle of 30°, which is achievable through removal or densification of the top layer in softer profiles.

It is crucial to note that these projections are applicable only under the infinite slope assumption. According to parametric studies employing finite element modeling (FEM),

Table A.5. Qualitative ranking of the prototype soil profiles around Jump Off Joe.

Soil Profile	Rank	Notes
BH-1	II	Second best. Has some weaker layers between strong basalt layers. Higher settlement but under acceptable limits.
BH-2	I	Best site with highest bearing capacity and lowest settlement.
BH-5_2	III	Primarily soft site interspersed with strong layers. Will require ground improvement to support gravity rails and minimize differential settlement.
BH-6	IV	Very soft layers. No bedrock encountered. Will require significant ground improvement to support gravity rails and minimize differential settlement.

depending on the slope's length-to-depth ratio and the soil's cohesion, the FOS may be decreased by 5% to 40%. Precise slope stability assessment requires thorough modeling, which falls beyond the scope of this project. Nonetheless, like the bearing capacity and settlement evaluations, the stiffer profiles at BH-1 and BH-2 are anticipated to adequately support the gravity rails system whereas the softer profiles, BH-5_2 and BH-6, will require soil stabilization, such as using soil nails.

A.3.2 Site Feasibility

Results of the geotechnical analysis are summarized in Table A.5. The ranking of sites shown in the table is contingent upon the site-specific conditions observed when detailed geotechnical investigation is carried out at Jump Off Joe in the next phase of the project. The topsoil (6"-12") should be removed at all sites and loose layers compacted for optimum dry density. This should be sufficient for the sites that may have profiles similar to BH-1 and BH-2. However, for softer sites like BH-5_2, ground improvement will be necessary to enhance the bearing capacity and minimize the differential settlement if it is adjacent to BH-1 and BH-2. Sites like BH-6 will require aggressive soil modification techniques like grouting to support the gravity rails.

For future investigations, it is recommended that at least two boreholes be drilled for every leg of a gravity rail site. This includes both storage (relatively flat ground) and the slope (inclined ground) areas to get a clear picture of the subsurface soil conditions present at the site. Lab tests are also critical to characterize the soil type, density, and strength parameters. The above computations used observed (BH-5 and BH-2) and approximated (BH-1 and BH-2) N-values from SPT tests. However, most accurate estimates for bearing capacity, total and differential settlement, and slope stability require

the strength parameters of soil—cohesion and angle of friction.

A.4 Hydrological Feasibility Analysis

A.4.1 Watershed Delineation and Drainage Patterns

To support hydrological feasibility assessment, high-resolution topographic, land cover, and soil datasets were integrated with NRCS TR-55 methods for estimating watershed runoff potential.

The raw 1-meter DEM (Figure A.12) was preprocessed using the `Fill` tool in the ArcGIS Spatial Analyst toolbox to eliminate spurious depressions or pits in the terrain that could interrupt flow routing. This sink-filling process ensures a hydrologically correct DEM suitable for flow analysis. Flow direction was then computed using the Deterministic 8 (D8) algorithm via the `Flow Direction` tool, which assigns flow direction from each cell to one of its eight surrounding neighbors based on steepest descent (Figure A.12). Using the resulting flow direction raster (in addition to slope and aspect) (Figure A.12), flow accumulation was calculated using the `Flow Accumulation` tool, which computes the number of upstream cells contributing to each grid cell.

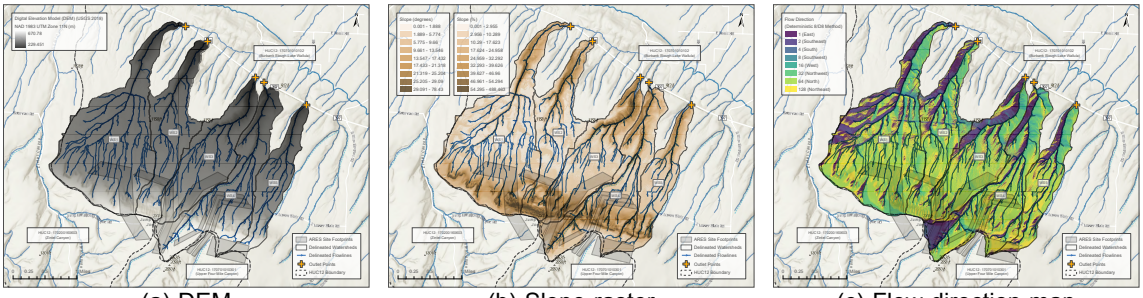

(a) DEM (b) Slope raster (c) Flow direction map

Figure A.12. (a) DEM shows elevation gradient across watersheds; (b) slope raster highlights areas of steep terrain that influence runoff speed and routing; (c) flow direction map to determine steepest descent pathways.

A flow accumulation threshold of 25,000 cells (equivalent to 25,000 m² or approximately 0.01 mi²) was applied to extract concentrated flow paths (Figure A.13). These were vectorized to delineate the flow network across the terrain. Five pour points were manually identified along State Highway 397 at key locations where concentrated flows intersected the highway and drained adjacent proposed site footprints. These pour points served as outlets for watershed delineation.

Using the `Watershed` tool, upstream contributing areas were delineated (Figure A.13) for each pour point based on the flow direction grid. The resulting drainage basins, labeled WS1 through WS5 from west to east, define the watersheds used for subse-

quent hydrologic analysis. To characterize flow path geometry within each basin, the `Flow Length` tool was applied to calculate the hydraulic length—defined as the maximum downslope distance from the most hydraulically distant cell in the watershed to its respective outlet (i.e., pour point) (Figure A.13).

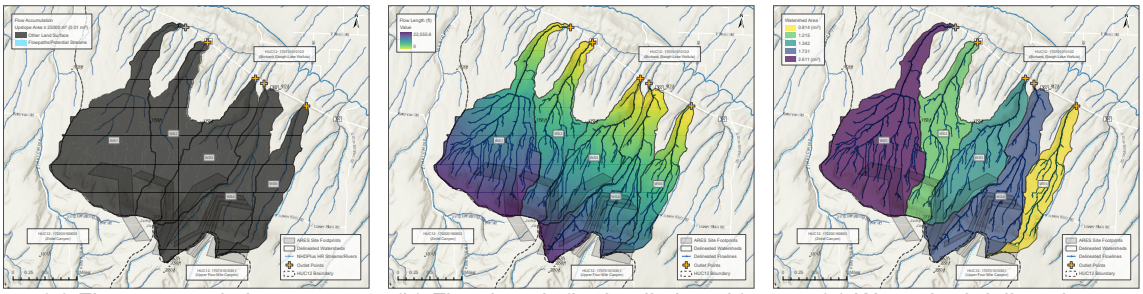

(a) Flow accumulation map (b) Flow length (hydraulic length) (c) Watershed delineation

Figure A.13. (a) Flow accumulation represents the number of upstream cells contributing flow to each cell, used to identify stream networks. (b) Flow length (hydraulic length) estimates the longest flow path from each cell to the outlet, useful for peak flow and travel time analysis. (c) Watersheds and flowlines delineated based on flow direction and accumulation, with outlet points along State Highway 397.

Land use and soil data were then used to estimate the runoff response of each watershed. Land cover classifications were obtained from the 30-meter resolution National Land Cover Database (NLCD 2023) (Figure A.14), while hydrologic soil groups (HSG) were derived from the USDA gridded SSURGO (gSSURGO 2024) database (Figure A.14). Curve Numbers (CNs) were assigned to each land cover–soil group combination using standard NRCS TR-55 guidance for average antecedent moisture condition (AMC II)[1]. The CN raster represents spatially distributed runoff potential within the watershed (Figure A.16).

Rainfall input was based on the 100-year, 24-hour design storm depth extracted from NOAA Atlas 2 (based on historical precipitation records from 1897–1970) (Figure A.14). Combining CN values with design storm depth using the TR-55 runoff equation, spatial runoff depth was estimated for each cell (Figure A.16) (detailed modeling in the next section).

[1] https://www.nrc.gov/docs/ML1421/ML14219A437.pdf

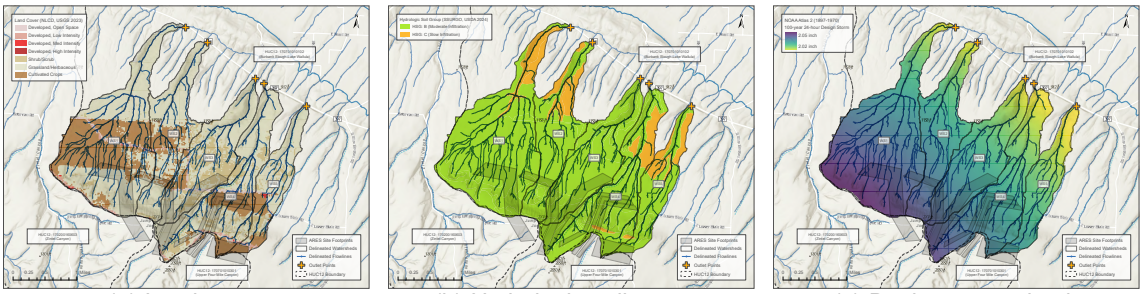

(a) Land cover (b) Hydrologic soil groups (c) Design storm depth

Figure A.14. (a) Land cover data used to define curve numbers, (b) USDA soil groups used for infiltration capacity classification, and (c) NOAA Atlas 2 design storm depth for 100-year, 24-hour events

Table A.6 summarizes the key datasets used for this analysis, including spatial resolution, year of publication, and source.

Table A.6. Datasets used for hydrological feasibility analysis.

Data	Source
1-meter DEM	USGS 2018-2019
30-meter Land Cover	NLCD, USGS 2023
HSG	gSSURGO, USDA 2024
100-year 24-hour Design Storm Depth	NOAA Atlas 2 (1897-1970)

A.4.2 Rainfall-Runoff Modeling

The NRCS (formerly SCS) Curve Number (CN) method in combination with the dimensionless unit hydrograph approach was applied to simulate runoff hydrographs for the delineated watersheds under a 100-year, 24-hour design storm using the NRCS Type II rainfall distribution. The methodology integrates spatially distributed watershed characteristics—such as curve number, drainage area, and hydraulic length—derived from land cover, hydrologic soil group, and topographic data. Rainfall excess was computed using the CN method, and resulting direct runoff hydrographs were generated using a convolution-based technique following the dimensionless unit hydrograph model described in NRCS TR-55[1] and NOAA guidance[2]. All analyses were performed in Python

[1] https://www.nrc.gov/docs/ML1421/ML14219A437.pdf
[2] https://www.nohrsc.noaa.gov/technology/gis/uhg_manual.html

3, and the full workflow is provided as an HTML output viewable in any standard web browser without requiring local Python installation.

A.4.2.1 Rainfall Distribution Calculation

We adopt the 24-hour SCS Type II rainfall distribution from the USDA NRCS National Engineering Handbook (Part 630, Hydrology) [1]. This distribution characterizes high-intensity, short-duration convective events typical of many U.S. regions. A normalized cumulative precipitation series $R_c(t)$ over a 24-hour window was interpolated to 0.5-hour intervals to increase temporal resolution. Incremental rainfall depth at each timestep was computed using:

$$\Delta P_t = P_{\text{total}} \cdot (R_c(t_i) - R_c(t_{i-1})) \tag{A.4}$$

where:

- ΔP_t is the incremental rainfall (in inches) at time t
- P_{total} is the total design storm depth (e.g., 2.03 inches for the 100-year event)
- $R_c(t)$ is the cumulative rainfall ratio at time t

The resulting temporal distribution of rainfall depth is illustrated in Figure A.15, which shows both cumulative and incremental rainfall profiles highlighting the front-loaded nature of the SCS Type II storm, where peak intensities occur near the midpoint of the event (between 12 to 13 hours).

A.4.2.2 Curve Number Runoff Calculation

The NRCS (formerly SCS) Curve Number (CN) method was used to estimate direct surface runoff depth (Q) from precipitation input. The curve number is an empirical parameter (ranging from 30 to 100) that reflects the combined influence of land use, hydrologic soil group, and antecedent moisture conditions. Curve numbers were assigned on a per-cell basis using the land cover and HSG raster datasets described previously, with results shown in Figures A.16a and A.16b.

[1] https://www.hydrocad.net/neh.htm

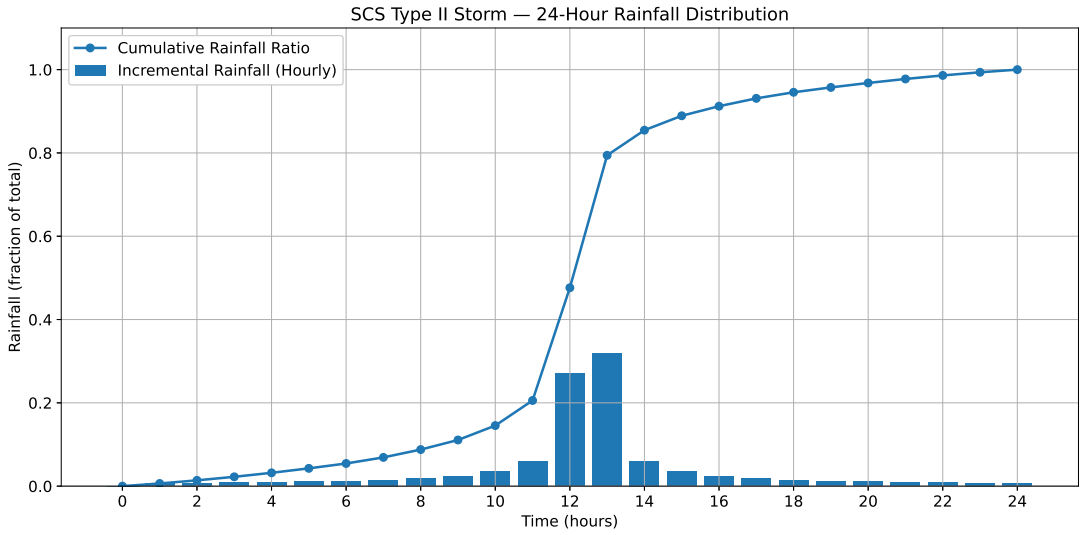

Figure A.15. SCS Type II 24-hour rainfall distribution based on the NRCS National Engineering Handbook (Part 630). The figure illustrates the cumulative and incremental rainfall profiles, highlighting the front-loaded nature of the storm.

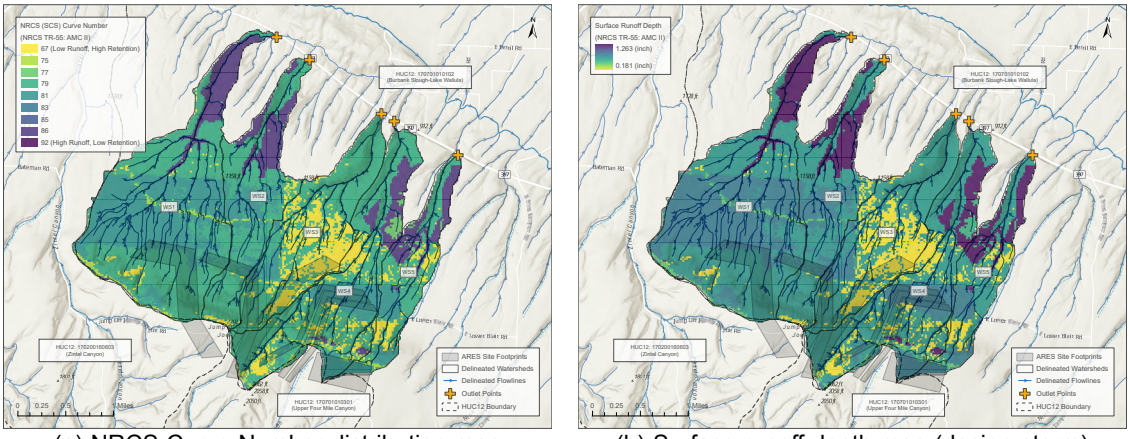

(a) NRCS Curve Number distribution map (b) Surface runoff depth map (design storm)

Figure A.16. Spatial distribution of curve number and estimated surface runoff depths based on a 100-year, 24-hour SCS Type II design storm under Antecedent Moisture Condition II (AMC II). Curve numbers are derived from land cover and HSG combinations. Runoff depths are computed using the NRCS runoff equation applied to each grid cell.

Runoff depth was calculated using the following equations:

$$S = \frac{1000}{\text{CN}} - 10 \qquad \text{(Potential maximum retention, in)} \qquad \text{(A.5)}$$

$$I_a = 0.2 \cdot S \qquad \text{(Initial abstraction, in)} \qquad \text{(A.6)}$$

$$Q = \begin{cases} \frac{(P-I_a)^2}{P+0.8S} & \text{if } P > I_a \\ 0 & \text{otherwise} \end{cases} \qquad \text{(A.7)}$$

where:

- P is the total rainfall depth (in inches)
- Q is the direct runoff depth (in inches)
- S is the potential maximum retention (in inches)
- I_a is the initial abstraction (in inches)

These equations were applied for each cell within the delineated watersheds using the storm depth from NOAA Atlas 2 (e.g., 2.03 inches for the 100-year, 24-hour event) and spatially varying CN values. The resulting runoff depth rasters provided the basis for computing excess rainfall time series used in hydrograph modeling.

A.4.2.3 Hydrograph Timing Parameters and Peak Discharge Calculation

Following the NRCS TR-55 methodology[1], the unit hydrograph parameters[2]—lag time, time to peak, and time base—were computed for each watershed based on its geomorphological properties. These parameters are essential for shaping the hydrograph response and are defined as follows:

- **Lag time (T_{lag}), in hours:**

$$T_{\text{lag}} = \frac{L^{0.8} \cdot (S+1)^{0.7}}{1900 \cdot \sqrt{Y}} \qquad \text{(A.8)}$$

- **Time of concentration (T_c), in hours:**

$$T_c = \frac{T_{\text{lag}}}{0.6} \qquad \text{(A.9)}$$

[1] https://www.nrc.gov/docs/ML1421/ML14219A437.pdf
[2] https://www.nohrsc.noaa.gov/technology/gis/uhg_manual.html

- **Rainfall duration (D), in hours:**

$$D = 0.133 \cdot T_c \tag{A.10}$$

- **Time to peak (T_p), in hours:**

$$T_p = T_{\text{lag}} + 0.5 \cdot D \tag{A.11}$$

- **Time base (T_b) of hydrograph, in hours:**

$$T_b = 2.67 \cdot T_p \tag{A.12}$$

- **Peak discharge (Q_p), in cfs:**

$$Q_p = \frac{484 \cdot A \cdot Q}{T_p} \tag{A.13}$$

Where:

- L = hydraulic length of watershed (ft)
- S = potential maximum retention (in)
- Y = average watershed slope (
- A = watershed area (mi^2)
- Q = runoff depth (in)

A.4.2.4 Unit Hydrograph Generation

To convert rainfall excess into a runoff hydrograph, the dimensionless unit hydrograph (UH) method was employed, following guidance from the Soil Conservation Service (SCS, 1972). A standardized dimensionless UH table, which provides normalized discharge values (q/q_p) as a function of normalized time (t/T_p), was linearly interpolated over the time axis and scaled to the actual peak discharge and time-to-peak for each watershed.

The scaled unit hydrograph $q(t)$ is defined as:

$$q(t) = Q_p \cdot \left(\frac{q}{q_p} \right)_{t/T_p} \tag{A.14}$$

where Q_p is the peak discharge and $(q/q_p)_{t/T_p}$ is the interpolated dimensionless ratio at normalized time t/T_p.

The effective hydrograph $q(t)$ was generated over the full time base T_b, and the direct runoff hydrograph $Q(t)$ was computed by convolving $q(t)$ with the excess rainfall time series $r(t)$:

$$Q(t) = r(t) * q(t) \tag{A.15}$$

where $*$ denotes discrete convolution. The resulting runoff hydrograph $Q(t)$ was truncated at 36 hours, beyond which no significant runoff was observed.

A.4.2.5 Volume Calculations and Runoff Ratio

For each delineated watershed, the following outputs were plotted:

- Rainfall and excess rainfall as bar plots (in/hr)
- Runoff hydrograph showing direct runoff flow rate (cfs)

Total rainfall volume (V_{rain}) and total runoff volume (V_{runoff}) were computed using:

$$V_{\text{rain}} = \sum \left(\Delta P_t \cdot \frac{A_{\text{acres}}}{12} \right) \tag{A.16}$$

$$V_{\text{runoff}} = \sum \left(r(t) \cdot \frac{A_{\text{acres}}}{12} \right) \tag{A.17}$$

where:

- ΔP_t = incremental rainfall at time t (inches)
- $r(t)$ = excess rainfall at time t (inches)
- $A_{\text{acres}} = A_{\text{mi}^2} \times 640$ = watershed area in acres
- Division by 12 converts inches to feet

The runoff ratio was also calculated for each watershed as:

$$\text{Runoff Ratio} = \frac{V_{\text{runoff}}}{V_{\text{rain}}} \tag{A.18}$$

This ratio provides an index of how much of the total rainfall contributes to surface runoff under the given design storm and watershed conditions.

A.4.3 Hydrological Analysis Results and Site Feasibility

The TR-55-based runoff analysis across the five watersheds (WS1–WS5) reveals variation in hydrologic response, driven by differences in watershed size, slope, and curve number (CN). WS1, the largest watershed at 1671 acres, exhibited the highest peak discharge (595.23 cfs) and the greatest runoff depth (0.5973 inches), a result of its expansive drainage area and elevated CN (80.25), indicating limited infiltration and higher imperviousness. In contrast, WS3—with a lower CN (75.55) and higher potential retention (S = 3.2363 inches)—generated the lowest runoff depth (0.4152 inches) and peak flow (260.50 cfs), underscoring the role of land cover and hydrologic soil group in reducing runoff.

Lag time (T_{lag}) and time of concentration (T_c) ranged from 0.8603 to 1.1415 hours and 1.4338 to 1.9025 hours, respectively, indicating a slightly delayed runoff response in WS1 due to its size, despite relatively steep slopes. The runoff ratio—defined as the proportion of rainfall converted into direct runoff—ranged from 0.2043 in WS3 to 0.2949 in WS2, with higher ratios correlating with greater imperviousness (i.e., higher CNs). These metrics collectively reveal how watershed characteristics influence both the timing and efficiency of runoff under uniform storm conditions. Tables A.7-A.8 summarize these results.

Table A.7. Watershed hydrologic characteristics using TR-55 method

Watershed	Area (ac)	Flow Len. (ft)	CN (-)	Slope (%)	P (in)	S (in)	I_a (in)	Q (in)
WS1	1670.976	22556.75	80.25	11.16	2.0395	2.4611	0.4922	0.5973
WS2	777.984	18386.31	80.39	13.52	2.0340	2.4394	0.4879	0.5998
WS3	859.008	18164.12	75.55	15.71	2.0324	3.2363	0.6473	0.4152
WS4	1108.032	21608.60	78.32	17.51	2.0333	2.7681	0.5536	0.5154
WS5	521.024	16896.27	79.30	13.13	2.0280	2.6103	0.5221	0.5509

Figure A.17 presents the TR-55 runoff hydrographs for the five delineated watersheds (WS1–WS5) and their comparative response. Each hydrograph illustrates the temporal distribution of surface runoff generated during a 24-hour SCS Type II design storm, reflecting the influence of watershed-specific characteristics such as curve number (CN), slope, and drainage area. Watersheds with higher CN values and steeper slopes (e.g., WS1 and WS2) exhibit sharper peaks and shorter times to peak (T_p), indicating faster runoff response and reduced infiltration. In contrast, WS3 and WS4, with relatively lower CNs and longer times of concentration, produce broader hydrographs with delayed peak flows. WS5 shows a moderately quick response, consistent with its intermediate hydro-

Table A.8. Runoff response metrics using TR-55 method

Watershed	T_{lag} (hr)	T_c (hr)	D (hr)	T_p (hr)	Q_p (cfs)	T_b (hr)	Runoff Ratio
WS1	1.1415	1.9025	0.2530	1.2680	595.23	3.3857	0.2929
WS2	0.8768	1.4613	0.1944	0.9740	362.33	2.6004	0.2949
WS3	0.9320	1.5533	0.2066	1.0353	260.50	2.7643	0.2043
WS4	0.9345	1.5575	0.2072	1.0381	416.05	2.7717	0.2535
WS5	0.8603	1.4338	0.1907	0.9556	227.17	2.5515	0.2717

logic properties. The composite plot consolidates these behaviors, offering a comparative visualization of flow dynamics across all subcatchments, which is essential for designing downstream hydraulic structures and assessing cumulative runoff impacts.

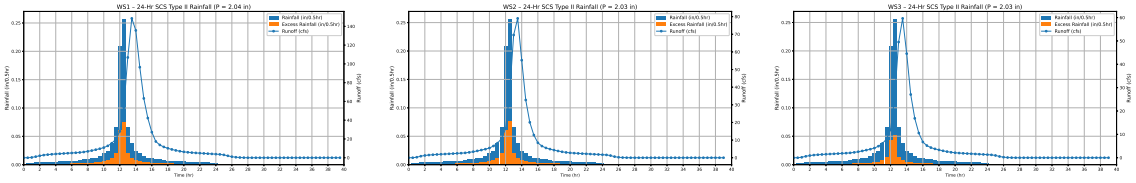

(a) Runoff hydrograph: WS1 (b) Runoff hydrograph: WS2 (c) Runoff hydrograph: WS3

(d) Runoff hydrograph: WS4 (e) Runoff hydrograph: WS5 (f) Runoff hydrograph: All WSs

Figure A.17. TR-55 runoff hydrographs for individual watersheds (WS1–WS5) and the comparative plot. These time series illustrate temporal variation in flow response based on watershed-specific hydrologic characteristics.

While Tables A.7–A.8 list peak flow values (Q_p) calculated using analytical TR-55 equations, the plotted hydrographs in Figure A.17 are derived from a discretized unit hydrograph convolution approach. The tabulated Q_p values represent *instantaneous peak discharges* under the assumption of a uniformly distributed, short-duration rainfall occurring entirely at once—akin to a flash flood scenario. In contrast, the hydrograph peaks reflect the *temporal distribution of flow* resulting from a 24-hour SCS Type II design storm. These peaks account for how rainfall excess is spread over time, producing smoother, lower-magnitude flow responses. Consequently, differences between tabulated and plotted peak flows are expected due to differences in temporal resolution and storm abstraction assumptions.

Table A.9. Statistics of intersecting streams, potential flowlines, and delineated watersheds for each site footprint

Footprint	No. of Stream/ River Reaches Intersec.	No. of Flowlines Intersec. ($\geq$0.01mi^2)	Length of Longest Intersec. Flowline (ft)	Avg. Length of Intersec. Flowline (ft)	Total Length of Intersec. Flowline (ft)	No. of Watersheds Intersec. (State HW 397)
EN 1	0	13	5180.45	2003.35	26043.31	4
EN 2	1	16	1719.16	639.96	10239.50	2
EN 3	0	6	5180.45	3456.92	20741.47	4
EN 4	0	18	5318.24	1892.13	34058.40	1
EN 5	2	8	2463.91	1256.56	10052.49	1
EN 6	1	6	2463.91	1744.32	10465.88	1
EN 7	1	10	2463.91	1465.55	14655.51	1

To assess hydrologic connectivity and potential design considerations, besides the delineated flowlines and watersheds, each site footprint was also intersected with the USGS NHDPlus High Resolution (HR) flow network [1]. Table A.9 summarizes the number of stream or river reaches, qualifying flowlines (with a minimum upstream drainage area of 0.01 mi^2), their lengths, and the number of intersected watersheds within the State HW 397 region.

Across all sites, the number of intersected flowlines ranged from 6 to 18, with **EN 4** having the highest count (18 flowlines) and the longest total flowline intersected length (34,058 ft). **EN 1** and **EN 3** shared the longest individual intersected flowline (5,180 ft), though **EN 3** had only 6 intersected flowlines. Average flowline lengths were highest in **EN 3** (3,457 ft), reflecting fewer but more extensive segments.

Stream or river reaches were sparse across most sites, with **EN 5** intersecting two reaches—the highest among the segments. **EN 1**, **EN 3**, and **EN 4** had no intersecting reaches, suggesting lower stream order segments dominate these footprints. Watershed intersections ranged from 1 to 4, with **EN 1** and **EN 3** overlapping with four watersheds, indicating broader catchment connectivity. These metrics provide insight into surface water complexity, which can influence both environmental assessment, hydrologic design feasibility, and stormwater drainage considerations.

[1] https://www.usgs.gov/national-hydrography/access-national-hydrography-products

Pacific Northwest National Laboratory

902 Battelle Boulevard
P.O. Box 999
Richland, WA 99352
1-888-375-PNNL (7665)

www.pnnl.gov